

2017

Acceleration of bridge construction with prolonged service life

Anmol Mohiniraj Pakhale
Iowa State University

Follow this and additional works at: <https://lib.dr.iastate.edu/etd>

 Part of the [Civil Engineering Commons](#)

Recommended Citation

Pakhale, Anmol Mohiniraj, "Acceleration of bridge construction with prolonged service life" (2017). *Graduate Theses and Dissertations*. 16188.
<https://lib.dr.iastate.edu/etd/16188>

This Thesis is brought to you for free and open access by the Iowa State University Capstones, Theses and Dissertations at Iowa State University Digital Repository. It has been accepted for inclusion in Graduate Theses and Dissertations by an authorized administrator of Iowa State University Digital Repository. For more information, please contact digirep@iastate.edu.

Acceleration of bridge construction with prolonged service life

by

Anmol M. Pakhale

A thesis submitted to the graduate faculty
in partial fulfillment of the requirements for the degree of
MASTER OF SCIENCE

Major: Civil Engineering (Structural Engineering)

Program of Study Committee:
Brent M. Phares, Co-Major Professor
Behrouz Shafei, Co-Major Professor
Jennifer S. Shane

The student author, whose presentation of the scholarship herein was approved by the program of study committee, is solely responsible for the content of this thesis. The Graduate College will ensure this thesis is globally accessible and will not permit alterations after a degree is conferred.

Iowa State University

Ames, Iowa

2017

Copyright © Anmol M. Pakhale, 2017. All rights reserved.

TABLE OF CONTENTS

LIST OF FIGURES	v
LIST OF TABLES	xi
ACKNOWLEDGMENTS	xii
ABSTRACT	xiii
CHAPTER 1. INTRODUCTION	1
1.1 Background	1
1.2 Objective and Approach	2
CHAPTER 2. CONSTRUCTION AND EVALUATION OF VICTOR AVENUE BRIDGE OVER PRAIRIE CREEK	4
2.1 Introduction	4
2.1.1 Background	4
2.1.2 Objectives	5
2.2 Bridge Description	6
2.2.1 General information	6
2.2.2 Internal curing concrete	11

2.3 Bridge Construction	14
2.3.1 Cast-on site beam construction	14
2.3.2 Tow truck lift/pull	18
2.3.3 Backhoe lift/move	21
2.4 Bridge Evaluation	28
2.4.1 Tow truck pull test results	28
2.4.2 Backhoe lift/move test results	32
2.4.3 Load Test	34
CHAPTER 3. INVESTIGATION OF TECHNIQUES FOR ACCELERATING THE CONSTRUCTION OF BRIDGE DECK OVERLAYS	44
3.1 Introduction.....	44
3.1.1 Objective and approach.....	46
3.2 Description of Different Types of Overlay Concrete Mixes	47
3.2.1 Class O Portland Cement Concrete.....	47
3.2.2 Class HPC-O High Performance Concrete	47
3.2.3 CTS Cement Rapid Set Low-P mixes.....	49
3.2.4 4×4 Concrete mix.....	52
3.2.5 Polyester Polymer Concrete.....	54
3.2.6 Very-Early-Strength LMC	56

3.3 Investigation of Ongoing Overlay Construction Project	58
3.3.1 Removal of temporary bollards	58
3.3.2 Removal of top 2 to 3 in. layer of deck concrete	59
3.3.3 Placing the compressed air line.....	62
3.3.4 Removal of substrate concrete using jackhammers	62
3.3.5 Sandblasting the deck	64
3.3.6 Overlay concrete placement.....	65
3.3.7 Other observations	66
3.4. Laboratory Testing.....	69
3.4.1 Methodology and study parameters	69
3.4.2 Pull-Off test.....	73
3.4.3 Push-Out test.....	91
3.4.4 Positive bending flexural test.....	110
3.4.5 Negative bending flexural test	123
CHAPTER 5. CONCLUSION.....	137
5.2 Limitations of the research.....	140
5.1 Future study	140
REFERENCES	142

LIST OF FIGURES

Figure 1. Plan and elevation view of the bridge	7
Figure 2. Abutment details (Section A-A).....	9
Figure 3. Sectional plan view of beam.....	9
Figure 4. Sectional elevation view of beam.....	10
Figure 5. Deck cross-section at the transverse ties	10
Figure 6. Beam interior span sections.....	11
Figure 7. Construction job site.....	15
Figure 8. Steel reinforcing cage for beam.....	16
Figure 9. Internal Instrumentation layout	17
Figure 10. Gage installation on reinforcement	18
Figure 11. Lifting/pulling setup	18
Figure 12. Beam lifted by the tow truck	19
Figure 13. Horizontal pulling loops after lift	20
Figure 14. Concrete spalling on non-pulling side of the beam	21
Figure 15. Strain gages layout used for backhoes lift/move	22
Figure 16. Installed strain gage and data collection system for lift/move	23
Figure 17. Beam launching using backhoes	24
Figure 18. Four beams placed over the creek on the concrete abutments	27
Figure 19. Fifth beam being moved to its position using backhoe	27
Figure 20. Typical top bar strain history (cross-section C top gages)	29
Figure 21. Typical bottom bar strain history (cross-section C bottom gage)	30

Figure 22. Horizontal pulling loop strain.....	31
Figure 23. Strain history for south cross-section	32
Figure 24. Strain history for north cross-section	33
Figure 25. Strain history for middle cross-section.....	33
Figure 26. Load cases	34
Figure 27. Instrumentation layout and nomenclature	35
Figure 28. Instrumentation mounted on the bridge.....	35
Figure 29. Relative displacement gage setup.....	36
Figure 30. Carrying out the load test on the bridge	36
Figure 31. Longitudinal strain distribution over the transverse mid-span (LC-1).....	38
Figure 32. Longitudinal strain distribution over the transverse mid-span (LC-5).....	38
Figure 33. Longitudinal strain distribution over the transverse mid-span (LC-8).....	39
Figure 34. History of the strain gages by J1 (LC-6)	40
Figure 35. History of the strain gages by J4 (LC-3)	41
Figure 36. History of relative displacement at J1 (LC-6)	42
Figure 37. History of relative displacement at J2 (LC-8)	42
Figure 38. History of relative displacement at J3 (LC-9)	43
Figure 39. History of relative displacement at J4 (LC-3)	43
Figure 40. Temporary bollards being detached by workers	59
Figure 41. Milling machine removal of top layer of the deck	60
Figure 42. Area marked for more in-depth removal	61
Figure 43. Removal of unsound concrete using jackhammer.....	63
Figure 44. Deteriorated area of the deck after removal of the substrate concrete	64

Figure 45. Ready-mixed concrete being placed on the deck	65
Figure 46. Manhole discovered near the approach to the westbound lane	66
Figure 47. Eastbound overlay construction schedule as observed.....	68
Figure 48. Different depths of concrete removal considered.....	71
Figure 49. Pull-off test specimen schematic (Case 1).....	74
Figure 50. Pull-off test formwork for substrate concrete placement	75
Figure 51. Pull-off test formwork for overlay concrete placement (Case 4)	76
Figure 52. Pull-off test steel plate with welded shear studs.....	77
Figure 53. Tapping the steel plate to embed the shear studs on a pull-off test specimen.....	78
Figure 54. Testing arrangement for pull-off test.....	79
Figure 55. Case 1 pull-off test specimen failure at concrete bond interface.....	81
Figure 56. Case 1 pull-off test specimen failure in concrete overlay	82
Figure 57. Case 2 pull-off test specimen failure at concrete bond interface.....	83
Figure 58. Case 2 pull-off test specimen failure in concrete overlay	84
Figure 59. Case 3 pull-off test specimen failure at concrete bond interface.....	85
Figure 60. Case 4 pull-off test specimen failure at concrete bond interface.....	86
Figure 61. Case 4 pull-off test specimen failure in concrete overlay	87
Figure 62. Average load at failure versus concrete removal depth (pull-off test)	89
Figure 63. Average tensile stress at failure versus concrete removal depth (pull-off test).....	89
Figure 64. Push-out test specimen schematic (Case 1).....	92
Figure 65. Push-out test specimen schematic (Case 4).....	93
Figure 66. Push-out test formwork for substrate concrete placement	94
Figure 67. Pair of push-out test sub-specimens after concrete removal (Case 4).....	95

Figure 68. Push-out test formwork for overlay concrete placement.....	95
Figure 69. Application of grout for push-out test specimen	96
Figure 70. Push-out test specimen after overlay concrete placement	97
Figure 71. Testing arrangement for push-out test.....	98
Figure 72. Case 1 push-out test specimen failure at concrete bond interface.....	100
Figure 73. Case 2 push-out test specimen failure at concrete bond interface.....	101
Figure 74. Case 3 push-out test specimen failure at concrete bond interface.....	102
Figure 75. Case 4 push-out test specimen failure at concrete bond interface.....	103
Figure 76. Load versus deflection (push-out test)	106
Figure 77. Average load versus concrete removal depth (push-out test).....	107
Figure 78. Average shear stress versus concrete removal depth (push-out test)	107
Figure 79. Average stiffness versus concrete removal depth (push-out test)	108
Figure 80. Positive bending flexural test specimen schematic (Case 1).....	112
Figure 81. Positive bending flexural test formwork for substrate concrete placement	112
Figure 82. Positive bending flexural test specimen after substrate concrete placement (Case 4).....	113
Figure 83. Positive bending flexural test specimen after roughening of substrate concrete (Case 1).....	114
Figure 84. Application of grout to positive bending flexural test specimen (Case 1)	115
Figure 85. Testing arrangement for positive bending flexural test.....	116
Figure 86. Case 1 positive bending flexural test specimen failure at concrete bond interface.....	117
Figure 87. Case 2 positive bending flexural test specimen failure at concrete bond	

interface.....	118
Figure 88. Case 3 positive bending flexural test specimen failure at concrete bond	
interface.....	118
Figure 89. Case 4 positive bending flexural test specimen failure at concrete bond	
interface.....	119
Figure 90. Average maximum load versus concrete removal depth (positive bending flexural test)	121
Figure 91. Average elastic shear stress at maximum load at interface versus concrete removal depth (positive bending flexural test)	121
Figure 92. Average stiffness versus concrete removal depth (positive bending flexural test).....	122
Figure 93. Negative bending flexural test specimen schematic.....	125
Figure 94. Negative bending flexural test formwork for substrate concrete placement.....	125
Figure 95. Chipping of substrate concrete for negative bending flexural tests	126
Figure 96. Negative bending flexural test specimen after concrete removal to required depth (Case 3)	127
Figure 97. Application of grout to negative bending flexural test specimen.....	127
Figure 98. Testing arrangement for negative bending flexural test	128
Figure 99. Case 1 negative bending flexural test specimen failure at concrete bond interface.....	129
Figure 100. Case 2 negative bending flexural test specimen failure at concrete bond interface.....	130
Figure 101. Case 3 negative bending flexural test specimen failure at concrete bond	

interface.....	130
Figure 102. Case 4 negative bending flexural test specimen failure at concrete bond	
interface.....	131
Figure 103. Average load versus concrete removal depth (negative bending flexural test).....	133
Figure 104. Average elastic shear stress versus concrete removal depth (negative bending flexural test)	134
Figure 105. Average stiffness versus concrete removal depth (negative bending flexural test).....	134

LIST OF TABLES

Table 1. Mix design for high performance concrete with internal curing	13
Table 2. Fresh properties for high performance concrete with internal curing (Air content and slump).....	14
Table 3. Fresh properties for high performance concrete with internal curing (Density and w/c ratio)	14
Table 4. Peak micro-strain values in longitudinal bar	30
Table 5. Properties of HPC concrete mix	49
Table 6. Properties of CTS Cement Rapid Set Low-P mixes	51
Table 7. Properties of 4×4 concrete mix	53
Table 8. Properties of polyester polymer concrete	55
Table 9. Properties of very-early-strength LMC.....	57
Table 10. C4 concrete mix strength values	72
Table 11. HPC-O concrete mix strength values.....	72
Table 12. Pull-off test results	88
Table 13. Push-out test results	104
Table 14. Positive bending flexural test results	120
Table 15. Negative bending flexural test results.....	132

ACKNOWLEDGMENTS

I would like to take this opportunity to express my thanks to those who helped me with various aspects of conducting research and the writing of this thesis. First and foremost, I thank Dr. Brent M. Phares for his guidance, patience and support throughout this research and the writing of this thesis. His insights and words of encouragement have often inspired me and renewed my hopes for completing my graduate education. I would also like to thank my committee members for their efforts and contributions to this work: Dr. Behrouz Shafei and Dr. Jennifer S. Shane. I would like to thank Dr. Lowell Greimann, for his help with my thesis writing and his endless hours of patience. I am grateful to Bridge Engineering Center (BEC) and Iowa DOT (Department of Transportation) which have funded my project and also its several engineers, who have helped in various aspects of the project.

I want to also offer my appreciation to Douglas L. Wood and Travis Hosteng who were willing to participate in my field testing, laboratory testing, and observations without whom, this thesis would not have been possible. Finally I would also like to thank my family, friends, colleagues, the department faculty and staff for making my time at Iowa State University a wonderful experience.

ABSTRACT

A large number of bridges in the US are close to their lifespan or are really old. These bridges either need a replacement or some kind of rehabilitation. This has led to increase in the bridge construction projects and with a simultaneous increase in traffic demand, there is a need to accelerate the bridge construction and prolong the bridge life while lowering the construction cost.

To achieve the objective of faster construction with prolonged life and reduced cost an approach known as the “get in, get out, stay out” was applied in one of the projects in this thesis. For this approach, three innovative concepts were included in the replacement of a bridge in Buchanan County of Iowa. The innovative concepts included Geo-synthetic Reinforced Soil (GRS) for the foundation, using prefabricated beams for superstructure and use of internal curing concrete for the beams. The constructed bridge was then monitored over three years through load testing and visual inspection. The bridge beams were found to be structurally sound over the three years of testing.

In addition to the construction of the new bridge with the innovative concepts, it is also important to improve the bridge service life. Bridge deck overlays significantly increase the service life of bridges. Current processes and practices are time-consuming and multiple opportunities may exist to reduce overall construction time by modifying construction requirements and/or materials utilized. This work included three major tasks with literature review, field investigation, and laboratory testing. Through the results and observations of these tasks, several conclusions were made, which could reduce bridge deck overlay construction time.

CHAPTER 1. INTRODUCTION

1.1 Background

Nearly half more than 250,000 of U.S. bridges according to the National Bridge Inventory are in the 25 to 50 year age range. This is a major concern for many State departments of transportation (DOTs) and the Federal Highway Administration (FHWA) because many bridges have a life expectancy of 50 years making them near the ends of their anticipated life cycles. The current goal with new bridge construction is a 100-year lifespan.

In addition to aging, about 26 percent of the bridges in the United States are deficient. Highway capacity also has increased little during the past two decades, but traffic demand has grown tremendously, causing increased congestion, with bridge construction projects compounding the problem. Increase in traffic demand leads to the deterioration of the bridge and additional maintenance cost and time. Traffic control represents anywhere from 20 to 40 percent of construction costs, and user delays are priced at thousands of dollars per day in heavy traffic areas.

There has been an increased interest in constructing bridges with longer life span, and lower construction cost and time and also accelerating constructions related to bridge maintenance. This thesis investigates acceleration of bridge construction and prolonging their service life, and is divided into two separate projects for the investigations.

The approach of constructing bridges faster and economical with longer life span is known as the “get in, get out, stay out” philosophy which has become popular because of the need to reduce traffic congestion caused by work zones. The first two portions of the philosophy

are self-explanatory. The "Stay Out" portion refers to the inherent lasting quality of prefabricated components that are produced in the controlled environment of a fabrication site. This philosophy was accomplished in the first project by incorporating several innovative concepts.

In addition to the construction of bridges, maintenance like rehabilitation of bridge deck with an overlay can also be time consuming. Due to exposure to extreme environmental conditions, heavy-truck wheel loadings, and deicing salts that corrode reinforcement, bridge decks are subject to the most severe conditions of all bridge components. This usually results in deck service lives being less than the other major bridge components. Rehabilitating damaged deck slab concrete with an overlay system can significantly increase the life of the reinforced concrete bridge deck and thus reducing the costs of constructing a new bridge (Ramey and Oliver 1998). An attempt to investigate the acceleration of bridge deck overlay construction was undertaken in the second project.

1.2 Objective and Approach

The primary objective of this thesis was to investigate on acceleration of bridge construction with longer life span, and lower construction cost. This objective was achieved through two separate projects as follows,

1. Construction and evaluation of victor avenue bridge over prairie creek

In this project, following the “get in, get out, stay out” philosophy was the objective. To follow this philosophy three innovative ideas were incorporated to build a box girder bridge in Buchanan County of Iowa.

2. Investigation of techniques for accelerating the construction of bridge deck overlays

The objective of this project was to investigate on techniques to accelerate the construction of bridge deck overlays. This objective was further divided into three techniques.

CHAPTER 2. CONSTRUCTION AND EVALUATION OF VICTOR AVENUE BRIDGE OVER PRAIRIE CREEK

2.1 Introduction

2.1.1 Background

Recently, there has been increased interest in constructing bridges that last longer, are less expensive, and take less time to construct. This is known as the “get in, get out, stay out” philosophy. The idea is to generally increase the cost-effectiveness of bridges by increasing their durability (i.e., useful life) and minimizing disruptions to the traveling public. A bridge in Buchanan County was constructed with innovative concepts to increase its durability while also striving to construct the bridge without the use of vertical lift equipment. The innovative concepts utilized in the bridge include high performance concrete with internal curing aggregates, a Geo-synthetic Reinforced Soil foundation, and an adjacent concrete box-beam superstructure that was intended to be placed using equipment other than a traditional overhead crane.

The bridge was constructed in Buchanan County with the assistance of the Iowa DOT, the Iowa State University Bridge Engineering Center (BEC), Concrete Pavement Technology (CPTech) Center, and Center for Earthworks Engineering Research (CEER)).

2.1.2 Objectives

This project consisted of four major tasks.

- Preliminary design support and documentation

To support Buchanan County and the Iowa DOT Office of Bridges and Structures, the Iowa State University team assisted with the preliminary bridge design process. Specifically, the research team assisted Buchanan County with the design of the GRS (Geo-synthetic Reinforced Soil) abutments and the Office of Bridges and Structures with the superstructure design.

- Construction inspection and documentation

The research team assisted the Office of Bridges and Structures with inspection of key phases of bridge construction. The construction process was observed and documented using photographs. Of particular interest were the fabrication of the precast bridge components, GRS abutment construction, and placement of the prefabricated superstructure on the GRS abutments. (The further details and results of this task is not included in this thesis because it was part of another team's work)

- Testing of concrete materials and mix used for the beams

High performance concrete with internal curing aggregates was used to fabricate the precast beams on site. The research team performed laboratory tests on the concrete

mix that was used and coordinated the results with both Buchanan County and Iowa DOT.

- Bridge inspection

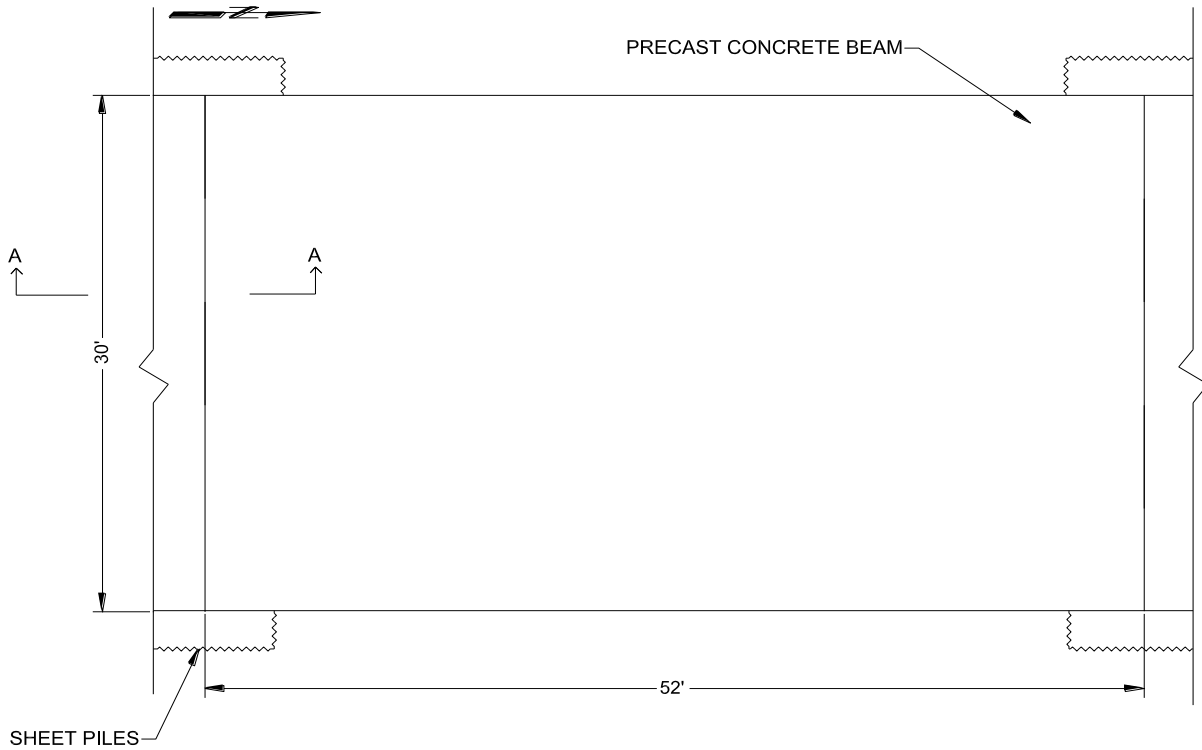
After the construction of the bridge, its performance was monitored for three consecutive years (2014, 2015, and 2016) via load tests and other data collection mechanisms. The research team mounted external instrumentation for each load test and carried out the load tests. The data from pore pressure sensors in the GRS abutment were also collected with all data analyzed to evaluate the structural performance of the bridge.

2.2 Bridge Description

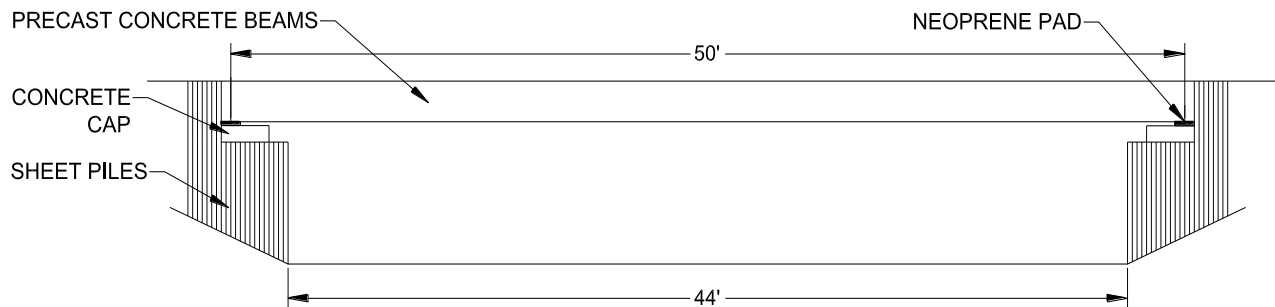
2.2.1 General information

The project that is the subject of this research was the replacement of an aged timber bridge with a cast on site, adjacent box beam bridge. The bridge is 50 ft long, 30 ft wide, with a 0° skew and is located on Victor Avenue, over Prairie Creek, in Section 15 of Fremont Township, T-89-N, R-7W. The bridge was designed for an HL93 loading plus 20 psf for a future wearing surface.

Figure 1 shows the plan and elevation view of the bridge. The bridge consists of precast box beams, guardrails, with a GRS abutment and sheet pile foundation system. Each of the five precast concrete beams is 6 ft wide creating the 30 ft bridge width.



a. Plan



b. Elevation

Figure 1. Plan and elevation view of the bridge

Figure 2 below shows a cross-sectional view of the substructure including details of the GRS abutments and concrete caps. As can be seen four different configurations of granular material and fabric with different lengths make up the GRS abutments. The vertical lifts of

granular material start just below the streambed and continue vertically to the bottom of the crushed stone road surface. The ends of the vertical lifts towards the streambed are covered by the steel sheet piles which help to hold them in place and to avoid the stream water from getting inside and loosening the soil. The sheet piles are driven to 8 ft below the streambed to provide stability.

A concrete cap is placed on top of the granular material and fabric, as shown in Figure 2, which then supports the precast concrete beams and transfers load to the substructure. This reinforced concrete cap is 4 ft wide, 2 ft high and 34 ft in length. A 1 in. by 8 in. neoprene pad is placed between the concrete cap and the concrete beams. The neoprene is placed with its centerline about one foot from each end of each beam.

The vertical lifts behind the concrete beams extend 10 ft past the concrete beam to provide support to the road leading to the bridge. The road surface consists of Class "A" crushed stone.

The bridge superstructure consists of five precast concrete box beams that are 2 ft high by 6 ft wide by 52 ft long (Figure 3 and Figure 4). Figure 3 shows the as-designed plan view of one beam for one-half of each beam. In this figure, the longitudinal reinforcement is not shown to improve clarity.

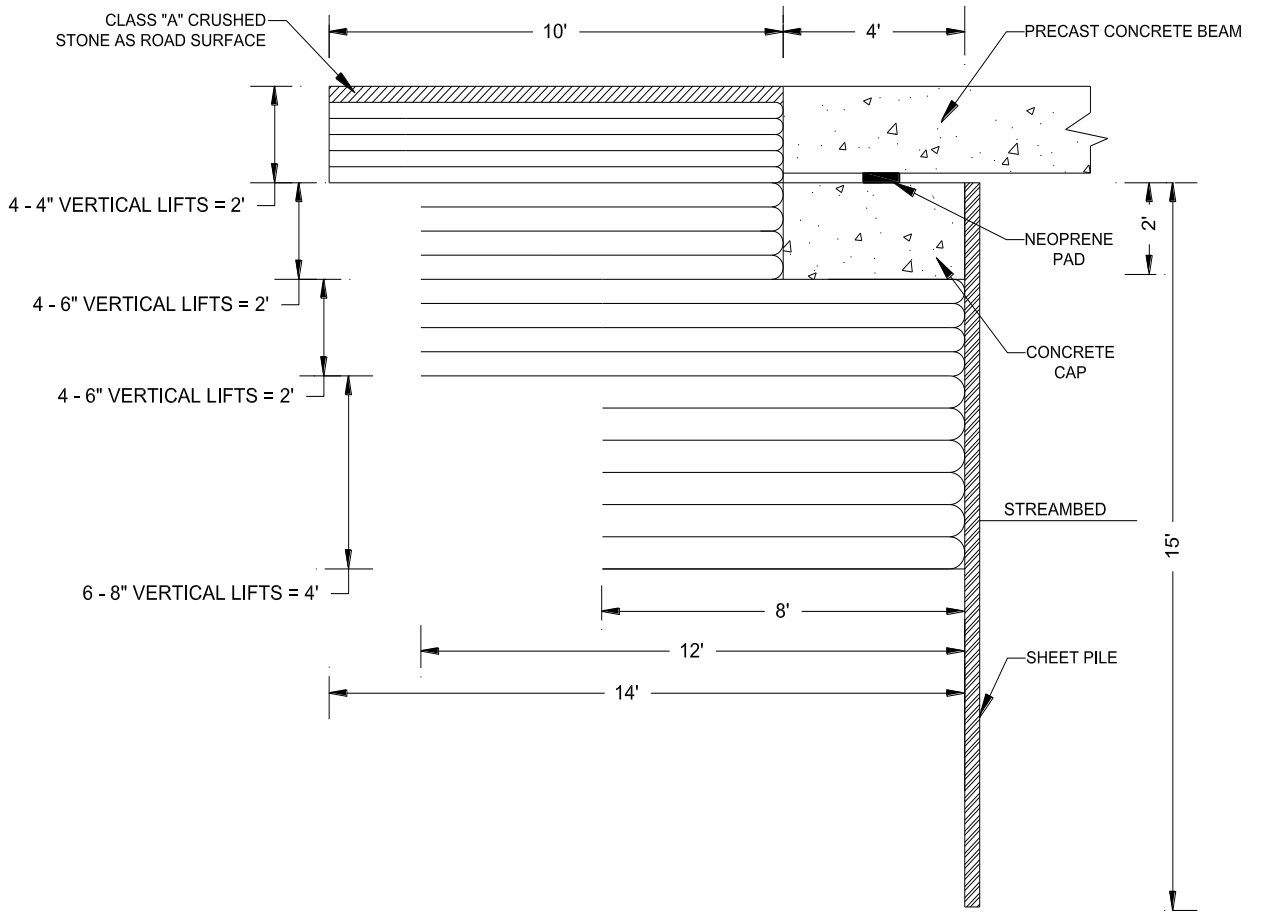


Figure 2. Abutment details (Section A-A)

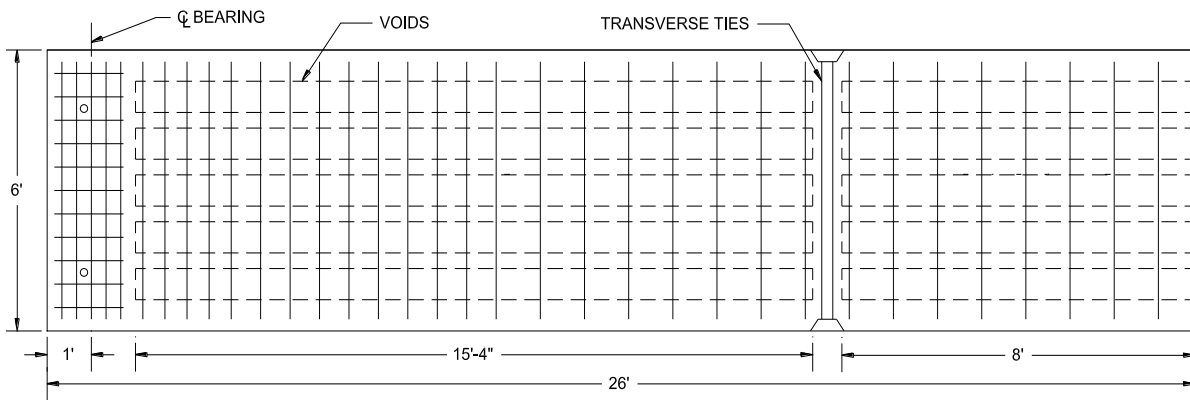


Figure 3. Sectional plan view of beam

Figure 4 shows an as-designed elevation view of the beam. There were two lifting loop provided on each end of the beam. To accommodate the dead load deflection at midspan, a variable thickness slab was provided.

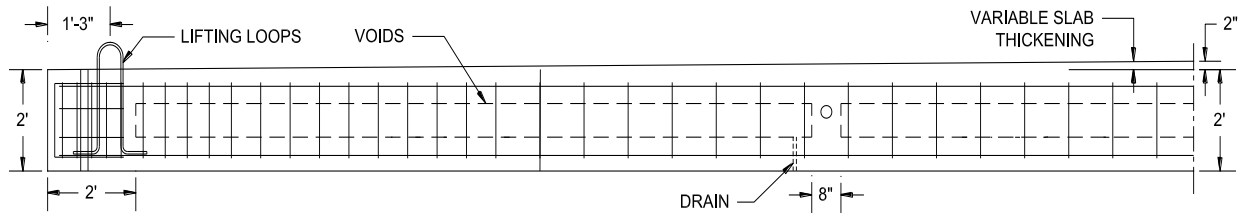


Figure 4. Sectional elevation view of beam

Figure 5 shows the bridge cross-section at a typical transverse tie. To connect the adjacent boxes, grouted shear keys were provided at the longitudinal joints between adjacent girders to ensure a load-sharing mechanism. Per the design plans keyway grout with 5.0 ksi compressive strength at 24 hours was to be used to fill the shear key.

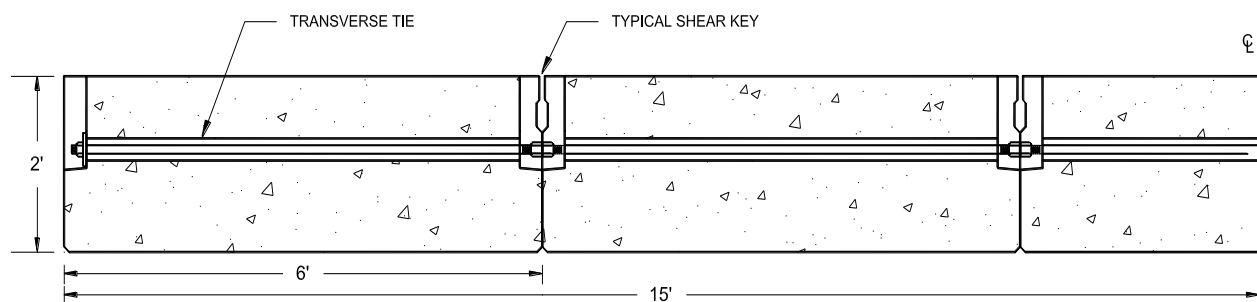
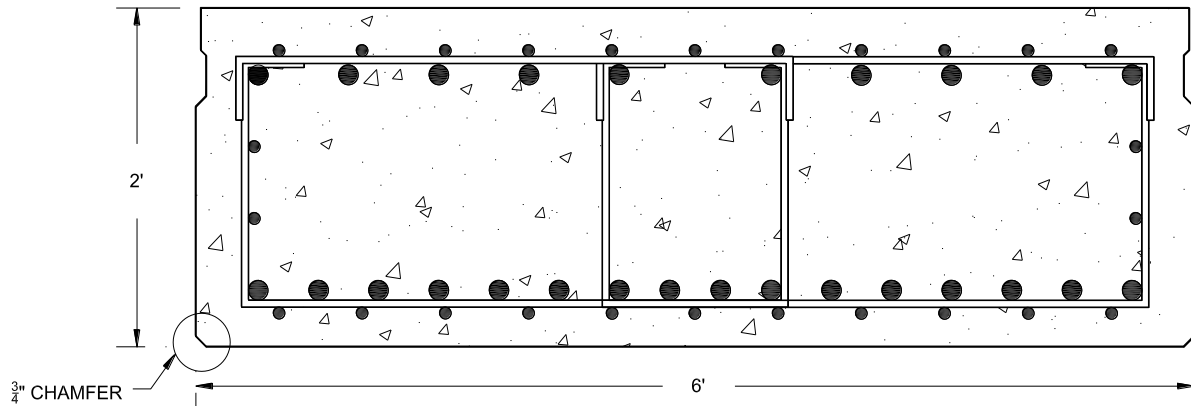


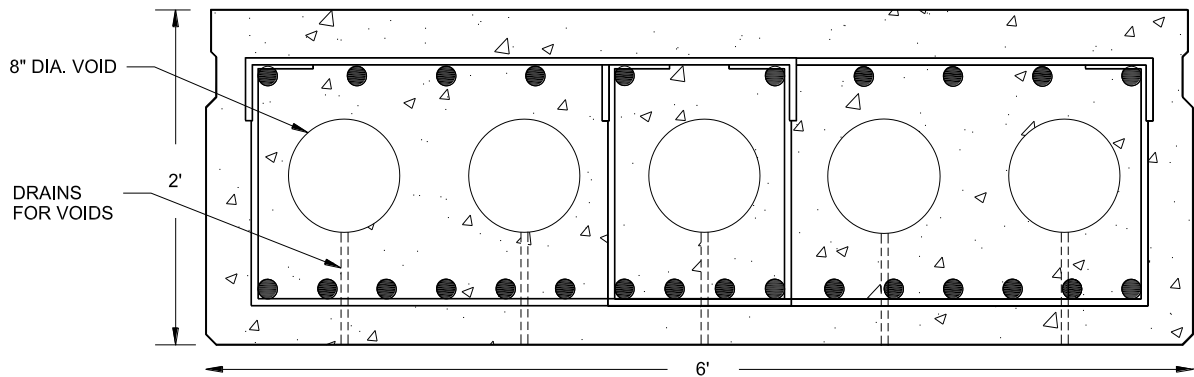
Figure 5. Deck cross-section at the transverse ties

Figure 6a shows the as-designed beam cross-section at the centerline of bearing while Figure 6b shows the beam cross-section at mid-span. In this figure five 8 in. diameter voids placed 5 in. (end to end) apart are shown. Every void was to be provided with a drain for water

as shown in Figure 6b. It should be noted that the contractor elected to not include the voids in the box beams.



a) Beam cross-section at centerline of bearing



b) Beam cross-section at mid-span

Figure 6. Beam interior span sections

2.2.2 Internal curing concrete

Curing plays a vital role in achieving high quality concrete elements. Cement hydration is a series of complex chemical reactions that require an adequate water supply and proper temperatures over an extended time period (Taylor 2013). Curing is defined as “action taken to maintain moisture and temperature conditions in a freshly placed cementitious mixture to allow

hydraulic cement hydration and (if applicable) pozzolanic reactions to occur so that the potential properties of the mixture may develop” (ACI 2016).

Conventional concrete is typically cured using so called external methods. External curing prevents drying of the surface, allows the mixture to stay warm and moist, and results in continued cement hydration (Taylor 2013). Internal curing is a relatively new curing technique that has been developed to prolong the cement hydration process by providing internal water reservoirs in a concrete mixture that do not adversely affect the concrete mixture’s fresh or hardened physical properties. Internal curing grew out of the need for more durable structural concretes that were resistant to shrinkage cracking (Babcock and Taylor 2015).

High performance concrete with internal curing aggregate was used to fabricate the precast Victor Avenue beams. Table 1 shows the details of the mix design, and Table 2 and Table 3 shows the fresh properties required. The 28-day average compressive strength of the concrete was 6,870 psi (ASTM C39), which was higher than the required strength of 4,000 psi and the surface resistivity was 13.90 k Ω -cm which is considered in the moderate range (AASHTO TP 95). Due to the use of the lightweight aggregate for internal curing processes, the beam weighed around 5% lighter than had the beam been fabricated using conventional concrete.

Table 1. Mix design for high performance concrete with internal curing

Material	Moisture Content %	Bulk Density lbs/ft ³	Loose Volume ft ³	Dry Weight lbs	Batch Weight lbs	Specific Gravity	Absolute Volume ft ³
Portland Cement	--	94.0	3.79	356	356	3.15	1.81
GGBFS	--	80.0	1.48	119	119	2.93	0.65
Fly Ash (Class C)	--	75.0	1.58	119	119	2.68	0.71
Coarse Aggregate	1.5%	95.0	15.60	1482	1504	2.62	9.06
Sand Fine Aggregate	3.0%	107.0	9.73	1041	1072	2.65	6.29
Buildex Fine Aggregate	21.0%	61.9	4.80	302	311	1.75	2.77
Water	--	62.4	3.56	--	222	1.00	3.56
Aggregates Surface Moisture	--	62.4	0.53	--	33	1.00	0.53
Air Content @ 6.0%	--	--	--	--	--	--	1.62
MRWR Admixture	--	--	--	--	--	--	--
Total Materials					3702		27.00

Table 2. Fresh properties for high performance concrete with internal curing (Air content and slump)

	As mixed	At placement
Air content	6.00%	4.5% to 5%
Slump	5" to 6"	4" to 5"

Table 3. Fresh properties for high performance concrete with internal curing (Density and w/c ratio)

Fresh concrete density (before pumping)	137.1 lbs/ft ³
Fresh concrete density (after pumping)	138.6 lbs/ft ³
Water/Cementitious materials ratio	0.43

2.3 Bridge Construction

2.3.1 Cast-on site beam construction

Figure 7 is a photograph of the Prairie Creek bridge construction site after removal of the existing bridge. At the time this photograph was taken the new abutments nor the replacement box beams had yet been constructed.



Figure 7. Construction job site

The timber formwork used for beam fabrication is shown in Figure 8. This figure also shows the top longitudinal and lateral reinforcement, and lifting loops at the end. Note that in this photograph a series of longitudinal sonotubes used to create the internal voids can be seen. Recall that one of the goals of this project was to construct the bridge without the use of a conventional crane. Along these lines, one of the original ideas for moving the beams in place was to use a large tow truck to “drag/launch” the beams into place. Given uncertainties in the practicality of this, a “test” beam was first constructed. This test beam was constructed

following the original design plans and is the beam shown in Figure 8. Beams used in the actual bridge were constructed similarly but did not include the internal voids.



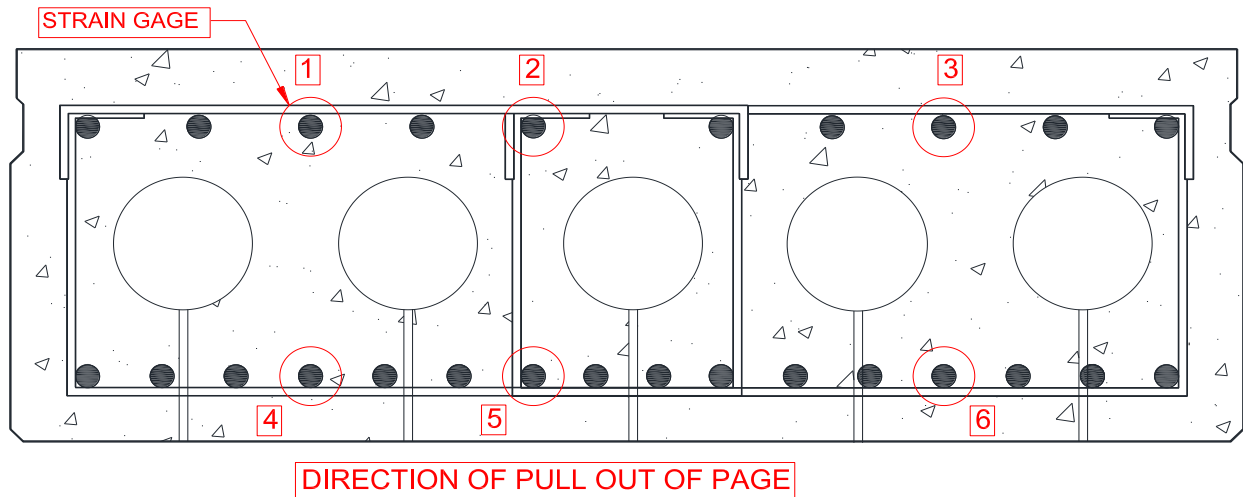
a)



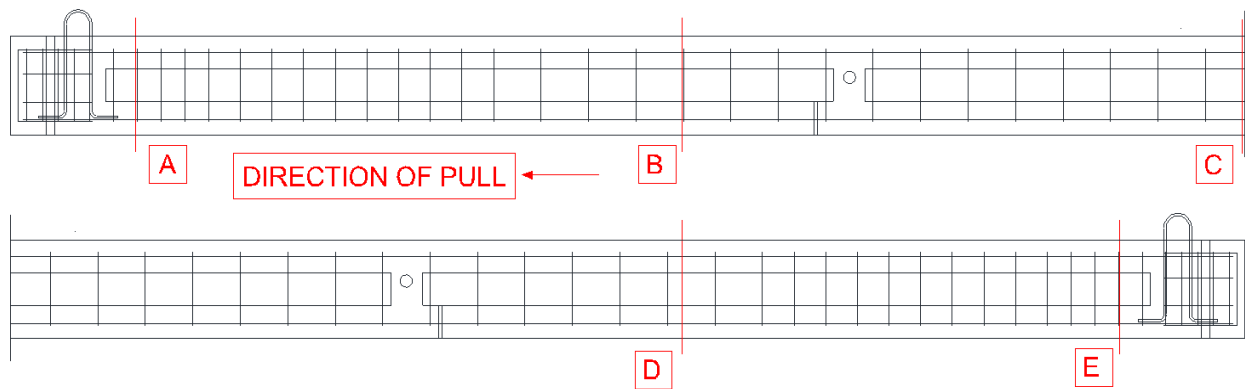
b)

Figure 8. Steel reinforcing cage for beam

For the test beam strain gages were mounted on six different longitudinal bars designated as 1, 2, 3, 4, 5 and 6 in Figure 9a. Five cross-sections were instrumented with strain gages. The location of the five cross-sections is called out as A, B, C, D and E in Figure 9b.



a) Stain gage locations on longitudinal bars (top and bottom) over a beam cross-section



b) Strain gages on longitudinal bars (top and bottom) at A, B, C, D, E

Figure 9. Internal Instrumentation layout

Figure 10 shows a typical installation of the strain gage on the longitudinal reinforcement.



Figure 10. Gage installation on reinforcement

2.3.2 Tow truck lift/pull

As mentioned previously the first attempt to position a beam was with a tow truck. Figure 11 shows the pulling loops on the sides (horizontal pulling loops) that were installed for this purpose. In theory, the beam was planned to be moved by putting wooden cylinders (shown in Figure 11) below it and then sliding it over those cylinders.



Figure 11. Lifting/pulling setup

Figure 12a and Figure 12b shows the beam when it was lifted about six to seven inches at one end. The lifting was stopped at this point to make observations. The lifting force was then gradually released to let the beam rest on the ground.



a) Beam lifted by tow truck



b) The beam when one end was lifted by the tow truck

Figure 12. Beam lifted by the tow truck

During the lift of the beam, three important observations were made. First, **Figure 13** shows the extreme bending of the pulling loops and a crack that propagated from the pulling loop. Second, Figure 14 shows concrete spalling on the other end (opposite to the pulling end) of the beam. Finally, although the tow truck could vertically lift the beam, it did not have sufficient capacity to “pull” the beam forward any appreciable distance. In the eyes of the design and construction teams, the use of a tow truck for this purpose was deemed unsuccessful.



Figure 13. Horizontal pulling loops after lift



Figure 14. Concrete spalling on non-pulling side of the beam

2.3.3 Backhoe lift/move

Realizing that the tow truck method of construction was likely not going to be feasible, it was decided to maintain the spirit of the project by including construction equipment restrictions in the bridge plan set. Specifically, it was stated that the contractor could not use a conventional crane to place the bridge beams. No other restrictions were included. The contractor selected for the project elected to use two backhoes to move the beams from their fabrication site to their final position on the bridge abutments. To document the behavior including peak behaviors, a series of externally mounted strain gages were installed on one beam prior to being moved. The external strain gages were mounted at three different cross-sections, one at 9 ft 8 in. from both (the north and the south) ends and one at the mid-span. The gage layout and the designations for those gages are shown in Figure 15.

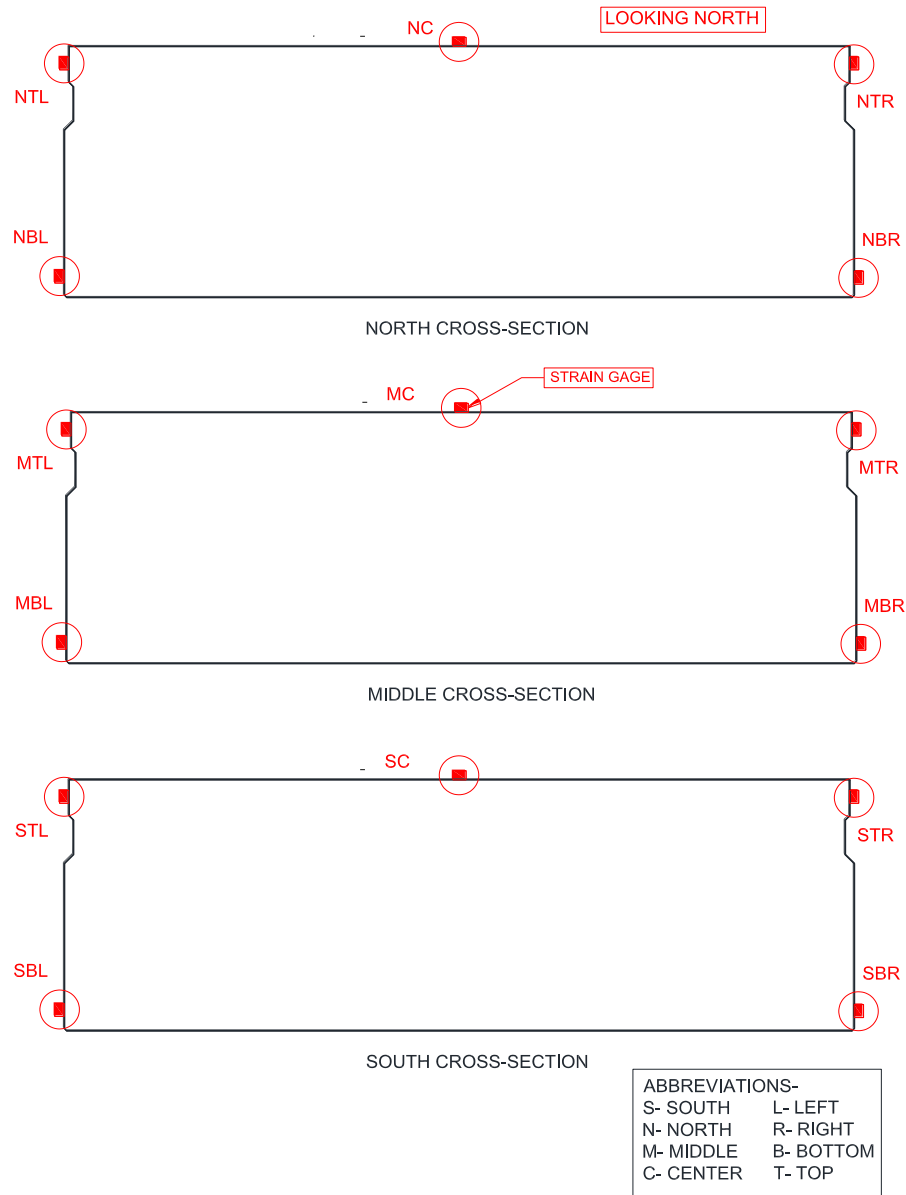


Figure 15. Strain gages layout used for backhoes lift/move

Figure 16 shows the strain gages mounted on the beam and data collection system that was used to record the strain during the beam move. All externally mounted gages had an effective gage length of 3-in.



Figure 16. Installed strain gage and data collection system for lift/move

To facilitate placing the beams, a temporary bridge was constructed over the creek by placing steel girders across the creek and placing timber deck panels over the girders to make a traversable surface. As shown in Figure 17a, the two backhoes lifted the beam using preinstalled lifting loops. After the beams were lifted, the backhoes moved the beams from where they were placed towards the creek by slowly tracking together in a coordinated fashion. Figure 17b shows one backhoe crossing the creek over the temporary bridge. Figure 18 shows four beams that had been placed on the concrete abutments while Figure 19 shows the fifth beam being moved to its designed location.

The lifting loops were cut off 2 in. below the top surface of the beams and the recessed area was filled with a grout material. The keyway between adjacent beams was filled with non-shrink grout and cured following the manufacturer recommendations. Backer rod was inserted

along the bottom of the joint to seal the joint. Galvanized rods were used to complete the transverse tie assembly mentioned previously. These 1 in. rods were tightened to a snug fit condition. Following “tightening” the pockets that received the transverse tie bar on the outside were filled with grout.



a) Beam lift



b) Beam move over the creek

Figure 17. Beam launching using backhoes



Figure 18. Four beams placed over the creek on the concrete abutments



Figure 19. Fifth beam being moved to its position using backhoe

2.4 Bridge Evaluation

2.4.1 Tow truck pull test results

During the lifting/pulling of the beam attempt, internal strain data were recorded. Figure 20 shows the strains from the three internal gages on top at mid-span (i.e., C1, C2 and C3 in Figure 9). The micro-strain values in Figure 20 are shown against time. Initially, an attempt was made to slide the beam without lifting it. However, while applying the pulling force, the front wheels of the tow truck lifted off the ground several inches. As a result, the pulling was stopped there. The strain values for this pull are shown around the 500 seconds time. Another attempt was then made to pull the beam after the truck was positioned on more solid ground. This attempt also caused lifting of the front of the truck. This attempt was between 1500 to 2000 seconds from the start of the test.

After the unsuccessful attempts at pulling the beam, it was decided to try to simply lift one end of the beam by applying a vertical force at one end. All the three gages reached their peak values during this activity which occurred between 2000 to 4000 seconds. Lifting of the beam resulted in positive bending (compression on top and tension at bottom).

Figure 21 shows the strain history of the bottom internal mid-span gage (C5 shown in Figure 9) with time. Similar to the top gages history, the bottom gage also reached peak strain values during the time when the beam was raised.

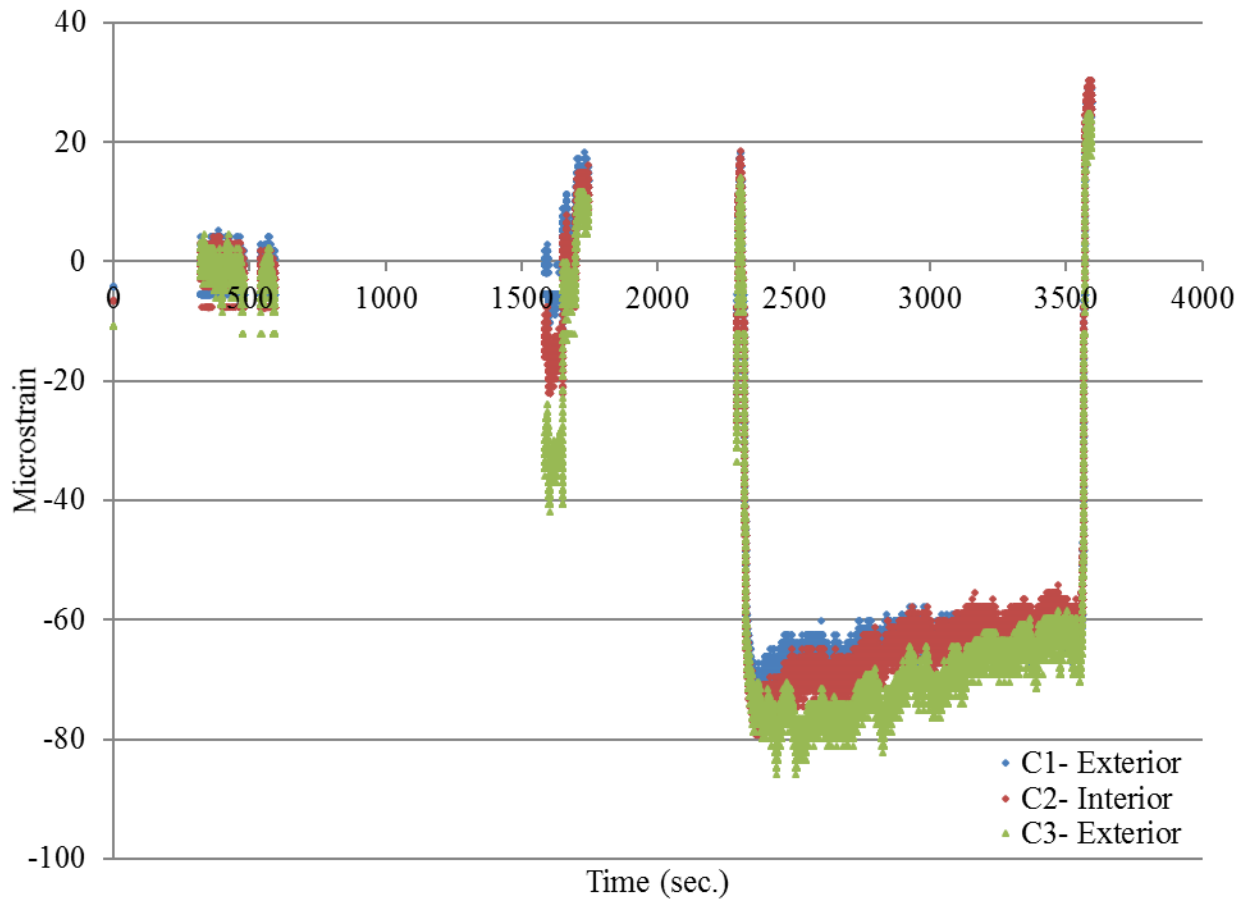


Figure 20. Typical top bar strain history (cross-section C top gages)

Table 4 shows the peak strain values for the top three and bottom three longitudinal bars at each instrumentation cross-section (i.e. A, B, C, D and E in Figure 9b). During the combined lifting/pulling attempts, a horizontal force was introduced into the beam that induced some additional tensile axial strain in the beam. This behavior resulted in larger tensile strains.

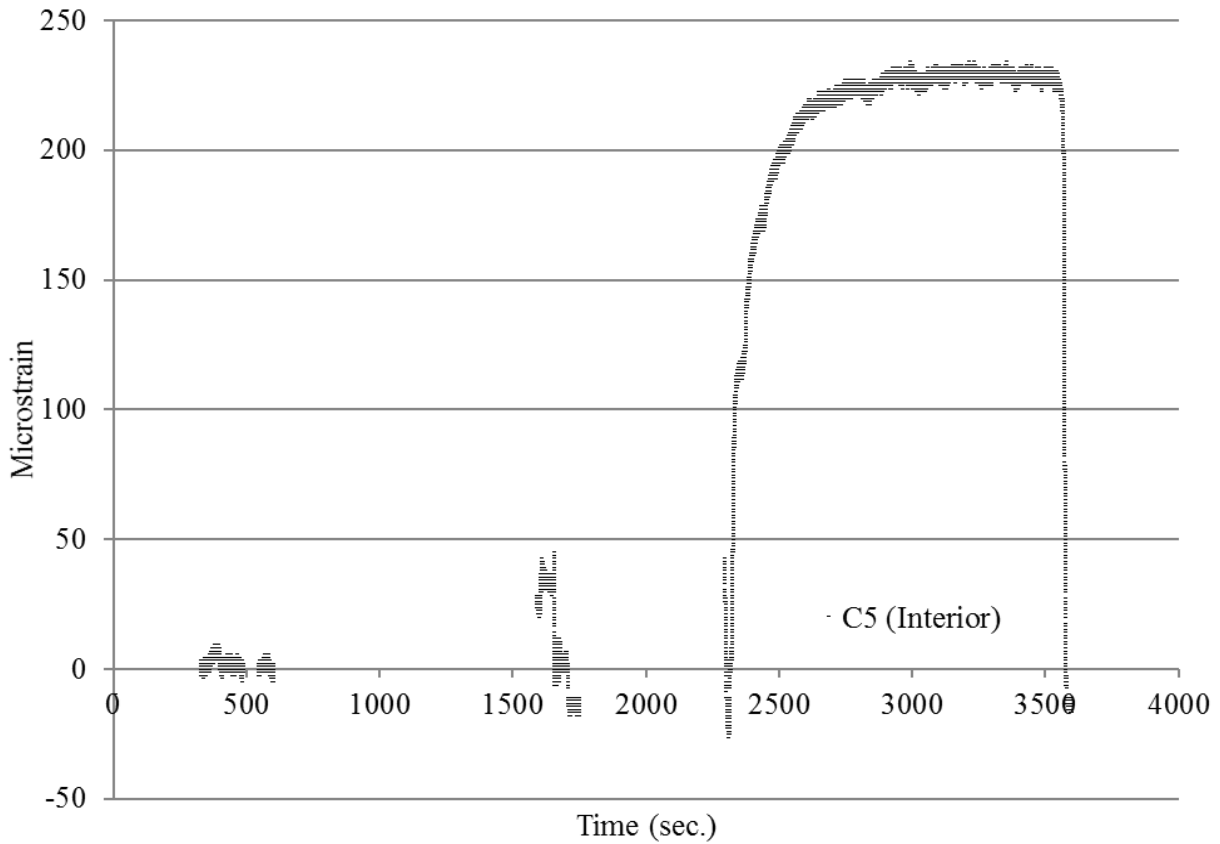


Figure 21. Typical bottom bar strain history (cross-section C bottom gage)

Location→	A	B	C	D	E
Bar↓					
Top	-35	-90	-80	-80	-30
Bottom	45	115	225	100	25

Table 4. Peak micro-strain values in longitudinal bar

In addition to the instrumentation on the longitudinal bars, one strain gage was installed on top of the horizontal pulling loop. Figure 22 shows the micro-strain values over time for the horizontal pulling loops that was used to lift the beam by the tow truck. The peak value in this case is over 10000 micro-strain due to the compression caused by the bending of the loop.

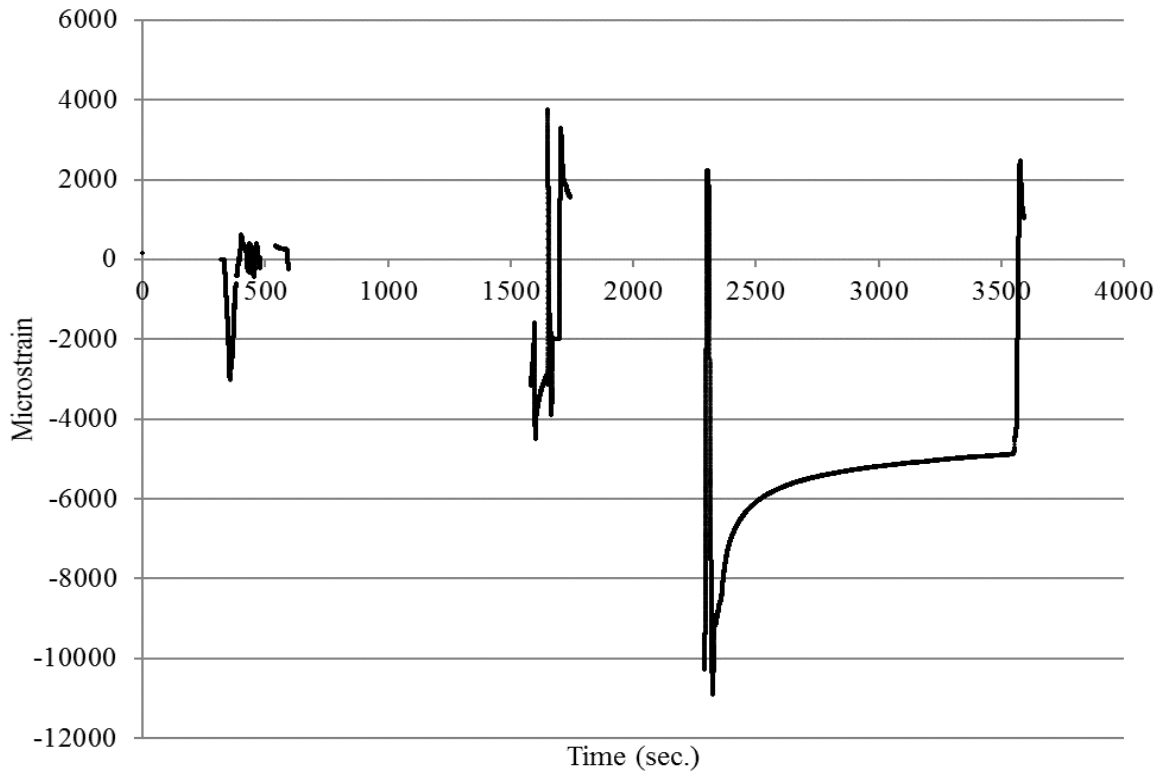


Figure 22. Horizontal pulling loop strain

As a result of the high strain in the lifting loops, cracking and spalling of concrete, coupled with the fact that the tow truck couldn't actually move the beam, hopes of using a tow truck to launch the beams seemed unlikely. However, as mentioned previously the spirit of the project was maintained by restricting the types of heavy construction equipment that could be used to construct the actual bridge. Specifically, it was envisioned that a county or small bridge contractor might not have a high capacity vertical crane available to place the beams. And, since the intent of this project was to demonstrate a bridge system that could be constructed by county forces, it was decided that the means and methods used to place the beams be determined by the bridge contractor.

2.4.2 Backhoe lift/move test results

As was previously mentioned, the contractor elected to use a pair of backhoes to lift, move, and place the bridge beams. Figure 23 shows the strain history for the external south cross-section gages (shown in Figure 15) during this process. It can be seen that the beam was placed into positive bending when initially lifted and that for the majority of the process, the strain magnitudes remained relatively constant. However, at just before 800 seconds following data collection initiation, it can be seen that a rapid strain change occurred.

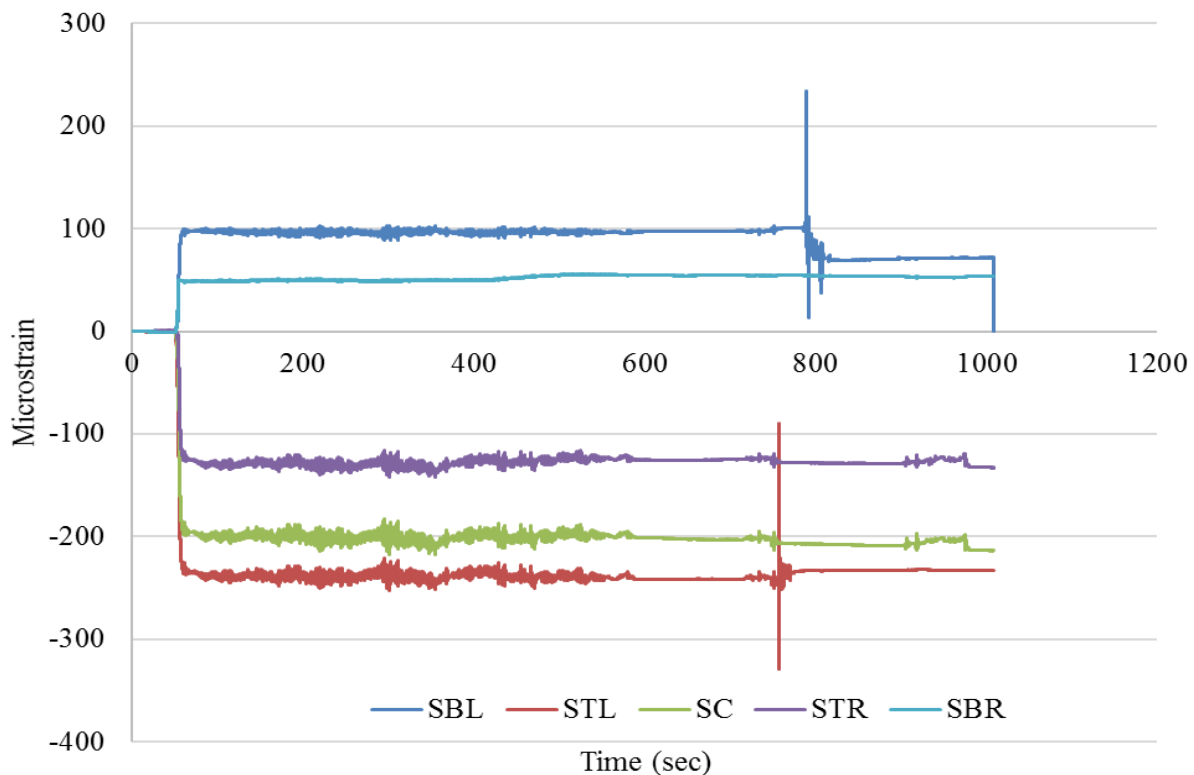


Figure 23. Strain history for south cross-section

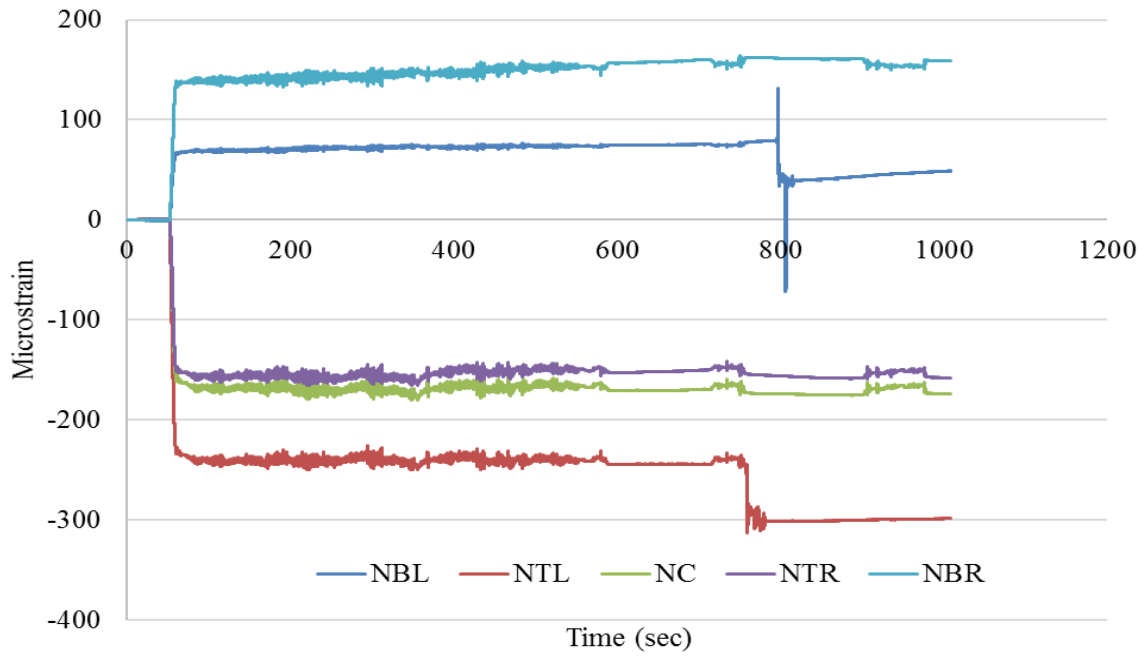


Figure 24. Strain history for north cross-section

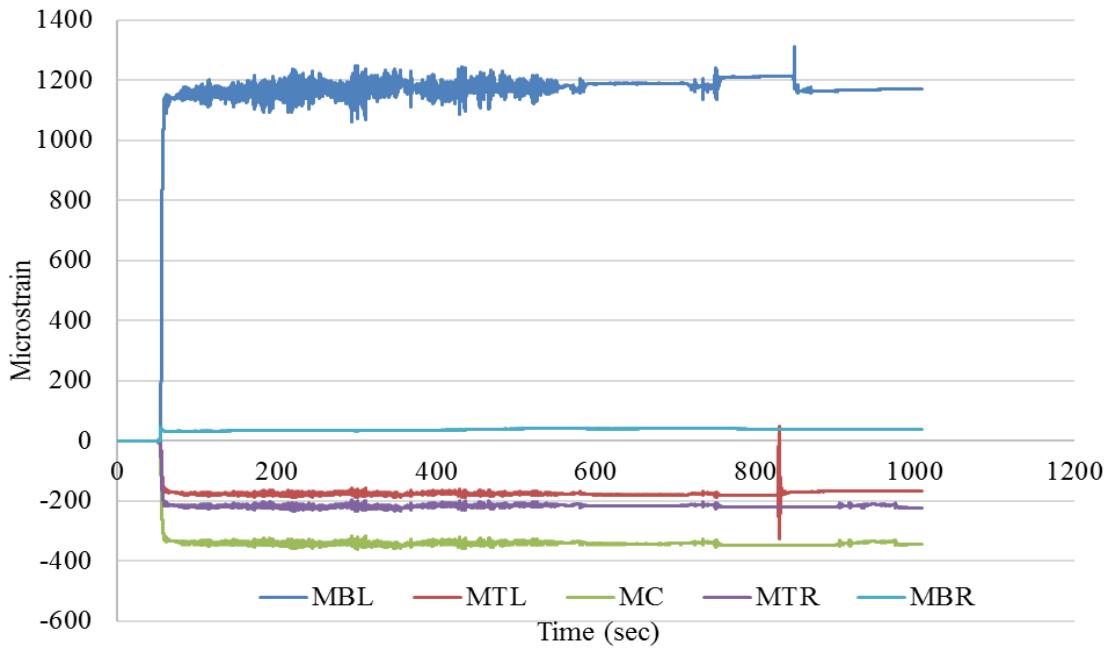


Figure 25. Strain history for middle cross-section

2.4.3 Load Test

After the construction of the bridge, testing of the bridge was carried out, annually, for three consecutive years (2014, 2015 and 2016) through load tests. For the load tests, the bridge beams were instrumented with externally mounted strains gages. Following instrumentation installation a loaded truck was driving over the bridge while recording the data from the gages. Figure 26 shows the different load cases that were used for the tests. In this figure the transverse location of the truck is shown.

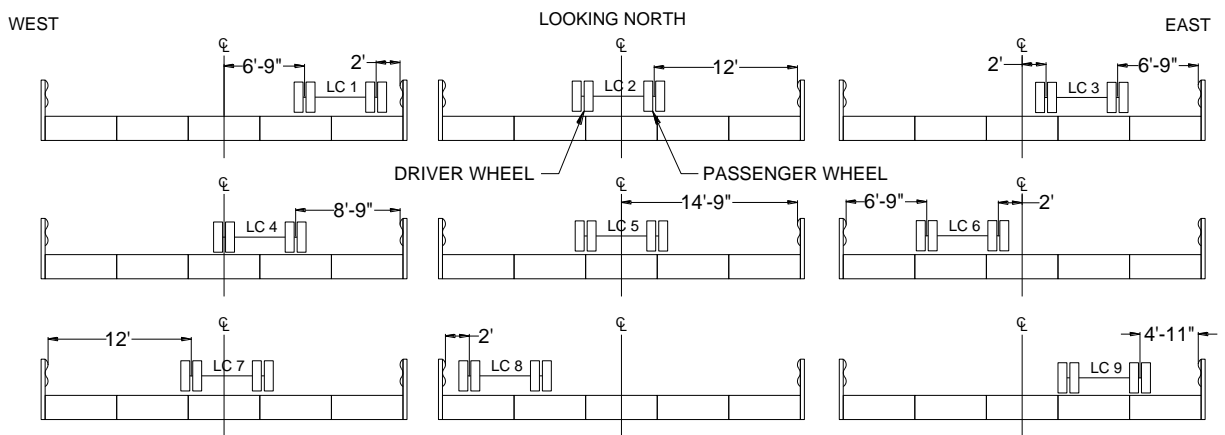


Figure 26. Load cases

Figure 27 shows the instrumentation layout and nomenclature for the same. Gages were installed on the beams to record the longitudinal strain in the beams and deflection transducers were installed to measure the relative displacement in between adjacent beams.

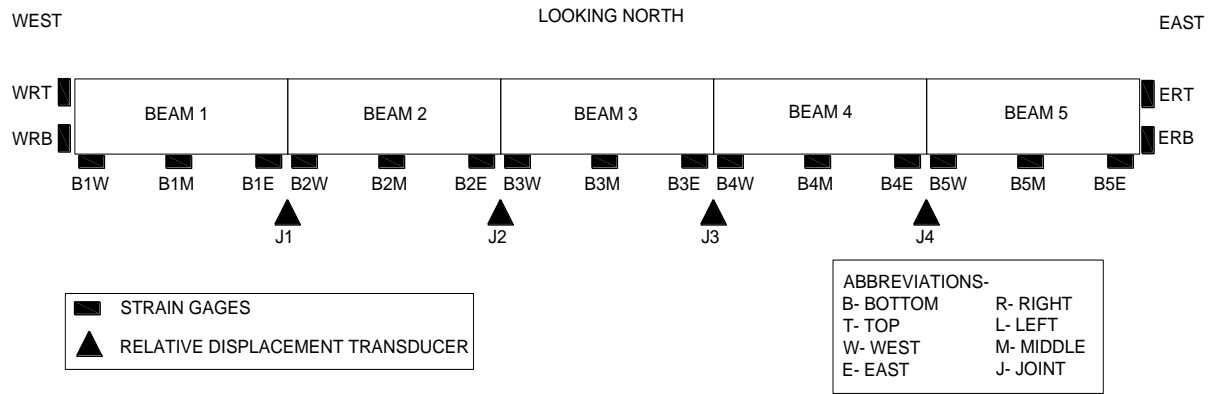


Figure 27. Instrumentation layout and nomenclature

Figure 28 shows the bridge after all external instrumentation had been installed. Figure 29 shows a close-up view of the relative displacement gage setup that was used to monitor for relative moment between adjacent beams.



Figure 28. Instrumentation mounted on the bridge



Figure 29. Relative displacement gage setup

Figure 30 shows the loaded tandem axle dump truck being guided across the bridge in a pre-designated truck position. For each load case, the truck was slowly driven (approximately 3mph) from one end to other while keeping the truck in a consistent transverse position.



Figure 30. Carrying out the load test on the bridge

2.4.3.1 Load test results

In general, the strain history from the load tests from all three years showed similar pattern. To simplify the analysis the test results were normalized to the weight of the truck used for the first load test (gross weight = 52,360 lbs.).

Figure 31 shows the strain distribution for Load Case 1 (LC-1) for all three years. The x-axis on the graph in the figure represents the strain gages from left (west) to right (east) when looking north. This figure shows the higher level of strains near the truck wheel locations. The B3E gage for year 2016 malfunctioned. The peak value in this case was 140 micro strain for year 2015, which is close to the tensile cracking strain of the concrete, indicating that there could have been a new or preexisting crack under the strain gage.

Figure 32 shows the strain distribution at mid-span for LC-5 in which the truck is centered laterally on the bridge. Similar to LC-1, the strain values under the truck location are higher compared to the other locations. The measured strains with the truck in this position are, as expected, lower than when the truck was not centrally placed with the highest strain value measured to be around 83 micro strain in 2015.

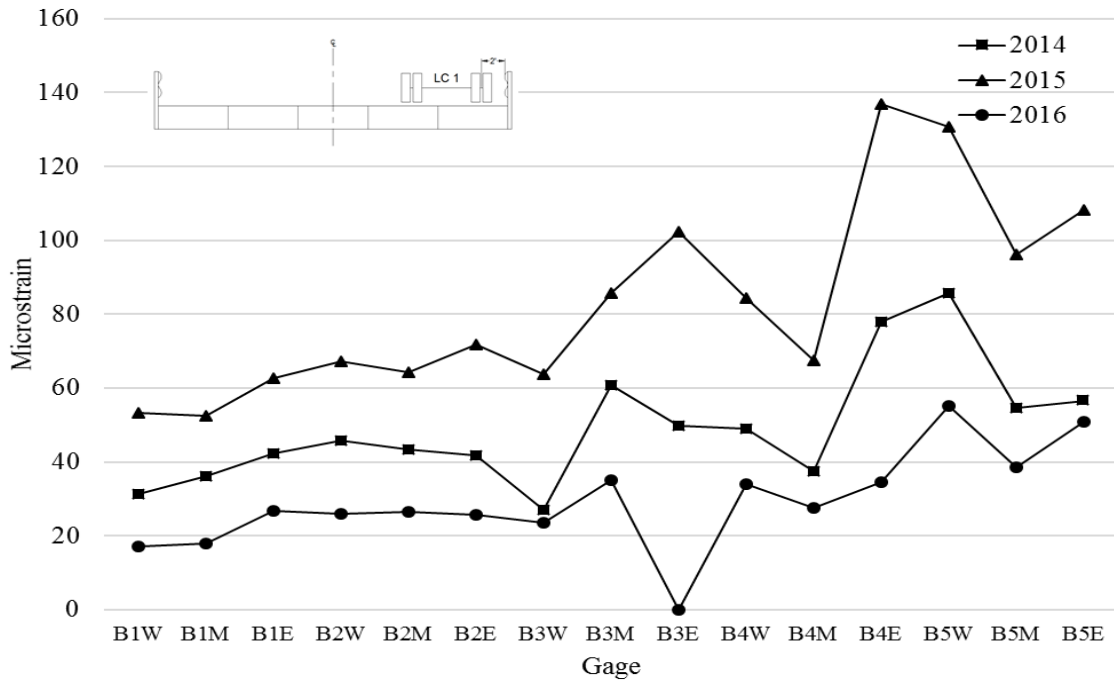


Figure 31. Longitudinal strain distribution over the transverse mid-span (LC-1)

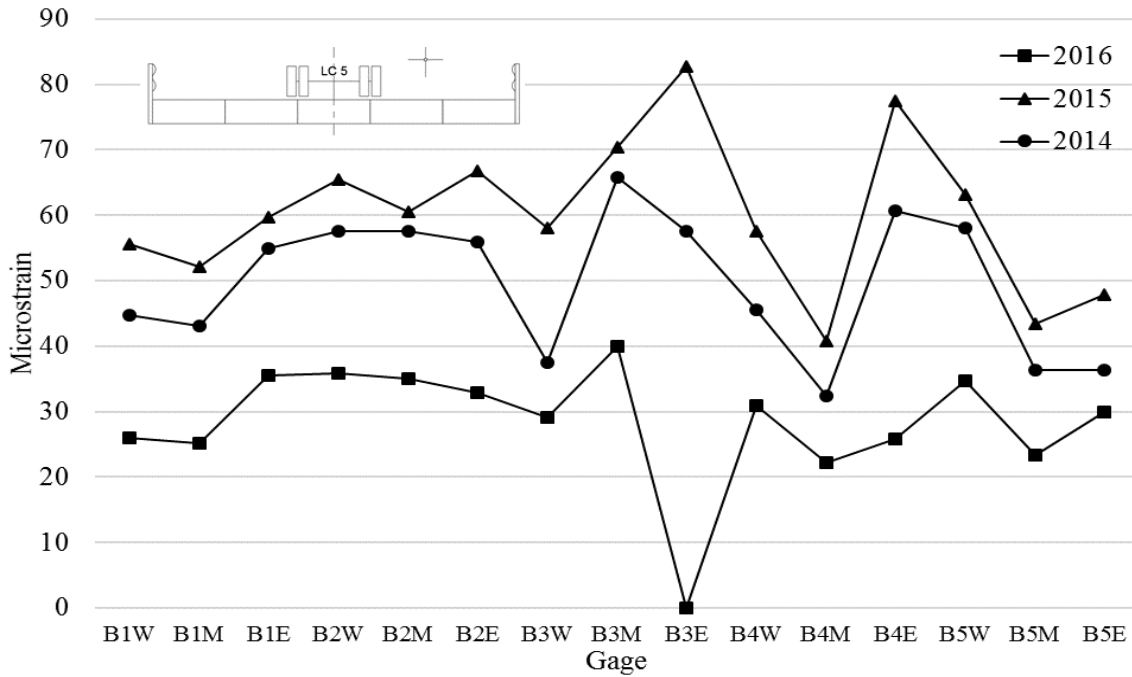


Figure 32. Longitudinal strain distribution over the transverse mid-span (LC-5)

Figure 33 shows the strain distribution at mid-span for LC-8 when the truck was driven very close to the west curb. The peak strain in this case was 90 micro strains.

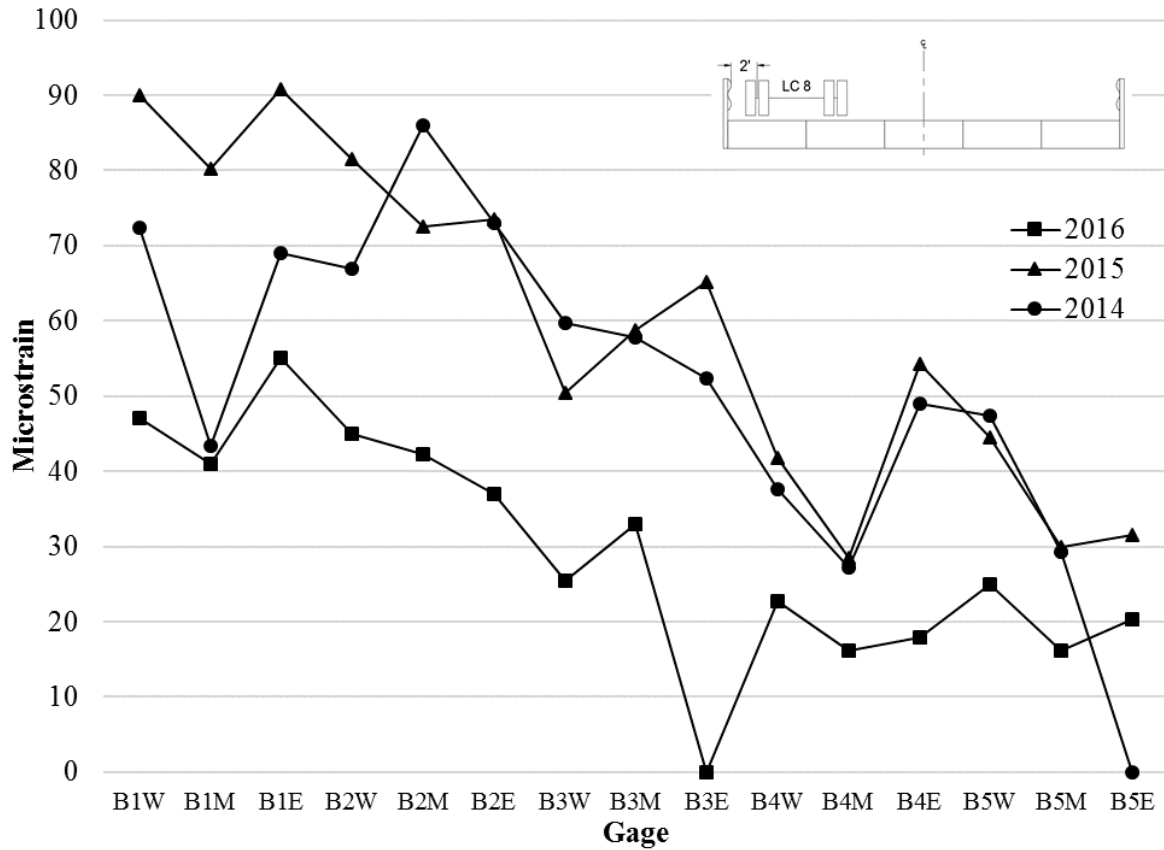


Figure 33. Longitudinal strain distribution over the transverse mid-span (LC-8)

Figure 34 shows the history of strain gages (B1E and B2W) mounted near joint J1 for LC-6. The peak strain value is reached when the truck is above strain gages i.e. mid-span.

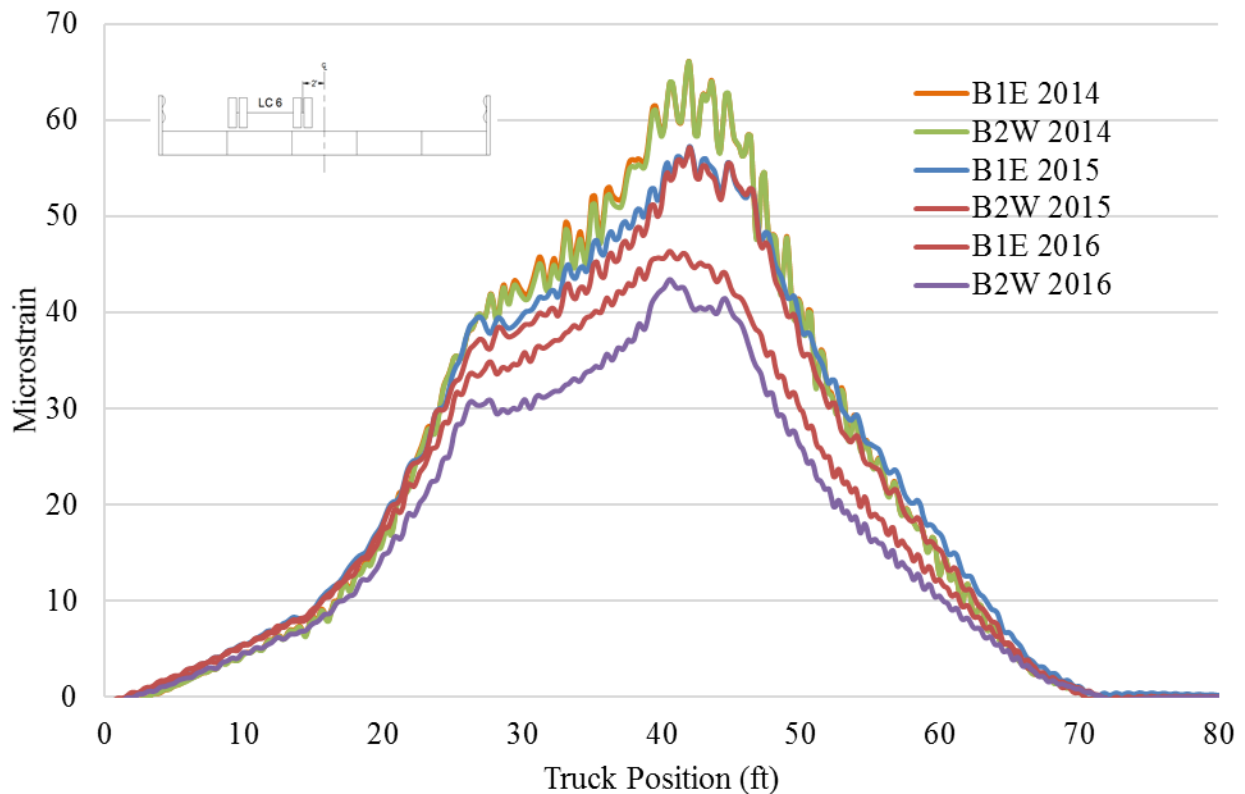


Figure 34. History of the strain gages by J1 (LC-6)

Figure 35 shows the history of strain gages (B4E and B5W) mounted near joint J4 in between for LC-3. Similar to the case of J1, LC-3 was used to determine peak strains for J4. From the strain history for these gages in Figure 34 and Figure 35, there is no significant difference in strain values and the peak strain values are low.

Figure 36 shows the history of relative displacement between Beam 1 and Beam 2 at joint J1 for LC-6 for all three years. From this history, it can be seen that, the relative displacement transducer for the year 2016 failed. The peak relative displacement value was around 0.00002 in., which is significantly small.

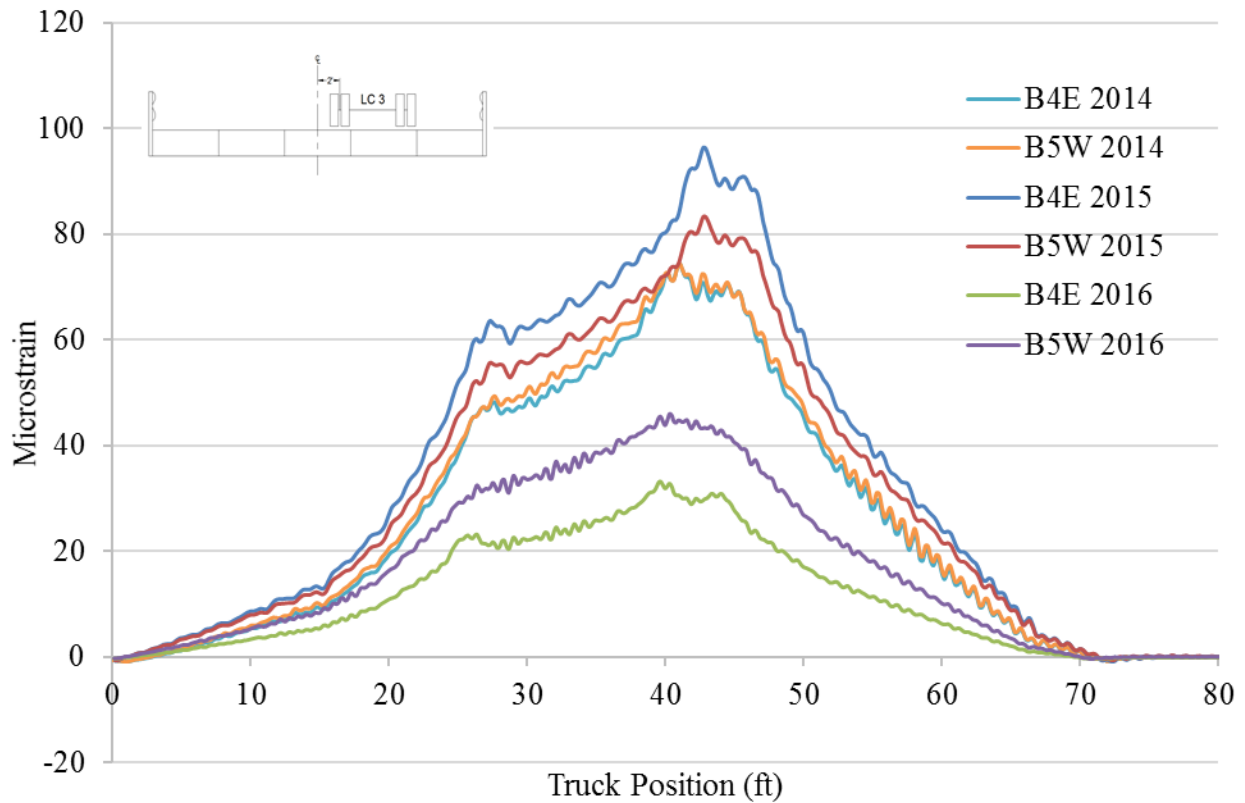


Figure 35. History of the strain gages by J4 (LC-3)

Similarly, Figure 37, Figure 38 and Figure 39 show the relative displacement at the joints J2 (LC-6), J3 (LC-9) and J4 (LC-3) respectively. These figures show the various patterns followed by the relative displacement transducers. The highest relative displacement was -0.0004 for J3 (LC-9) for the year 2014. The year 2016 load test had the least relative displacement compared to other two years. Relative displacement history of J3 for year 2014 is not shown because the transducer for it malfunctioned.

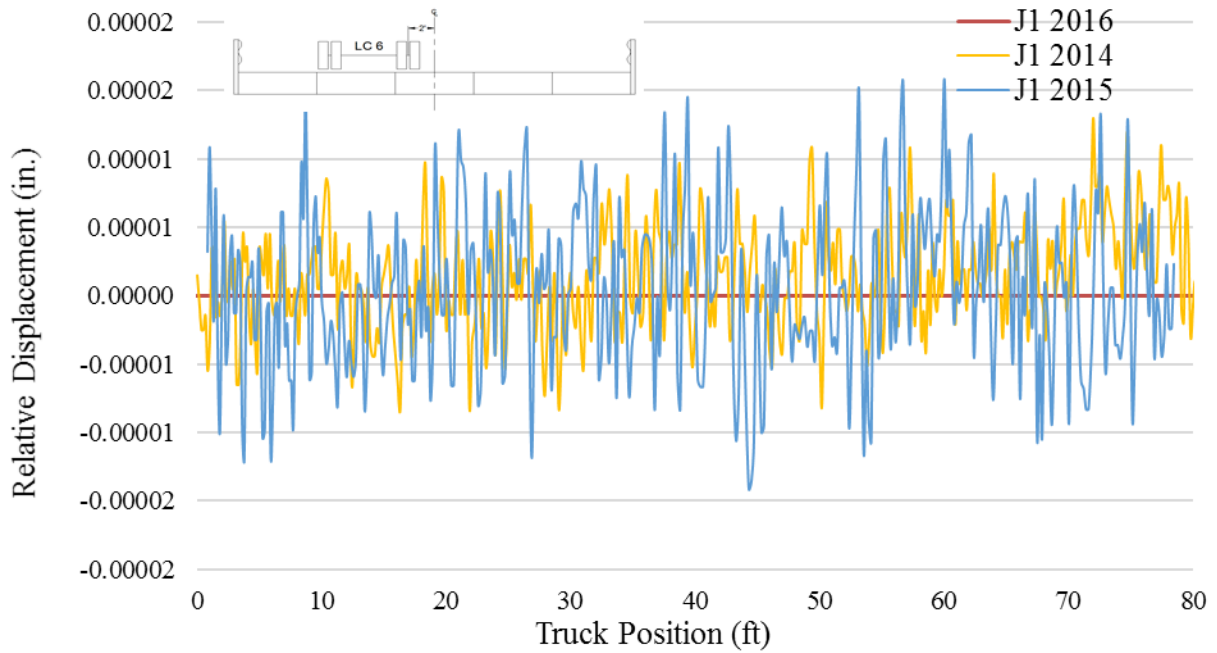


Figure 36. History of relative displacement at J1 (LC-6)

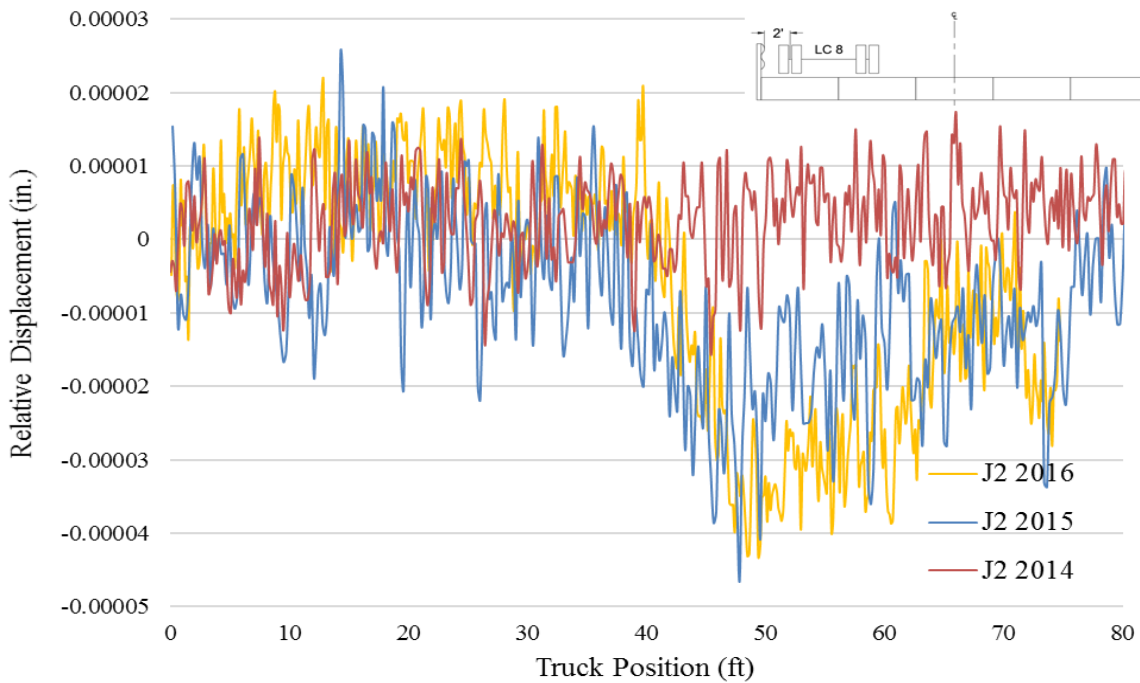


Figure 37. History of relative displacement at J2 (LC-8)

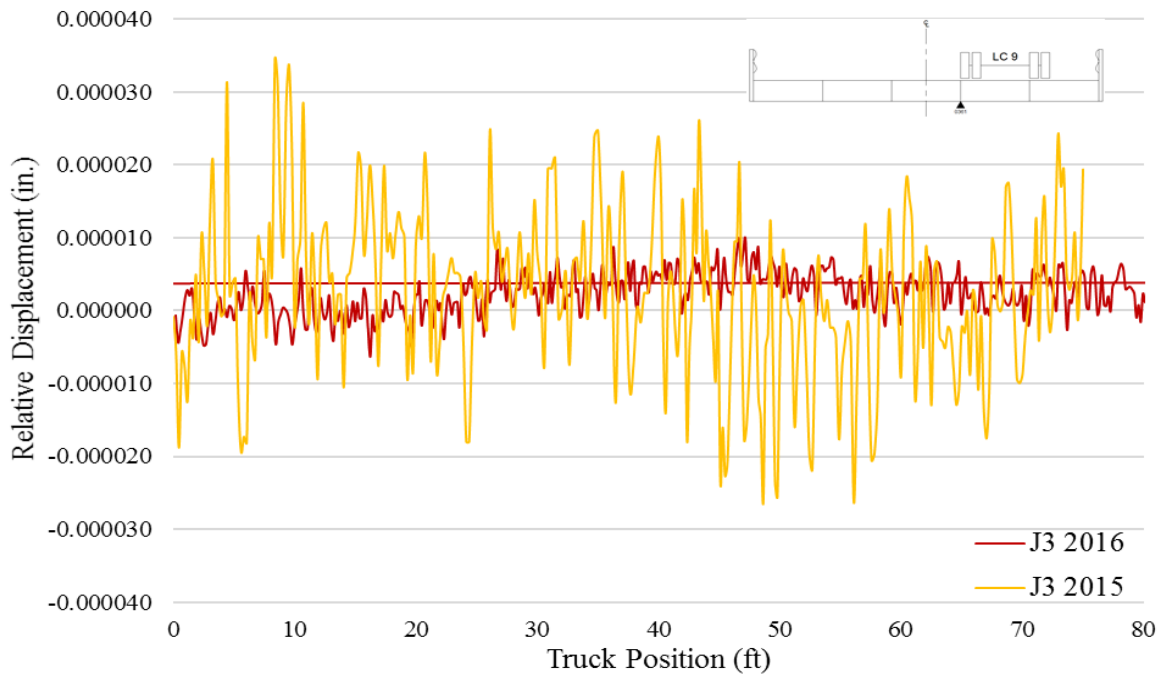


Figure 38. History of relative displacement at J3 (LC-9)

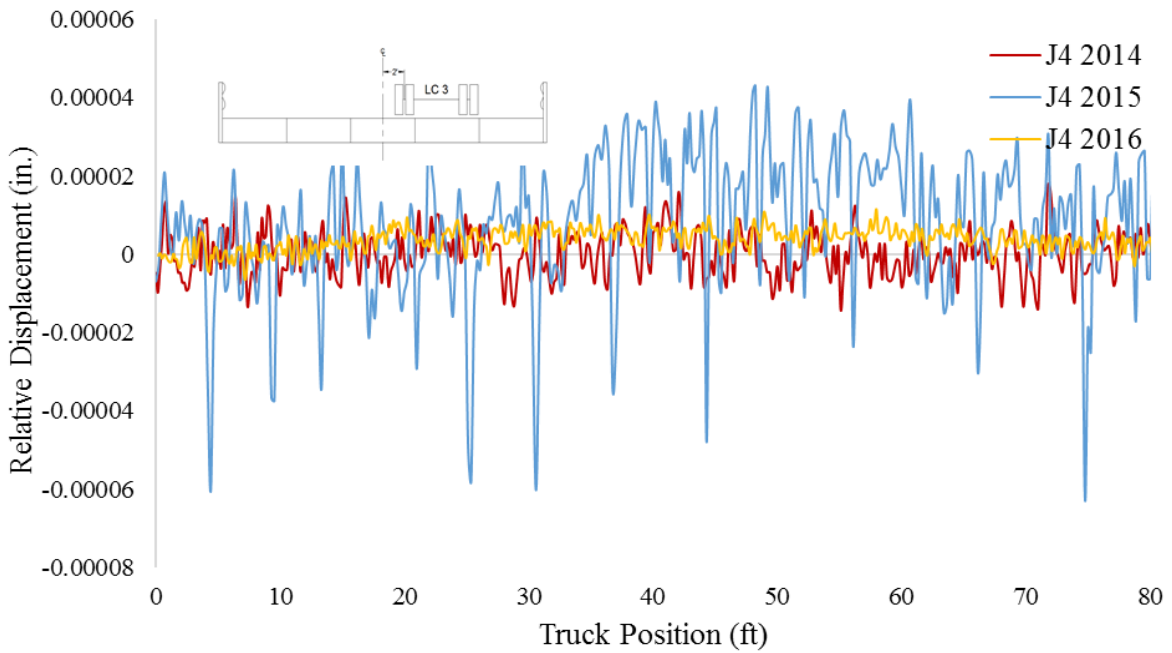


Figure 39. History of relative displacement at J4 (LC-3)

CHAPTER 3. INVESTIGATION OF TECHNIQUES FOR ACCELERATING THE CONSTRUCTION OF BRIDGE DECK OVERLAYS

3.1 Introduction

Due to exposure to extreme environmental conditions, heavy-truck wheel loadings, and deicing salts that corrode reinforcement, bridge decks are subject to the most severe conditions of all bridge components. This usually results in deck service lives being less than the other major bridge components.

Rehabilitating damaged deck slab concrete with an overlay system can significantly increase the life of the reinforced concrete bridge deck and thus reducing the costs of constructing a new bridge (Ramey and Oliver 1998). Published literature reveals that many states use overlay systems to prolong bridge decks service lives.

Generally, the Iowa Department of Transportation (DOT) uses high-performance concrete (HPC) Class HPC-O or Class O concrete for overlay construction. For the bridge to be open to traffic after overlay construction, the overlay concrete must reach a flexural strength of 400 psi. HPC-O concrete generally takes about three days to reach the required strength.

The Ohio DOT (ODOT) Office of Materials and Management Cement and Concrete Section reported that CTS Cement Rapid Set mixes are able to achieve the flexural strength of 400 psi in just two hours (Ohio DOT 2007). Part of this project was to identify if any other types of concrete mixes could reduce the curing time by a marked amount.

One of the major concerns about the construction of an overlay is the time it takes to open the bridge to traffic. As with other construction activities, attempts to minimize construction time must not compromise the structural soundness or longevity of the bridge. However, reducing the construction time could have a great effect on reducing societal costs and inconvenience to travelers. In this research, various ways of accelerating the construction of overlays were investigated.

Additionally, according to standard practice for overlay construction in Iowa, during removal of existing concrete, if more than half of the reinforcing steel bar becomes exposed, additional concrete needs to be removed so that the entire bar is exposed (Iowa DOT 2012). This process of removing additional, possibly sound, existing concrete material can be a significant part of the construction process, particularly if the work is completed using handheld tools. Although this concrete removal approach has resulted in satisfactory performance for many years, questions exist as to how, when, and why this requirement was enacted.

Thus, questions remain regarding how much removal is actually needed while still maintaining adequate structural stability. Answers are particularly important if hydrodemolition is utilized to remove the deteriorated material, because hydrodemolition equipment can usually be “dialed in” to remove quite precise depths of concrete.

3.1.1 Objective and approach

The primary objective of this project is to accelerate the construction of bridge deck overlays. This objective is divided into three parts as follows:

1. Investigation into faster curing concrete alternatives for overlays

The time required to cure traditional concrete is one aspect of the construction process that requires a notable amount of time. Current practice in Iowa requires three days of curing for HPC-O concrete. However, new types of concrete have been introduced that require far less curing time. Therefore, an investigation of other concrete mixes was completed by studying the available literature.

2. Observation of the overlay construction process to identify any opportunities for reducing construction time

In this activity, an ongoing overlay project was observed and documented. Throughout construction, the process was carefully observed and the time required for each process was noted. The goal of these observations was to identify if there were opportunities for increased efficiency. The intent was not to suggest that changes or mandates to contractor's means and methods should be made.

3. Laboratory testing to determine the required amount of existing concrete that must be removed

Removal of the substrate concrete to replace it with new overlay concrete requires a significant amount of time in the construction of an overlay. The standard practice in Iowa requires the contractor to remove the deteriorated substrate concrete, but if the removal depth exceeds half the diameter of the reinforcing bar, it is required that the contractor remove the concrete to 0.5 to 1 in. below the bar. To investigate the efficacy of this practice, laboratory testing was completed to determine the relationship between removal depth and the bond between the substrate concrete and the new overlay concrete.

3.2 Description of Different Types of Overlay Concrete Mixes

3.2.1 Class O Portland Cement Concrete

The Iowa DOT currently uses Class O Portland cement concrete (PCC) as an overlay concrete to replace the unsound, top-of-deck concrete during overlay construction. The water-to-cement (w/c) ratio is intended to be controlled by the slump specified when these mixtures are used. A water-reducing agent is typically required for this mix. Class O mixes require coarse aggregate specifically intended for repair and overlay.

3.2.2 Class HPC-O High Performance Concrete

Class HPC-O is also a highly used overlay concrete by the Iowa DOT for bridge deck overlay construction (Iowa DOT 2012). HPC is a concrete mix proportion that has been designed to provide several benefits that cannot always be achieved routinely using conventional ingredients, normal mixing, and normal curing practices.

HPC possesses high durability and high strength when compared to conventional concrete. This concrete contains one or more cementitious materials, such as fly ash, silica fume, or ground granulated blast furnace slag, and usually a super plasticizer. The use of some mineral and chemical admixtures like silica fume and super plasticizer enhance the strength, durability, and workability qualities to a very high extent. The maximum w/c ratio is 0.42 and, just like Class O mix, Class HPC-O mix is also specified as low slump concrete for overlay construction (Iowa DOT 2012).

Table 5 lists various HPC mix properties.

Curing

The Iowa DOT *Standard Specifications for Highway and Bridge Construction* include the following curing instructions: Allow the surface to cure using wet burlap for at least 72 hours. The burlap should be wet at all times by means of an automatic sprinkling or wetting system. When Class HPC-O is used on projects with a deck overlay quantity greater than 1,800 square yards (1500 m²), allow the surface to cure for 168 hours (Iowa DOT 2012).

Table 5. Properties of HPC concrete mix

Property	Value	Curing time
Traffic return time	72 hrs	72 hrs
Compressive strength (psi)	3000	as little as 3 hrs
	up to 10,000	28 days
Flexural strength (psi)	300	as little as 3 hrs
	1000	28 days
Permeability (coulombs)	500-2000	
Chloride penetration	less than 0.07% Cl at 6 months	
Modulus of elasticity (psi)	5800000	
Abrasion resistance	0-1mm depth of wear	
Absorption	2% to 5%	
Freeze-thaw resistance (durability factor for 300 to 1000 cycles)	95 to 100	
Cost (\$/yd ³)	119	

Source: Kosmatka et al. 2003

3.2.3 CTS Cement Rapid Set Low-P mixes

CTS Cement launched a cement product called Rapid Set Low-P, that, when incorporated into a concrete, provides very low permeability, high durability, and corrosion resistance. These attributes are highly desirable for structural repairs and bonded overlays in exterior and harsh

environments. Low-permeability concrete inhibits the passage of salt solution through the concrete, which in turn results in less corrosion of the internal reinforcing steel. Rapid Set Low-P Cement requires the addition of aggregates, water and, in some cases, a retarder such as citric acid. (CTS Cement 2016)

Due to the fast setting nature of Rapid Set Low-P cement, tensile strength development occurs very rapidly. This shortens the amount of time that vibrations from adjacent traffic lanes can be a factor in early-age stress cracking in the concrete.

Table 6 lists CTS Cement Rapid Set Low-P mix properties.

Other advantages (CTS Cement 2014):

- Single component cement – just add water and aggregates
- Provides corrosion protection
- High sulfate resistance
- Easy to place, high slump, non-segregating formula
- Hydraulic cement based formula – provides excellent long-life durability

Table 6. Properties of CTS Cement Rapid Set Low-P mixes

Property	Value	Curing time
Traffic return time	4 hrs	4 hrs
Compressive strength (psi)	4000-4500	3 hrs
	5000-6000	6 hrs
	8000-9000	28 days
Tensile bond strength (psi)	200-250	24 hrs
	600	7 days
	700	28 days
Slant shear bond strength (psi)	1200	24 hrs
	1900	7 days
	2200	24 days
Initial set	30 min	
Final set	40 min	

Source: CTS Cement 2014

Curing

The CTS Cement *Rapid Set*[®] *Low-P*[™] *Cement Datasheet* includes the following curing information: For overlays, the surface should be covered promptly after final finishing with a single, clean layer of wet burlap followed by a layer of clear polyethylene film. Patches can be water cured by maintaining a moist sheen on the surface. Curing should continue until the concrete has reached the strength desired. Depending on temperatures and specified strength, this

will usually be within 1 to 3 hours after final finishing. During the entire period, apply more water, as needed, to keep the entire concrete surface continuously wet (CTS Cement 2014).

3.2.4 4×4 Concrete mix

The Iowa DOT specifications for highway and bridge construction state that the overlay concrete needs to reach a minimum flexural strength of 400 psi to re-open the bridge (Iowa DOT 2012). “The name 4×4 concrete originates from a concrete that obtains at least 400 psi of flexural strength within 4 hours of placement... The flexibility of 4×4 concrete is such that it can be modified to meet many different specified strength conditions simply by adjusting the mixture proportions and admixture dosages.” (BASF 2016)

With 4×4 concrete, it is possible to proportion a mixture using locally available Portland cements, aggregates, and selected admixtures. With 4×4 concrete, a synthetic high-range water-reducing admixture is used to provide fluidity and strength, a hydration control admixture is used to provide workability control, and an accelerating admixture provides early strength (Meyers n.d.). Air-entraining admixtures can be used where the concrete has to be air-entrained (BASF 2011).

Smith, Alarcon, and Glauz mention that 4×4 concrete has met all of the technical and performance expectations of the California DOT (Caltrans) highway engineers (Smith et al. 2001). For example, no cracks have been observed four hours after placement of the material.

Table 7 lists 4×4 concrete mix properties.

Table 7. Properties of 4×4 concrete mix

Property	Value	Curing time
Traffic return time	4 hrs	4 hrs
Compressive Strength (psi)	4130	4 hrs
	7740	24 hrs
	8250	28 days
Flexural strength (psi)	480	4 hrs
	855	24 hrs
	1250	28 days

Source: Meyers n.d.

Other advantages (BASF 2011, Meyers n.d., Smith et al. 2001):

- Very user-friendly and easy to place and finish since it can be mixed on site
- Uses portable dispenser system for accelerating admixtures on site
- Exceptional high-early strength permits rapid opening to traffic minimizing lane closures
- No cracks observed 4 hours after placement when a loaded ready mix truck was driven onto the slab
- High abrasion resistance
- Uses DOT-approved admixtures and locally available cement and aggregates
- Mixed and delivered in ready-mixed concrete trucks

Curing

The researchers did not find any printed instructions readily available on curing 4×4 concrete mixes for overlays, but the manager/chief engineer with BASF Admixture Systems replied to our inquiry saying moist curing or curing compounds are used insulating blankets are used to retain heat resulting from the hydration process ((Nmai 2016).

3.2.5 Polyester Polymer Concrete

Polymer concrete is an expensive overlay material that can cost twice as much as conventional PCC and slightly more than latex-modified concrete. However, an increasing number of highway engineers are choosing polymer concrete for concrete bridge deck rehabilitation, finding that its advantages as an overlay material might justify its high cost.

Some benefits of polymer concrete include improvement in abrasion and skid resistance of the deck surface and also protection against corrosion of the internal steel reinforcement. Additionally, it is impermeable to water, deicing salts, and chemicals that can accelerate corrosion.

Polyester concrete is a composite of dry aggregate in an unsaturated or thermoset, polyester resin binder. Certain polymer content, well-graded aggregates, fibers, and coupling agents influence the various properties of polyester polymer concrete. When the liquid resin cures into a hardened, cross-linked state, a polyester concrete is formed.

Maggenti stated that Caltrans' use of polyester polymer concrete for 20 years has been successful and proved to be very effective in terms of durability, crack resistance, chloride ion intrusion resistance, bonding, ease of construction, and lane closure time (Maggenti 2001).

Table 8 lists polyester polymer concrete properties.

Table 8. Properties of polyester polymer concrete

Property	Value	Curing time
Traffic return time	2-4 hrs	2-4 hrs
Compressive strength (psi)	3982	24 hrs
	7000	7 days
	8030	28 days
Flexural strength (psi)	2200	28 days
Tensile strength (psi)	800	28 days
Chloride permeability (coulombs)	0-200	
Modulus of elasticity (psi)	$1 \times 10^6 - 2 \times 10^6$	
Abrasion (mm/year)	4 (8 to 10 times more than PCC)	
Cost (WSDOT- weighted avg \$/sq ft)	10.73	

Sources: Oberoi 2012, Anderson et al. 2013

Curing

The Washington State DOT (WSDOT) Materials Laboratory included the following instructions on curing in a 2013 report: Polyester polymer concrete shall be placed immediately

after the prime coat is applied to the bridge deck. The prime coat shall cure for a minimum of 30 minutes before placing the polyester concrete overlay. After placement, a 30 to 90 minute set time will be produced by implementing initiators. Depending on environmental conditions such as weather, accelerators or inhibitors may be added to the mix to help produce the specified cure time.

Traffic and construction equipment shall not be permitted on the polyester polymer concrete overlay for at least two hours and until the polyester polymer overlay has reached a minimum compressive strength of 3,000 psi as verified by the rebound number determined in accordance with ASTM C805. No vehicles or personnel will be allowed to travel on the finished polyester concrete overlay during the curing process.

The contractor will utilize a Schmidt hammer to determine the proper time to open the roadway to traffic. A 3,000 psi reading on the rebound hammer will be achieved in order to open the roadway to traffic (Anderson et al. 2013).

3.2.6 Very-Early-Strength LMC

Latex-modified concrete (LMC) is a PCC in which an admixture of styrene butadiene latex particles suspended in water is used to replace a portion of the mixing water. LMC has been used on highway bridges for overlay rehabilitation for more than 40 years (Sprinkel 1998).

Compared to concrete without latex, LMC is reported to be more resistant to intrusion of chloride ions, to have higher tensile, compressive, and flexural strength, and to have greater

freeze-thaw resistance. The use of LMC overlays is one of the most popular ways to extend the time to corrosion initiation. The resistance to chloride intrusion is said to be attributable to the lower w/c ratio and a plastic film produced by the latex particles within the concrete (Sprinkel 1998).

Table 9 lists very-early-strength LMC properties.

Table 9. Properties of very-early-strength LMC

Property	Value	Curing time
Traffic return time	3 hrs	3 hrs
Compressive strength (psi)	3000	3 hrs
	4000	6 hrs
	6500	5 days
Chloride permeability (coulombs)	300-1400	28 days
	0-10	1 year
	0-60	9 years
Drying shrinkage (%)	0.02	170
Tensile adhesion bond strength (psi)	153-276	1-6 months
	176-301	9-10 years
Cost (\$/yd ³)	140	

Source: Sprinkel 2011

Curing

The overlay is to be quickly covered with wet burlap and polyethylene to provide a moist environment during the three-hour curing period (Sprinkel 1998).

3.3 Investigation of Ongoing Overlay Construction Project

The acceleration of the construction of bridge deck overlays may be achieved through management of time, labor, and materials. As part of this research, a team observed a portion of an ongoing overlay construction project to document the time required for different activities and to observe possible activities where construction time could be reduced. It should, again, be noted that the observations and comments are not intended to suggest that changes to contractor's means and methods associated with overlay construction are needed or should be required.

Overlay construction for the bridge on IA 163 over Fourmile Creek, 1.7 miles west of US 65 (FHWA No. 40941, overlay project number BRFN-163-1(87)--39-77), was observed. The bridge was 256 ft long and 56 ft wide. For this research, the team observed overlay construction of only the eastbound lanes. A summary of the team's investigation of the construction activities follows.

3.3.1 Removal of temporary bollards

Temporary bollards were installed on the bridge deck during construction of the westbound overlay. These bollards were installed between the eastbound and westbound lanes to

direct traffic safely. The bollards that were used were bolted to the deck and had to be detached using a hand drill as shown in the Figure 40.



Figure 40. Temporary bollards being detached by workers

It took two hours for 10 workers to remove all of the bollards.

3.3.2 Removal of top 2 to 3 in. layer of deck concrete

After the temporary bollards were removed, a milling machine was lined up with the deck surface and prepared for operation. Preparing the road milling machine took about an hour.

One person operated the machine and four workers watched over the machine and guided the operator. The milled concrete was transferred to a dump truck by a conveyor connected to the milling machine as shown in Figure 41.



Figure 41. Milling machine removal of top layer of the deck

In one pass from one end of the bridge to the other, the milling machine was able to remove about 2 to 3 in. of concrete, so that there would be only 0.5 to 1 in. deep concrete on top of reinforcing steel. The milling required an hour to finish one pass and, once a pass was done, it took 15 to 20 minutes to turn around and start working on the next pass.

After half of the deck was milled, the cutting drum of the road milling machine was changed, which took 30 to 45 minutes. The overall time for the removal of the top layer of concrete was seven hours.

After doing five passes, all of the top layer of concrete on the deck was removed and the residual concrete was cleaned off. Alongside cleaning, the cleaned deck portion was inspected

for unsound and damaged areas, which were marked for more in-depth removal as shown in Figure 42.



Figure 42. Area marked for more in-depth removal

Throughout the removal of the top layer of concrete, three dump trucks were used to take milled concrete from the construction site to the dump site. Even though three trucks were used, many times, after a truck was filled with concrete, a new truck was not ready to continue the road milling machine's operation. Access to the bridge site required long travel times and, as a result, a truck was not yet available at times and the milling operation had to be halted for several minutes. Providing one more dump truck could reduce that downtime.

3.3.3 Placing the compressed air line

Jackhammers were used to further remove the unsound concrete after removal of the top 2 to 3 in. layer. To power the jackhammers along the length of the bridge, a pipeline for compressed air was installed on the outer side of the bridge railings. Five workers were working on the installation of the compressed air pipeline while the top layer of the deck was being removed using the milling machine.

3.3.4 Removal of substrate concrete using jackhammers

The removal of substrate concrete using the jackhammers was completed by nine workers over the course of three days. On the first day, it took an hour to prepare for the task and then removal took about six hours. By the end of second day, all marked, unsound concrete was removed. On the third day, all areas were carefully inspected and marked for additional concrete removal. After the inspection, removal of the marked concrete took place for seven additional hours. Figure 43 shows a worker removing the marked patch of concrete using a jackhammer.

Considering that it took three days for removal of the substrate concrete, utilizing additional workers could lead to shorter completion time. Also, according to standard practice for overlay construction in Iowa, if more than half of the bar becomes exposed during substrate removal, additional sound concrete needs to be removed such that the entire bar is exposed. Considering the large area of concrete needing removal, removing the additional sound concrete around the bar may have taken a significant amount of time.

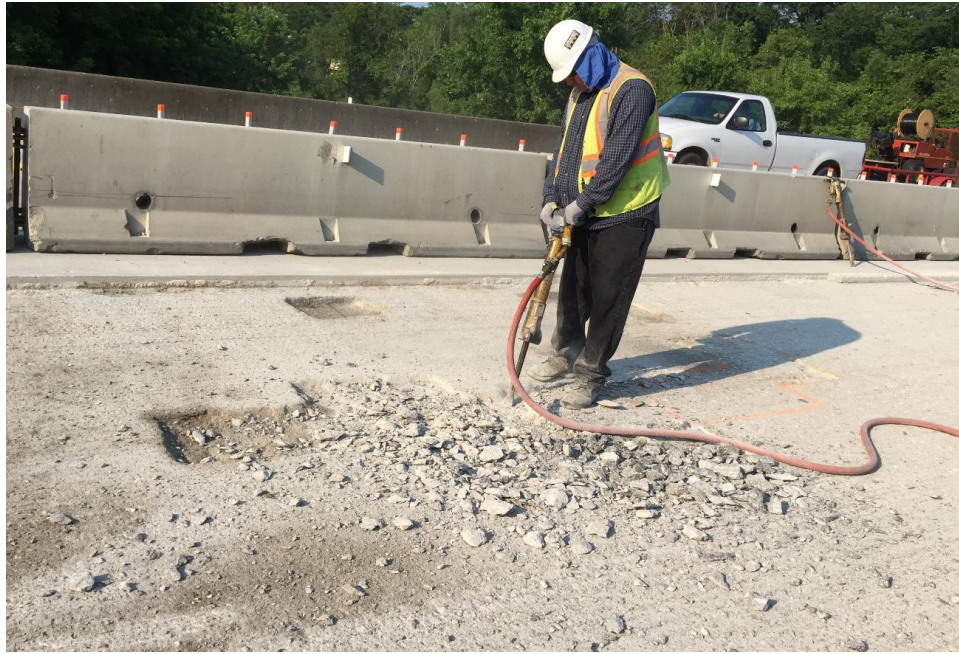


Figure 43. Removal of unsound concrete using jackhammer

On the third day, the deck was inspected for areas where the entire reinforcing steel bar needed to be exposed. According to the contractor, about 30% of the time, the damaged concrete level is between half the diameter to the full diameter of the bar and the workers need to expose the entire reinforcing steel bar. This extra removal may take many hours to complete depending on how deep the deteriorated concrete is and over how much area it extends. In a best case scenario, it may have been possible for the entire third day of concrete removal to have been almost entirely avoided if the deteriorated concrete was just barely below the half diameter point. It seems fair to say that this additional removal may have taken 4 to 8 hours. Figure 44 shows a deteriorated area of deck concrete after removal of the substrate concrete.



Figure 44. Deteriorated area of the deck after removal of the substrate concrete

In this figure, the concrete has been removed below the reinforcing steel for almost the entire area.

3.3.5 Sandblasting the deck

The entire deck was then sandblasted to provide the roughness needed for a proper bond between the concrete and the new overlay concrete. Sandblasting also removed any corrosion on the exposed reinforcing steel. Six people were simultaneously working on the sandblasting process, either operating the sandblasting equipment or cleaning the sand off the deck. Preparing

for sandblasting and sandblasting the whole deck took about nine hours. Two sandblasting crews working on the deck simultaneously would require less time, but would also require more workers.

3.3.6 Overlay concrete placement

Preparatory work for overlay placement took about five hours with ten workers.

Followed by the preparation work, the ready-mixed concrete was placed on the deck as shown in Figure 45.



Figure 45. Ready-mixed concrete being placed on the deck

About 20 workers worked on the overlay placement at the same time. Many tasks were carried out by workers including watching over the overlay concrete for proper placement, operating the machinery, laying wet burlap for curing, moving the machinery and equipment, and scooping extra concrete from one place and dumping it to another place. The whole process took about four hours. The concrete was cured for three days before opening to traffic.

3.3.7 Other observations

During overlay installation on the westbound lanes prior to the research team's observations on the eastbound lanes, a fiber optic cable was found near the bridge. In addition, the contractor found a manhole at the approach to the westbound lanes, which was not shown in the plans, as shown in Figure 46. Although the true impact of these observations on the project schedule are not known, the contractor, when asked, did mention this as an unexpected factor.



Figure 46. Manhole discovered near the approach to the westbound lane

The as-built overlay construction schedule of the eastbound lanes observed by the researchers (64 hours over the course of 7 working days) is shown in **Figure 47**.

The schedule does not show curing time after overlay placement nor the time to actually open the eastbound lanes to traffic.

Removal of the substrate concrete on the deck and along the barrier rail using jackhammers took the most time (33 hours over the course of 4 working days). Based on the above mentioned observation regarding the amount of sound concrete removed below the one-half diameter point, it is possible that 4 to 8 hours may have been saved had this requirement not been in place. In bridges with more extensive areas of deteriorated concrete that is not as “deep,” it is possible that relaxing or eliminating this requirement could have notable time saving implications. Such a reduction could have an impact on the critical path for the entire project.

The contract proposal for the entire bridge deck overlay construction (eastbound and westbound lanes) shows a contract period of 40 working days. During this project, however, the research team only observed the overlay portion of the project, as the goal was to identify areas when traffic mobility was impacted. Collectively, the two most time-consuming operations were old concrete removal and overlay placement. If the rapid set alternatives briefly described in section 3.2 were shown to provide the durability, permeability, abrasion resistance, freeze-thaw resistance, etc. that is needed, and if the additional concrete removal below the one-half bar diameter requirement was eliminated, it seems possible that up to 77 hours of the estimated 136 could have been saved.

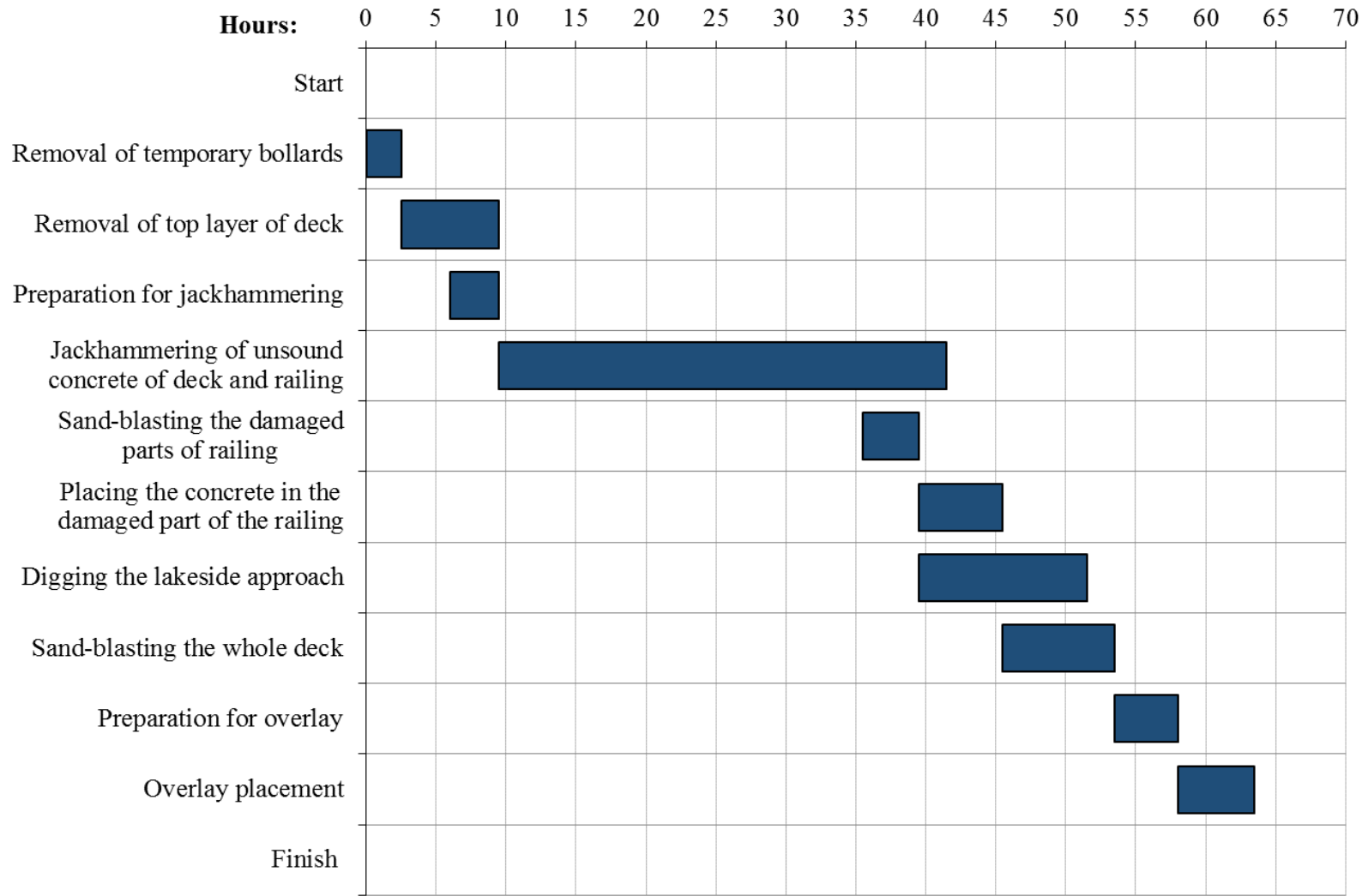


Figure 47. Eastbound overlay construction schedule as observed

3.4. Laboratory Testing

3.4.1 Methodology and study parameters

With this project, one of the approaches investigated for accelerating overlay construction was to determine if the change in depth of overlay concrete affects the bond strength between the substrate concrete and the new overlay concrete. Currently, if the concrete needs to be removed up to half of the diameter of the reinforcing steel, then it is not necessary to remove it any further; but, if there is a need to remove the concrete any deeper than half the diameter of the reinforcing steel, it is removed to expose all of the bar plus an extra 0.5 to 1 in. of concrete. This need for extra removal takes extra construction time.

Four different cases of reinforcing steel exposure were considered in four tests so that, the bond strength between the substrate and the overlay concrete could be studied. Three specimens were tested for every removal depth level.

The following four cases of removal depth levels were considered, as also shown in Figure 48.

Case 1. Concrete removed down to the upper surface of the reinforcing steel

In this case, the substrate concrete was removed down to the top surface of the reinforcing steel so that there would be virtually no exposure of the reinforcing steel to the new overlay concrete.

Case 2. Concrete removed down to half the diameter of the reinforcing steel

The substrate concrete was removed up to half the diameter of the reinforcing steel leaving the top half of the reinforcing steel exposed to the new overlay concrete.

Case 3. Concrete removed down to the full diameter of the reinforcing steel

In this third case, the substrate concrete was removed to the bottom of the reinforcing steel, so that the entire diameter of the reinforcing bar would be exposed to the new overlay concrete.

Case 4. Concrete removed down to the full diameter of the reinforcing steel plus an additional 0.5 to 1 in. below it

To get deeper, an additional 0.5 to 1 in. concrete was removed in addition to the full bar exposure condition.

For these four different cases of removal depth, the bond between the substrate concrete and the new overlay concrete was evaluated using four different tests:

- Pull-off test
- Push-out test
- Positive bending flexural test
- Negative bending flexural test

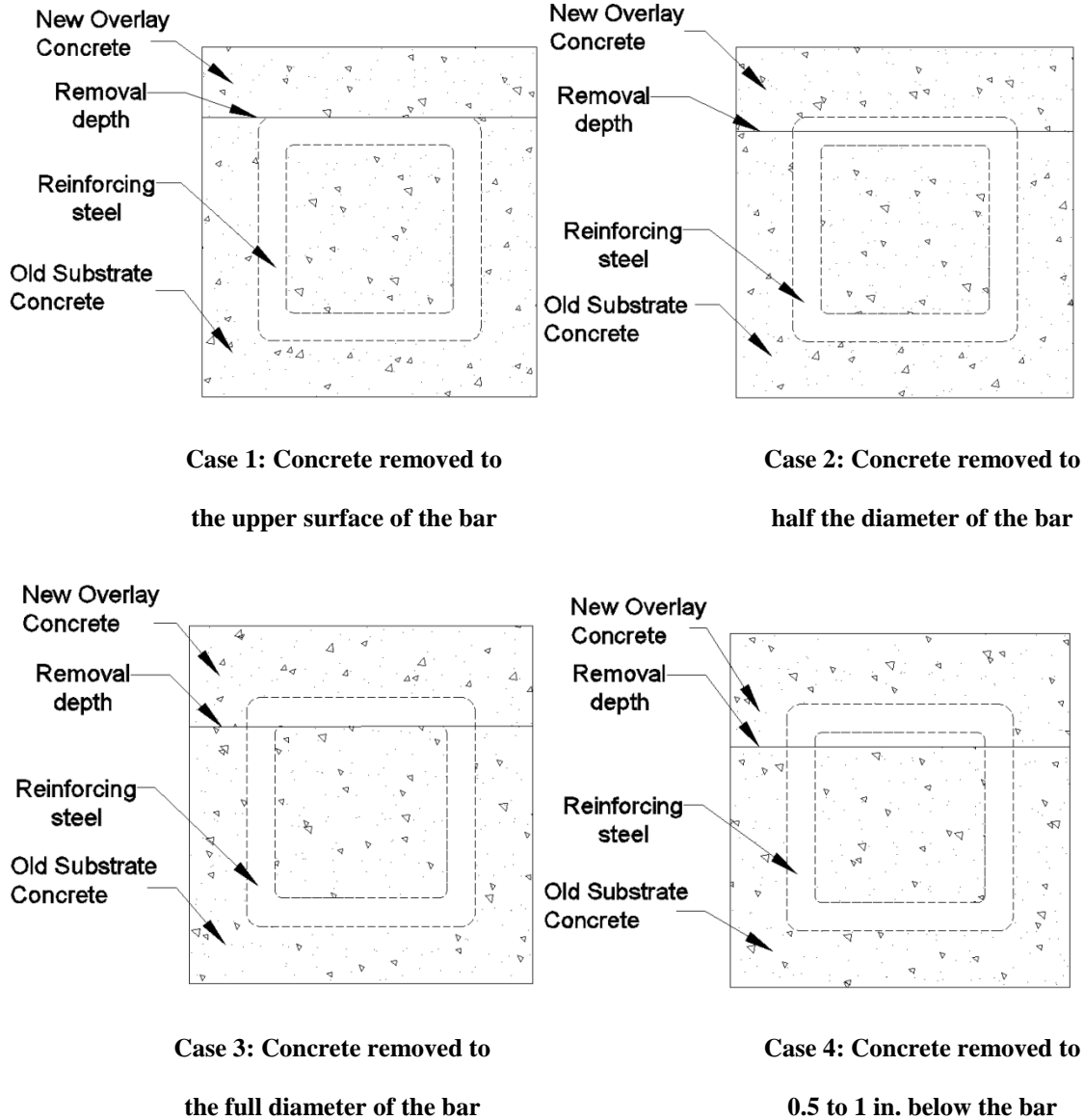


Figure 48. Different depths of concrete removal considered

Factors that were taken into consideration for comparing the bond strength were load at stiffness changes, maximum load, shear stresses at stiffness change and at failure, and stiffnesses.

Two types of concrete mixes were used for all of the tests. For the substrate concrete, C4 concrete was used; and, for the new overlay concrete, HPC-O concrete was used. The strength values for these concrete mixes are shown in Table 10 and Table 11.

Table 10. C4 concrete mix strength values

Age (days)	Compressive	Splitting tensile
	strength (psi)	strength (psi)
7	4767	495
21	4765	508
28	5190	515

Table 11. HPC-O concrete mix strength values

Age (days)	Compressive	Splitting tensile
	strength (psi)	strength (psi)
3	3947	420
21	6008	549
28	6501	573

This chapter further describes the methodology that was followed for the four different tests. Each of the tests and their results are described in the following sections.

3.4.2 Pull-Off test

The pull-off test was used to determine the tensile bond strength between the old concrete and the new overlay concrete with variable removal depth levels.

3.4.2.1 Specimen details

The specimens were fabricated to resemble a bridge deck slab. The dimensions of each specimen, the reinforcing steel spacing, and the detailing are all similar to an actual deck slab and are shown in Figure 49 for Case 1 (concrete removed down to the upper surface of the reinforcing bar).

Wooden formwork (as shown in Figure 50) was fabricated for the construction of the pull-off test specimens. The shaded part in Figure 49 was to be filled by the new overlay concrete after the concrete being used for the substrate concrete had cured. To create the voids to be filled later, foam was used to fill the shaded parts until the substrate concrete hardened and the overlay concrete could be placed. To keep the foam stable, the formwork was built upside down and the reinforcing steel was placed on the foam. An extra reinforcing steel bar was used to keep the main reinforcing steel stable horizontally. The reinforcement arrangement can be seen in Figure 50.

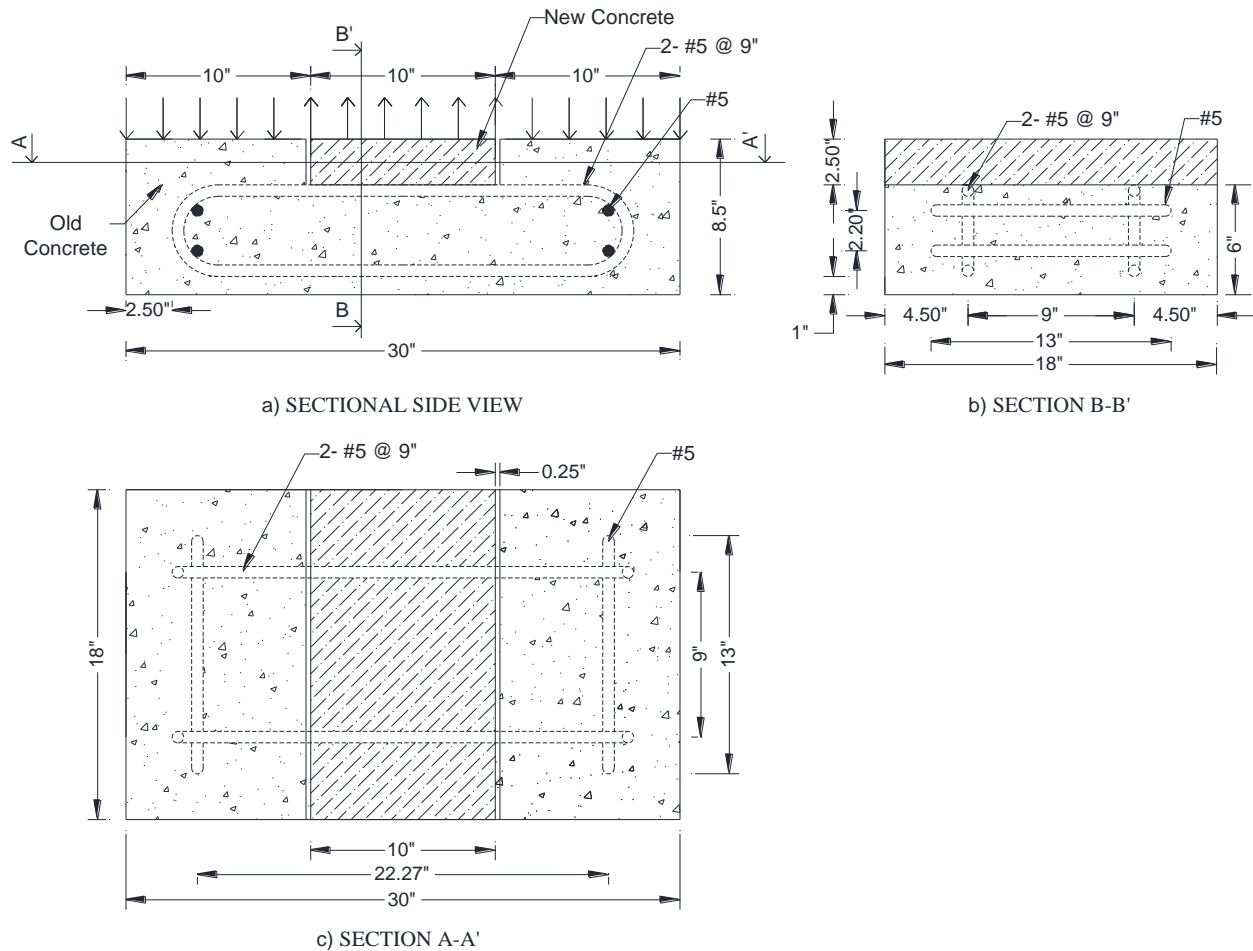


Figure 49. Pull-off test specimen schematic (Case 1)

C4 concrete was placed into the formwork and the specimens were vibrated appropriately. The specimens were covered with plastic and wetted periodically to maintain the moisture level inside. After curing the specimens for three days, the foam and formwork were removed. The depth of the foam was only up to the face of the reinforcing steel (i.e., 2.5 in.) deep. To achieve the different depth conditions, the portions where foam was used were chipped below the face of the bar and the exposed C4 concrete was then roughened using a jackhammer (Case 1 specimens only needed to have the C4 concrete roughened).



a) Top view



b) Angle view

Figure 50. Pull-off test formwork for substrate concrete placement

As shown earlier in the Figure 49 schematic (upper left), a gap is needed between the substrate concrete and the new overlay concrete for pull-off test placement of the overlay

concrete. Without the gap, at the time of pull-off test loading, the vertical bond between the substrate concrete and the new overlay concrete along the edges of the overlay concrete would provide shear bond strength to resist the load in addition to the tensile bond strength provided by the horizontal bond at the bottom of the overlay concrete. To get only the tensile strength resistance, foam with a 0.25 in. thickness was glued to the C4 concrete on each side to create the voids as shown in Figure 51.

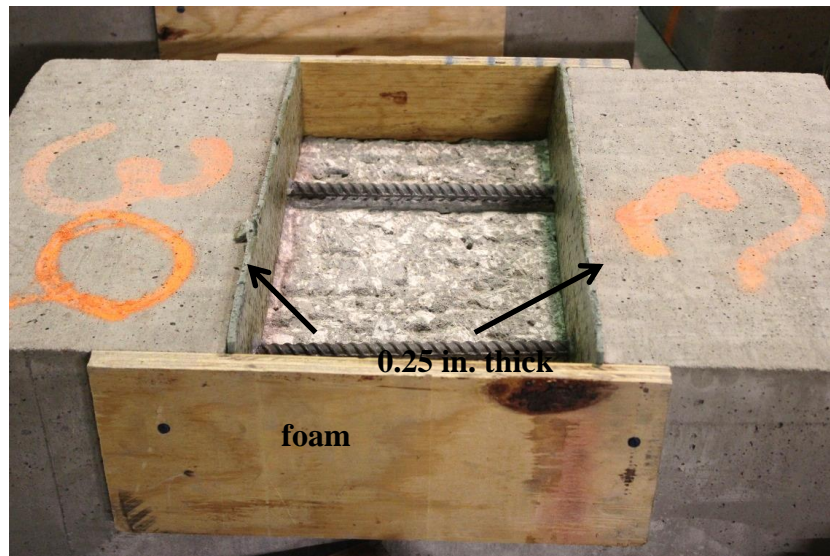


Figure 51. Pull-off test formwork for overlay concrete placement (Case 4)

The most challenging aspect of this test was to figure out a method to apply the pull-off force to the new overlay concrete. After much discussion, shear studs welded to a steel plate, as shown in Figure 52, were used.

Eight shear studs were welded to each steel plate. The shear studs were 1.5 in. long and the diameter of the head was 1 in. The plate was 10 x 18 x 0.5 in. The steel plate also had four 3/8 in. threaded holes, in which four bolts were fastened to connect it to a thicker plate, which

was used to apply the pull-off force. The shear studs of each steel plate were embedded in the overlay concrete of each pull-off test specimen at the time of concrete placement.

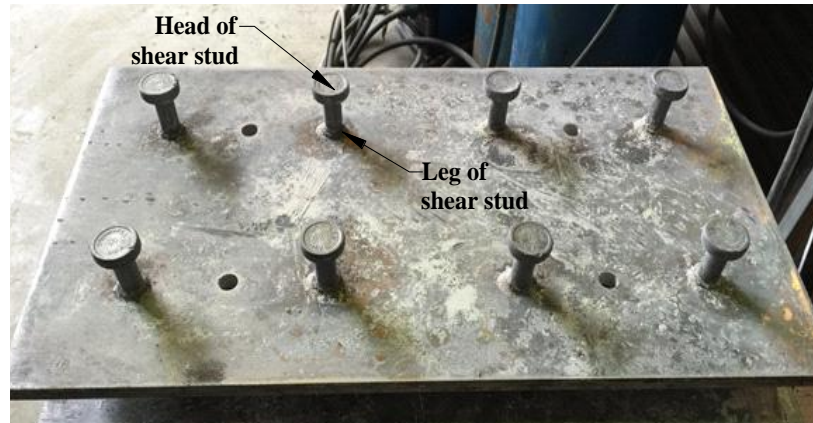


Figure 52. Pull-off test steel plate with welded shear studs

To bond the new overlay concrete to the previously placed concrete, a grout consisting of a mixture of about 5 to 6 gallons of water to each 94 lb bag of cement (12.5 to 13.8 in³ of water per lb of cement) was used. The grout material was applied to the chipped portion using a stiff hand brush, just prior to placing of the overlay concrete. As soon as the grout was applied, the overlay concrete was placed so that the applied grout would still be wet when the concrete was placed. After the concrete was placed, the steel plate studs were embedded in it by firmly tapping the plate using a rubber hammer as shown in Figure 53.

All specimens were covered with a plastic sheet to maintain the moisture level. The forms were removed after two days of curing so that the specimens would be ready for testing after the third day.



Figure 53. Tapping the steel plate to embed the shear studs on a pull-off test specimen

3.4.2.2 Testing arrangement

The Iowa DOT cures the overlay concrete for 72 hours and then opens the bridge to traffic. To simulate the same conditions, each pull-off test started two hours prior to 72 hours of curing and each test continued for approximately four hours.

Figure 54 shows the testing arrangement for the pull-off test. Closer views of the specimens are shown in the next section.

Each steel plate with the studs that were embedded in the overlay concrete of a specimen had four threaded holes for bolts. Using these bolts, the embedded steel plate was attached to a thicker steel plate to which the pulling force (upward) was applied.

One displacement transducer was attached on each side of the overlay to measure the displacement. A hydraulic loading system was used to apply the pull-off load. The load was

gradually increased up to a point where the specimen failed (i.e., the two concrete pieces separated either at the interface of the bond or in the overlay concrete material).

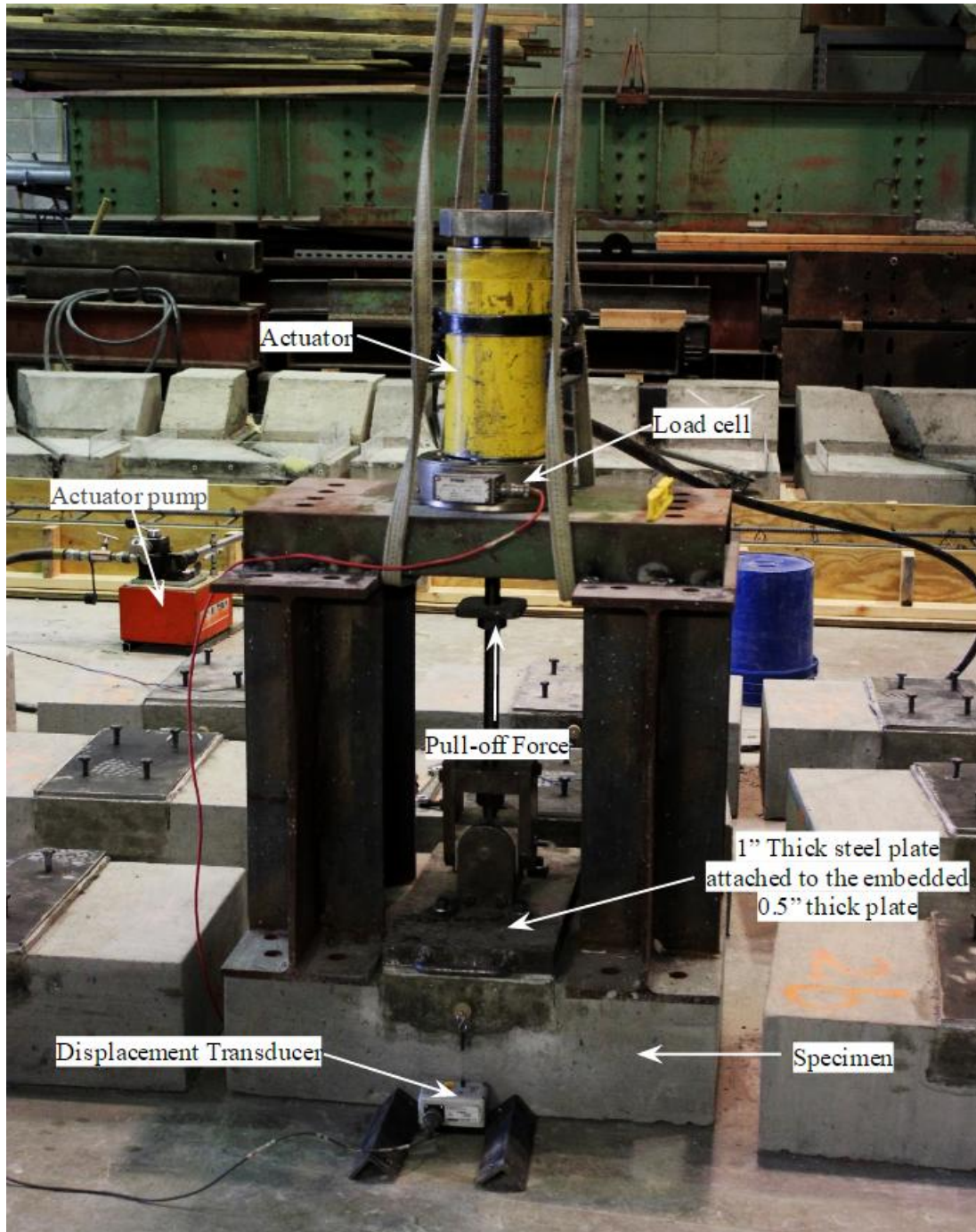


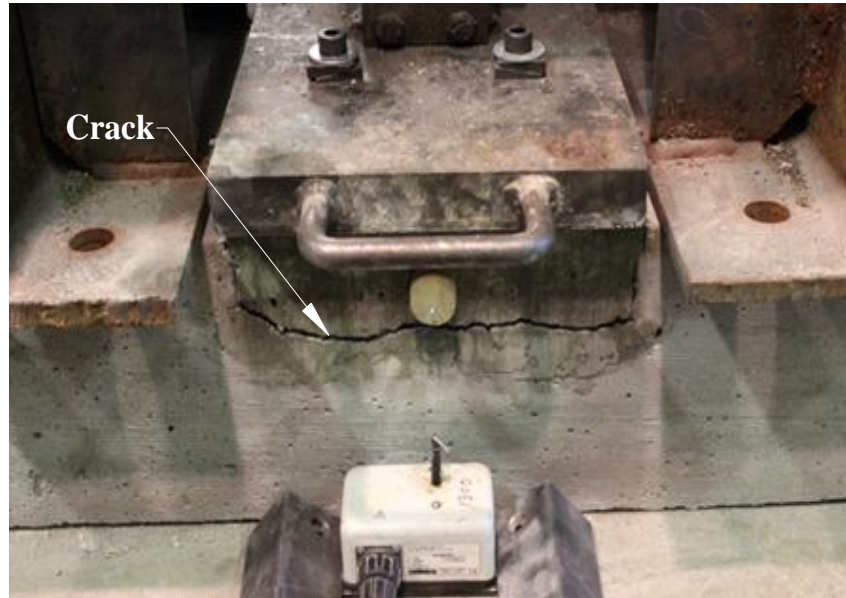
Figure 54. Testing arrangement for pull-off test

3.4.2.3 Results

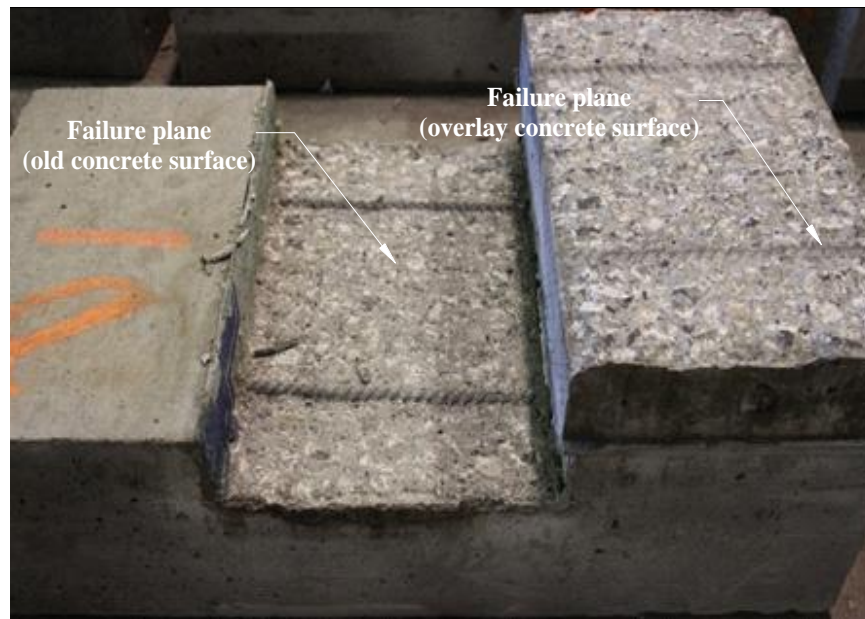
The results from the pull-off tests and the comparisons between different parameters are provided here. Observations of all tests made it clear that the shear studs created a potential failure plane at the head of the shear studs. In fact, some specimens failed at the heads of the shear studs in the overlay and some failed at the bond interface. In each case, a sudden failure was observed. Following are the results for the different concrete removal depth levels studied (Case 1 through 4).

Case 1– Concrete Removed to the Top of the Reinforcing Steel

For Case 1, two of the specimens failed at the bond interface and one specimen failed in the overlay. Figure 55 shows a side view of the failure (total separation of the bond) at the interface of the substrate and new overlay concrete and a top view of the interface surface after the failure.



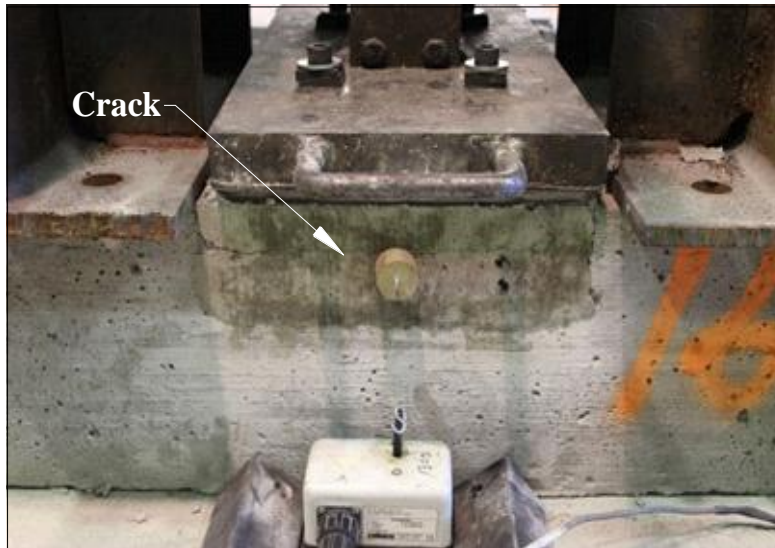
a) Side view



b) Top view

Figure 55. Case 1 pull-off test specimen failure at concrete bond interface

Figure 56 shows a side view of the failure of the specimen in the overlay concrete at the heads of the shear studs and a top view of the failure plane at the break in the bond.



a) Side view

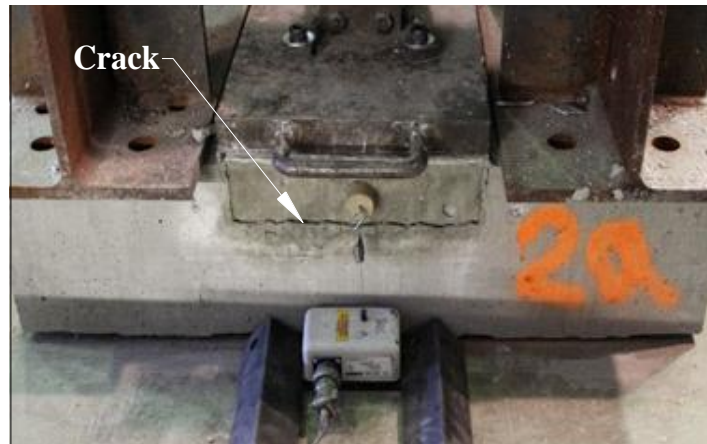


b) Top view

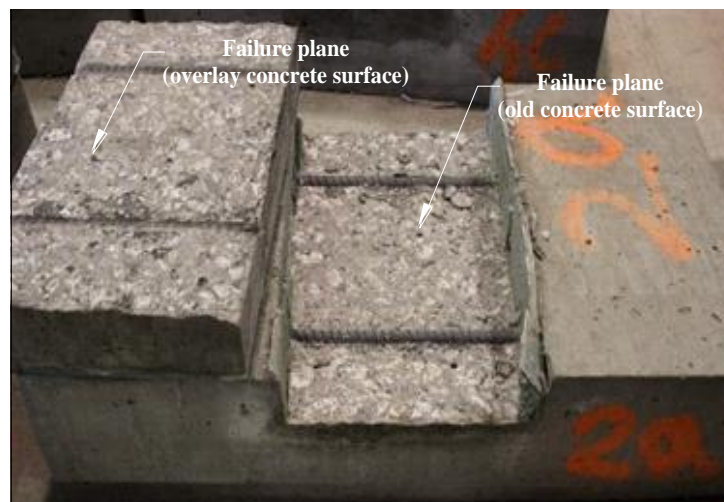
Figure 56. Case 1 pull-off test specimen failure in concrete overlay

Case 2– Concrete Removed to Half the Diameter of the Reinforcing Steel

In this case, two specimen failures were observed at the bond interface and one specimen failed in the overlay concrete at the heads of the shear studs. Figure 57 shows the failure of the specimen at the interface of the substrate and new overlay concrete.



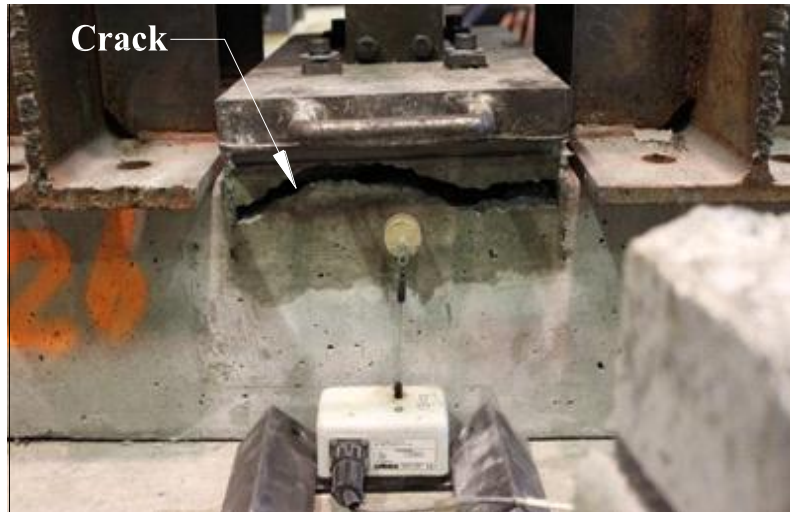
a) Side view



b) Top view

Figure 57. Case 2 pull-off test specimen failure at concrete bond interface

Figure 58 shows the failure of the specimen in the overlay concrete at the heads of the shear studs and the surface at which the break in the bond was observed.



a) Side view



b) Top view

Figure 58. Case 2 pull-off test specimen failure in concrete overlay

Case 3– Concrete Removed to the Full Diameter of the Reinforcing Steel

All of the specimens in this case failed at the interface level as shown in the Figure 59.

The figure shows the pattern of the crack and the interface surface.



a) Side view

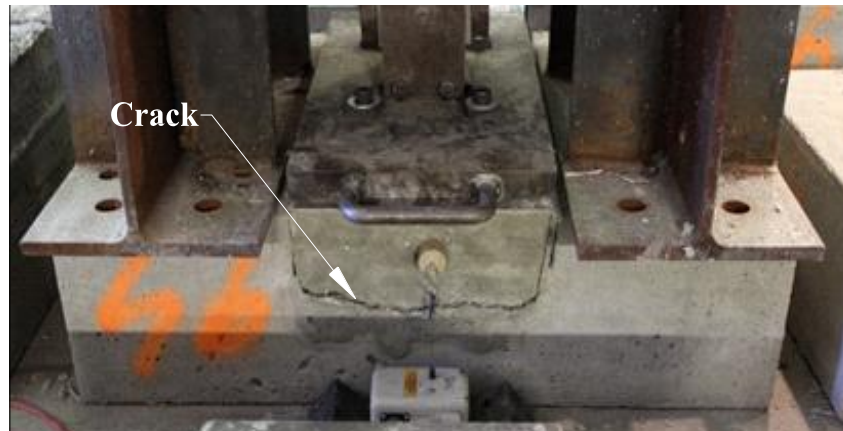


b) Top view

Figure 59. Case 3 pull-off test specimen failure at concrete bond interface

Case 4– Concrete Removed to the Full Diameter of the Reinforcing Steel Plus 0.5 to 1 in.

In this case, two of the specimens failed in the overlay and one specimen failed at the interface. Figure 60 shows the failure of the specimen at the interface of the substrate concrete and new overlay concrete.



a) Side view



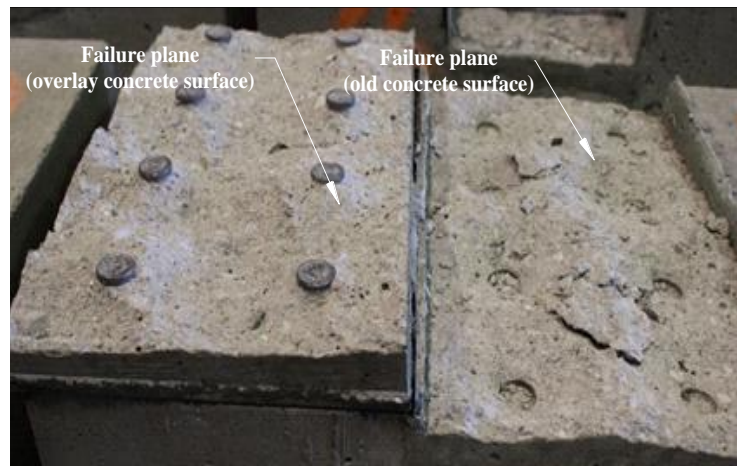
b) Top view

Figure 60. Case 4 pull-off test specimen failure at concrete bond interface

Figure 61 shows a side view of the failure of the specimen in the overlay concrete at the heads of the shear studs and a top view of the interface surface after the failure.



a) Side view



b) Top view

Figure 61. Case 4 pull-off test specimen failure in concrete overlay

Table 12 shows the peak tensile stresses for all specimens and the average values for each concrete removal depth (Case 1 through 4).

Table 12. Pull-off test results

Concrete Removal		Tensile		
Depth/ Case No.	Specimen No.	Load at Failure (kips)	Stress at failure (psi)	Failure plane location
1	1	15.1	84	Bond interface
1	2	16.9	94	At shear stud head
1	3	18.2	101	Bond interface
1	Average	16.8	93	
2	1	17.6	98	Bond interface
2	2	19.1	106	At shear stud head
2	3	15.0	83	Bond interface
2	Average	17	96	
3	1	14.5	81	Bond interface
3	2	15.8	88	Bond interface
3	3	19.1	106	Bond interface
3	Average	16	92	
4	1	19.8	110	At shear stud head
4	2	17.5	97	Bond interface
4	3	20.1	112	At shear stud head
4	Average	19	106	

Removal Depth/Case No.:

- 1 - To top of the reinforcing steel
- 2 - Half the diameter of the reinforcing steel
- 3 - Full diameter of the reinforcing steel
- 4 - Full diameter of the bar and 0.5 to 1 in. additional

Figure 62 shows the variation of the average load at failure versus the concrete removal depth level (Case 1 through 4).

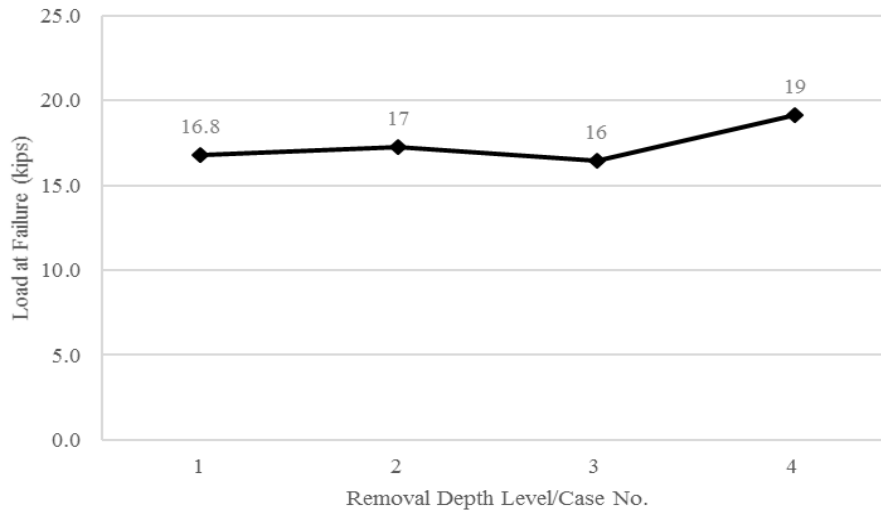


Figure 62. Average load at failure versus concrete removal depth (pull-off test)

Figure 63 shows the variation of the average tensile bond stress versus the concrete removal depth level (Case 1 through 4).

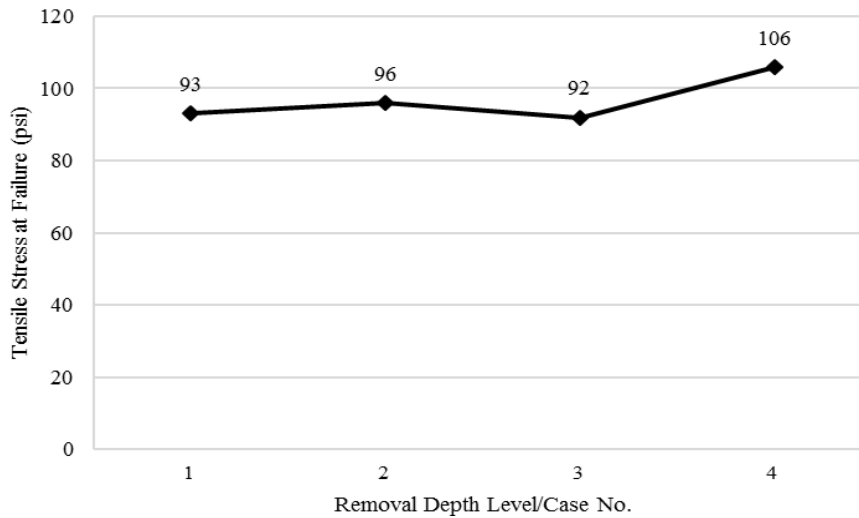


Figure 63. Average tensile stress at failure versus concrete removal depth (pull-off test)

3.4.2.4 Statistical analysis of the test data

A multiple comparison with Tuckey's procedure (the T Method) was performed using the load at failure values against the exposure depth. The recorded data values are independent of each other, the number of data points is too small and hence assumed to be normally distributed and there is equal within-group variance across the groups associated with each mean, which satisfies the assumptions for the Tuckey's procedure.

The analysis results showed that the mean values for the load at failure for all the different exposure depths were statistically indifferent. The P-value was 0.3669 which is greater than α ($\alpha = 0.05$), which means there is not enough evidence to say that the load at failure is dependent on the exposure depth.

3.4.2.5 Summary

Two failure plane locations were observed during pull-off testing. One failure plane was at the bond interface between the substrate concrete and the new overlay concrete and the other failure plane occurred at the shear studs in the overlay concrete. Even though a greater number of specimens failed at the bond interface, no criteria could predict the location of failure. It is possible that the load was not evenly distributed over the surface and perhaps the failure was caused by peeling. As the depth of concrete removal increased, the reinforcing steel held down more overlay concrete and retained that concrete upon the failure of the bond.

A very slight variation was seen in the peak load for the first three removal depth cases and the fourth case had a slightly greater failure load compared to other three. The variation in the tensile stress was similar to the variation of the peak load. Overall, the failure load and the

stress at failure had a 13% increase from Case 1 to Case 4, but Case 2 values were closer to Case 4 values.

3.4.3 Push-Out test

The push-out test was used to determine the shear bond strength between the substrate concrete and the overlay concrete for the four removal depths (Case 1 through 4). A shear load was applied to the bond on each of the specimens and the shear stress at failure was calculated for comparison between the four levels of concrete removal.

3.4.3.1 Specimen details

The specimens for the push-out test were designed to determine shear strength. The bar spacing used was similar to that for a typical deck slab. The shape and dimensions of the specimens are shown in Figure 64 (Case 1) and Figure 65 (Case 4).

For each of the test specimens, two sub-specimens of substrate concrete (C4 mix) were prepared and then bonded to each other with the overlay concrete between them. The two bonds between the substrate concrete sub-specimens and the new overlay concrete (between them) were then subjected to shear stresses to determine the shear strength.

The shaded portions in Figure 64 and Figure 65 represent the portion where the overlay concrete was placed. Foam that was 2.5 in. thick, as shown in Figure 66, was used to create the voids in the substrate concrete for placement of the overlay concrete later.

An additional steel bar was placed along the length on top of the reinforcement to prevent any horizontal movement during the concrete placement.

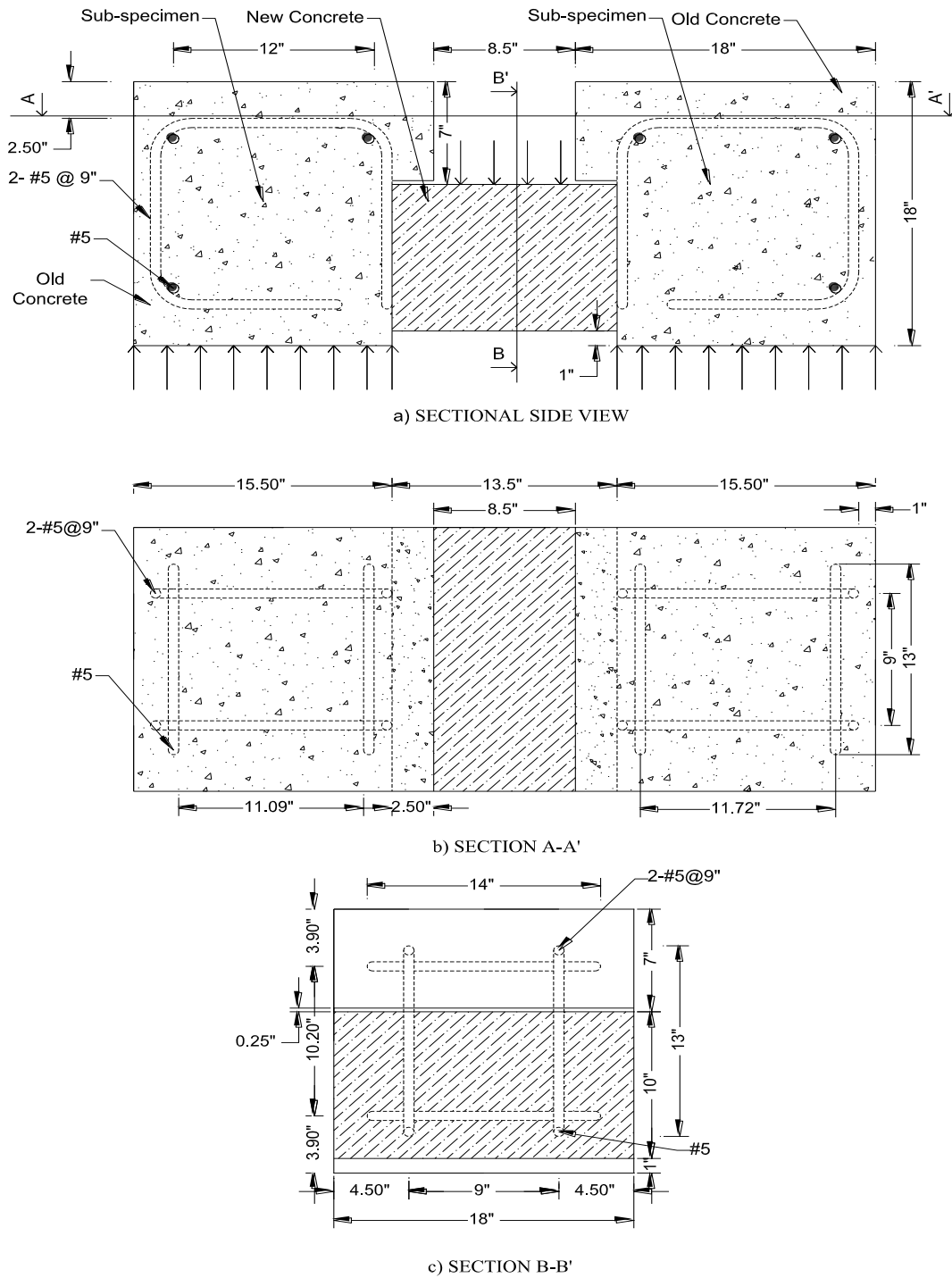
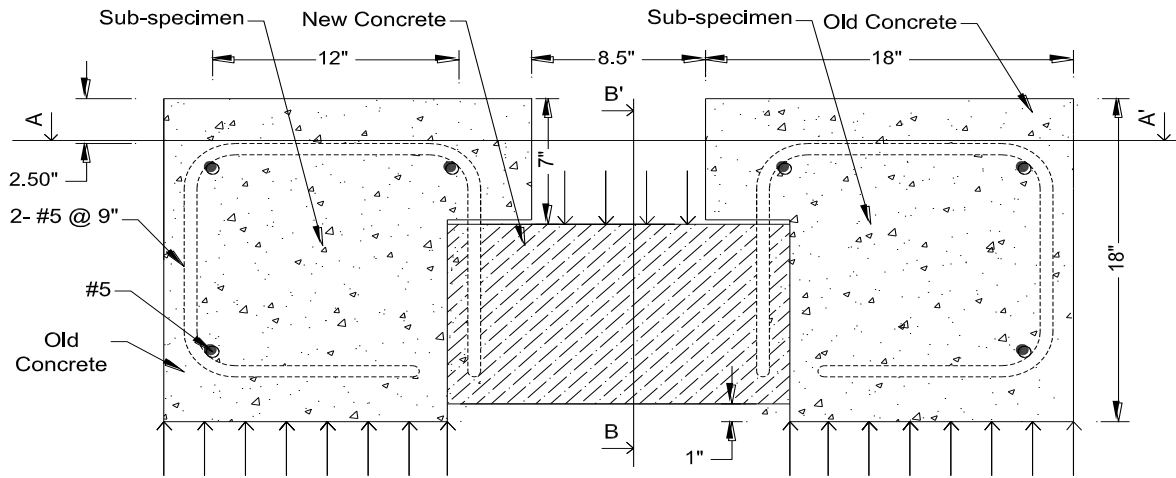
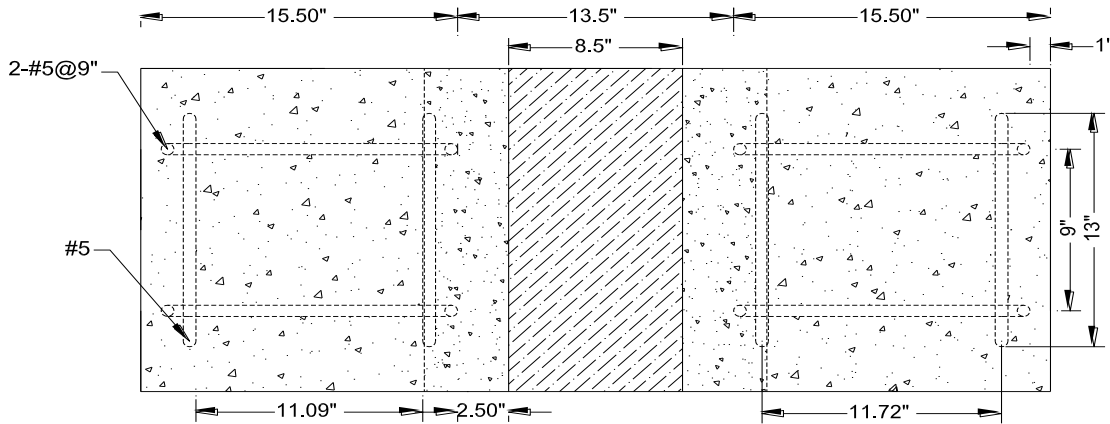


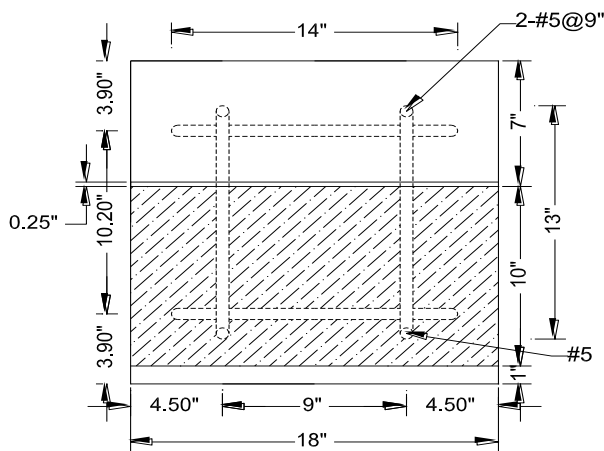
Figure 64. Push-out test specimen schematic (Case 1)



a) SECTIONAL SIDE VIEW



b) SECTION A-A'



c) SECTION B-B'

Figure 65. Push-out test specimen schematic (Case 4)

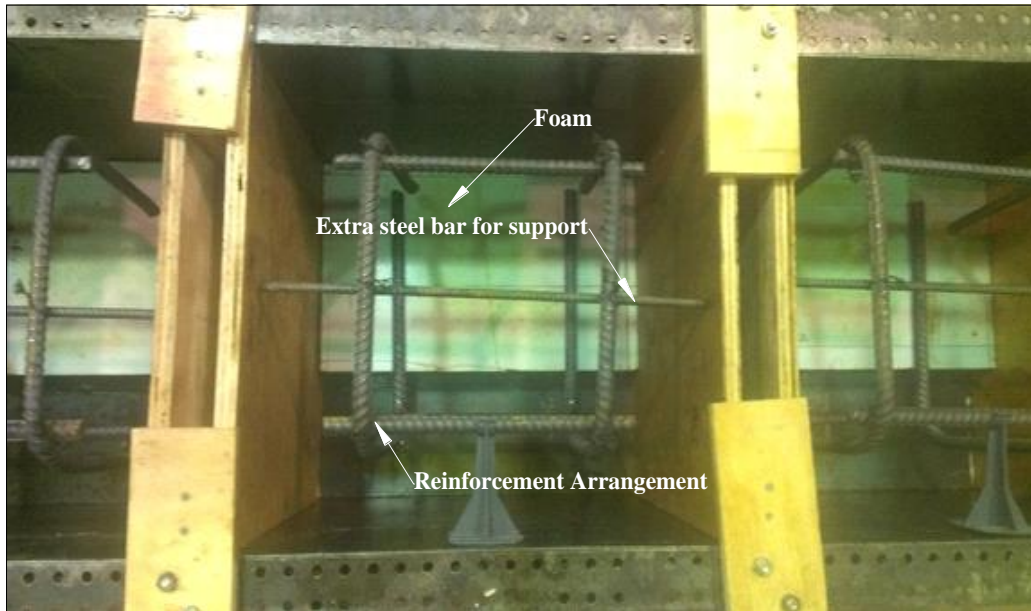


Figure 66. Push-out test formwork for substrate concrete placement

After curing the specimens for three days, the foam and the formwork were removed. The depth of the foam was only up to the face of the reinforcing steel (2.5 in.). Therefore, to achieve the different simulated concrete removal depths, additional concrete was removed and roughened using a jackhammer to the required depths, as shown in Figure 27 (Case 1 specimens only needed to have the concrete roughened).

Note that a small (0.25 in.) gap was needed between the substrate concrete and the top of the overlay concrete (as shown in the schematic in Figure 64) to eliminate any tensile bond between the substrate concrete and the top of the overlay concrete. To create this gap, 0.25 in. thick foam was glued to the substrate concrete. Wooden forms were attached to the sides of each pair of sub-specimens as shown in Figure 68 to create the space for the placement of the overlay concrete.



Figure 67. Pair of push-out test sub-specimens after concrete removal (Case 4)



Figure 68. Push-out test formwork for overlay concrete placement

To fill the 1 in. gap below the overlay concrete, a 0.75 in. thick sheet of plywood coupled with 0.25 in. thick foam was used. To bond the overlay concrete to the previously placed substrate concrete, a grout consisting of a mixture of about 5 to 6 gallons of water to each 94 lb bag of cement (12.5 to 13.8 in³ of water per lb of cement) was used. The grout material was

applied to the roughened concrete using a stiff hand brush just prior to placement the overlay concrete as shown in Figure 69.



Figure 69. Application of grout for push-out test specimen

The overlay concrete was placed until it touched the bottom of the foam, which was used to break the bond between the substrate concrete and the top of the overlay concrete on each specimen. The overlay concrete was vibrated and wet-cured on the top exposed surface. Figure 70 shows a specimen after placement of the overlay concrete.



Figure 70. Push-out test specimen after overlay concrete placement

3.4.3.2 Testing arrangement

Each push-out test started 4 hours prior to 72 hours after overlay concrete placement.

Figure 71 shows the testing arrangement.

The specimens were carefully moved to the testing area to be sure to not affect the shear bond of the substrate concrete and the overlay concrete. The specimens were set on the floor of the structural testing laboratory and the push-out load was applied to the overlay concrete from the top. Deflection transducers were mounted on both sides of the overlay concrete. A layer of neoprene was laid on top of the loading area to distribute the applied load.

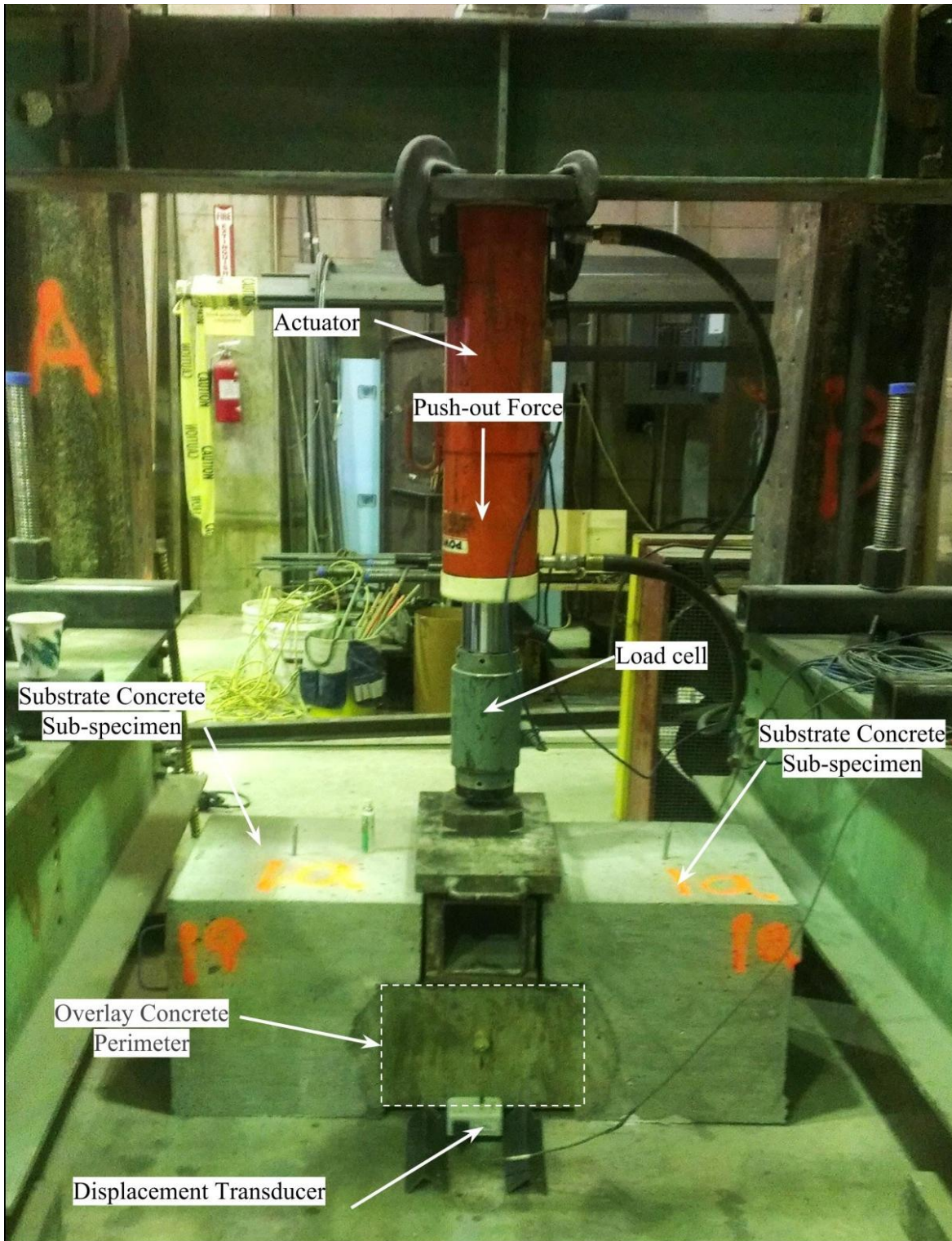


Figure 71. Testing arrangement for push-out test

3.4.3.3 Results

Each of the specimens had two bond interfaces, with one on each side of the overlay concrete. Only one bond failed in shear for all of the specimens. The results for the different concrete removal depths follow.

Case 1– Concrete Removed to the Top of the Reinforcing Steel

During application of the loads, sudden failures (a large drop in load and separation of one of the bonds) were observed. Figure 72(a) shows a failure surface with a crack and Figure 72(b) and (c) show an interface surface between the substrate concrete and the overlay concrete after failure.



a) Side view



b) Bond interface (substrate concrete)



c) Bond interface (overlay concrete)

Figure 72. Case 1 push-out test specimen failure at concrete bond interface

Given no exposure of the reinforcing steel to the overlay concrete for the Case 1 specimens, the entire bond broke after the crack formed.

The overlay concrete for Case 2 specimens was exposed to half the diameter of the reinforcing steel. After the first cracks were observed, as shown in Figure 73(a), the specimens had not completely failed.

Case 2– Concrete Removed to Half the Diameter of the Reinforcing Steel

The overlay concrete after the initial crack development was still bonded to the reinforcing steel. After further load application, a final break of the bond took place. Total separation of a bond and two interface surfaces after the separation are shown in Figure 73(b), (c), and (d).



a) Propagation of crack



b) Separation at interface



c) Bond interface (substrate concrete)



d) Bond interface (overlay concrete)

Figure 73. Case 2 push-out test specimen failure at concrete bond interface

Case 3– Concrete Removed to the Full Diameter of the Reinforcing Steel

Failures similar to Case 2 were observed for Case 3 specimens; but, due to the additional exposure of the reinforcing steel to the concrete, the bonds were stronger between the concrete and the reinforcing steel, withstanding a greater load after crack initiation. Figure 74 shows the failure of a specimen.



a) Propagation of crack



b) Separation at interface



c) Bond interface (substrate concrete)



d) Bond interface (overlay concrete)

Figure 74. Case 3 push-out test specimen failure at concrete bond interface

Case 4– Concrete Removed to the Full Diameter of the Reinforcing Steel Plus 0.5 to 1 in.

The loads for total separation of a bond were greatest for Case 4 specimens. Figure 75 shows a crack and total separation at a bond interface.



a) Propagation of crack



b) Separation at interface



c) Bond interface (substrate concrete)



d) Bond interface (overlay concrete)

Figure 75. Case 4 push-out test specimen failure at concrete bond interface

Perhaps not surprising, the concrete bonded to more of the reinforcing steel on these specimens, as shown in Figure 75(d).

Table 13 shows the shear stresses at first stiffness change and at maximum load for all specimens and the average values for each concrete removal depth (Case 1 through 4).

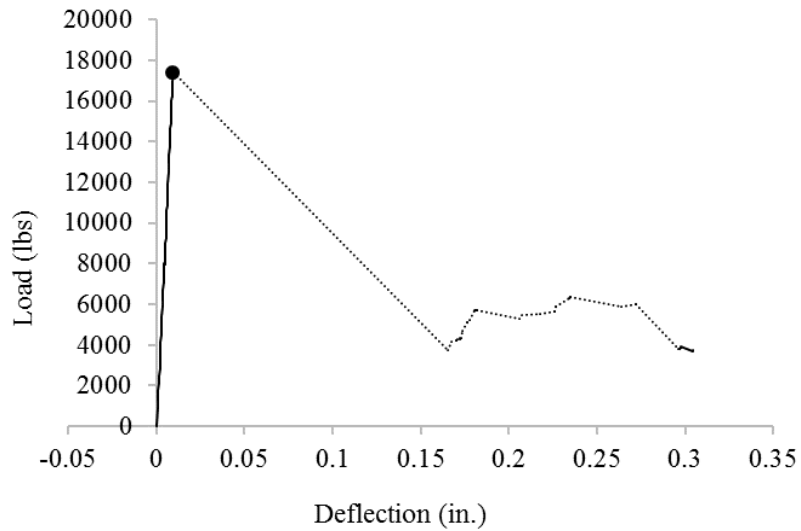
Table 13. Push-out test results

Concrete Removal Depth/ Case No.	Specimen No.	Shear				
		Load at First Stiffness Change (kips)	Stress at First Stiffness Change (psi)	Maximum Load (kips)	Shear Stress at Maximum Load (psi)	Maximum Stiffness (kips/in.)
1	1	17	48	17	48	2000
1	2	23	63	23	63	2000
1	3	17	48	17	48	3000
1	Average	19	53	19	53	2333
2	1	20	55	31	86	600
2	2	19	52	33	92	3000
2	3	22	62	27	75	4000
2	Average	20	57	30	84	2533
3	1	15	42	24	67	600
3	2	19	52	40	112	2000
3	3	21	58	39	108	4000
3	Average	18	51	34	96	2200
4	1	25	68	36	99	1000
4	2	18	49	40	110	3000
4	3	27	76	43	120	4000
4	Average	23	65	40	110	2667

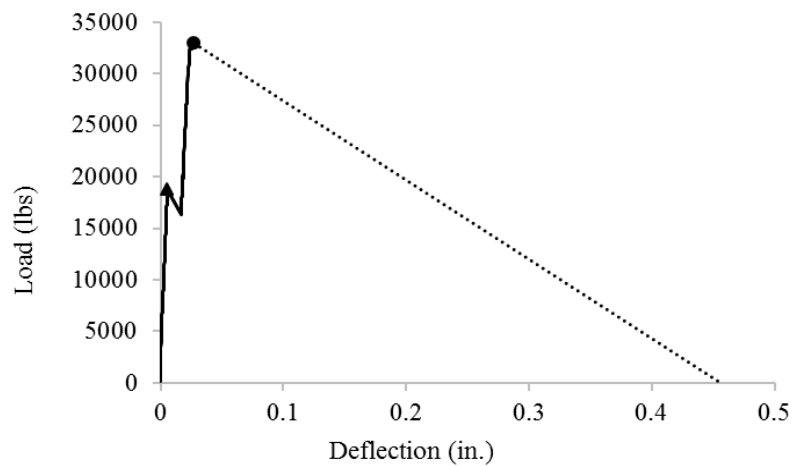
Removal Depth/Case No.:

- 1 – To top of the reinforcing steel
- 2 - Half the diameter of the reinforcing steel
- 3 - Full diameter of the reinforcing steel
- 4 - Full diameter of the bar and 0.5 to 1 in. additional

Figure 76 shows the load versus deflection graph for one specimen for each of the four concrete removal depth cases. The solid circular mark on each graph represents the maximum load value for that particular specimen and the solid triangular mark represents the point where first stiffness change was observed.



Case 1



Case 2

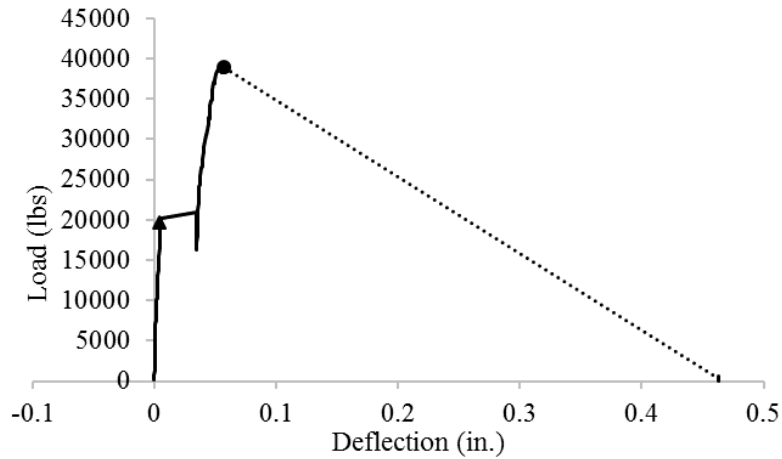
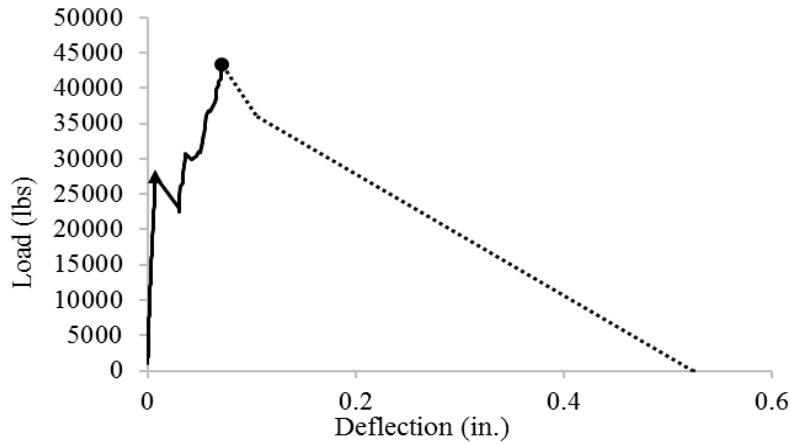
**Case 3****Case 4****Figure 76. Load versus deflection (push-out test)**

Figure 77 shows the average load at the stiffness change (triangles) and the maximum load (squares) versus the concrete removal depth case.

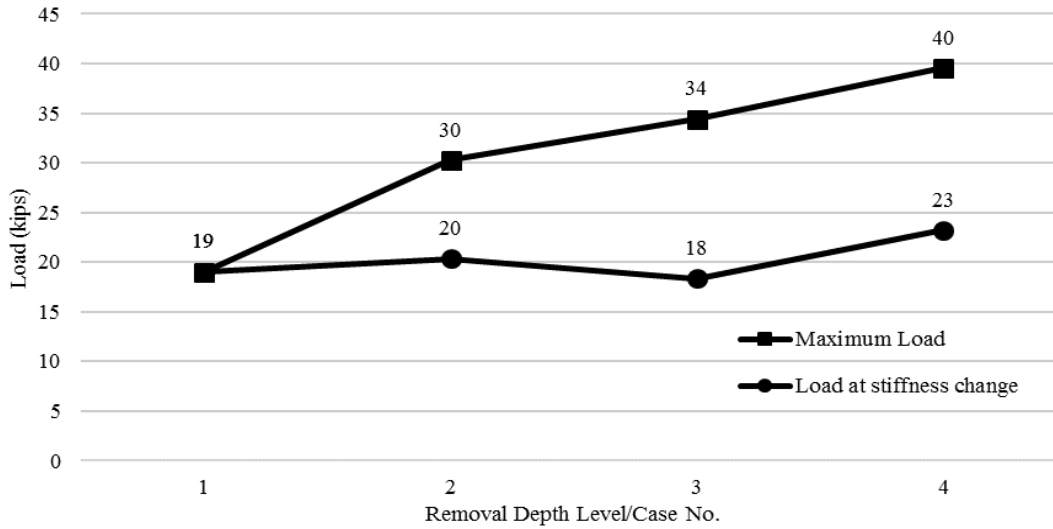


Figure 77. Average load versus concrete removal depth (push-out test)

Figure 78 shows the variation of the average shear stress at the stiffness change (triangles) and at the maximum load (squares) with change in the concrete removal depth level.

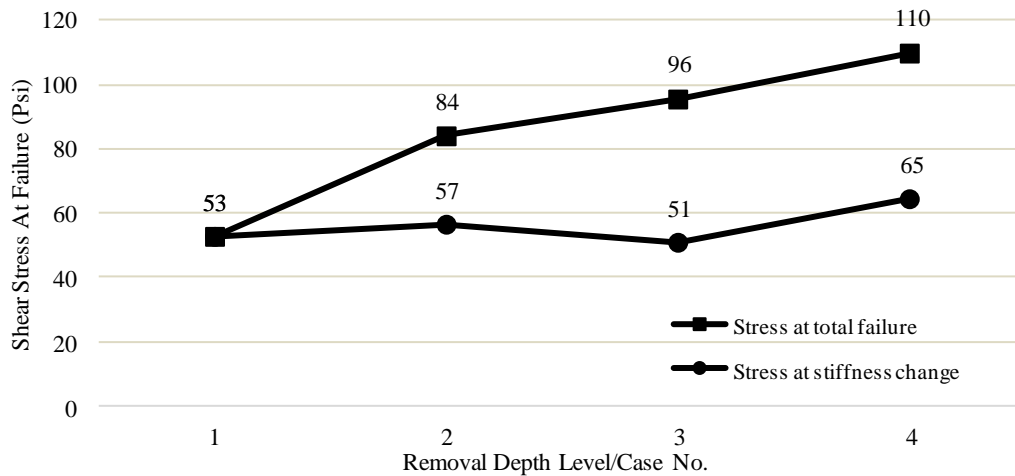


Figure 78. Average shear stress versus concrete removal depth (push-out test)

Figure 79 shows the variation of the average stiffness before the stiffness change with respect to the concrete removal depth level or case.

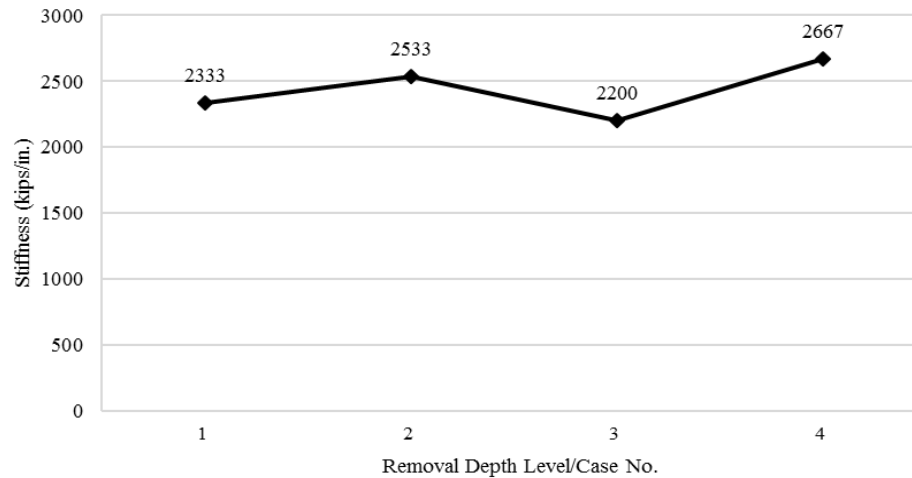


Figure 79. Average stiffness versus concrete removal depth (push-out test)

The stiffness was calculated as the initial slope of the load versus deflection from zero load to the point where the specimen started showing a non-linear behavior or a large stiffness change.

3.4.3.4 Statistical analysis of the test data

A multiple comparison with Tuckey's procedure (the T Method) was performed using the load at first stiffness change values against the exposure depth. The recorded data values are independent of each other, the number of data points is too small and hence assumed to be normally distributed and there is equal within-group variance across the groups associated with each mean, which satisfies the assumptions for the Tuckey's procedure.

The analysis results showed that the mean values for the load at first stiffness change for all the different exposure depths were statistically indifferent. The P-value was 0.3446 which is greater than α ($\alpha = 0.05$), which means there is not enough evidence to say that the load at first stiffness change is dependent on the exposure depth.

The analysis on the maximum load values showed that the average maximum load value for the exposure depth 1 and 4 differ from each other, 1 and 3 differ from each other but none of those three means are significantly different from 2. The P-value is 0.0083 which is less than 0.005, meaning that the maximum load values are dependent on exposure depth.

3.4.3.5 Summary

Case 1 specimens had a very small amount of exposure of the reinforcing steel to the overlay concrete, so a sudden failure was typically observed. As a result of this sudden failure, the load values at the stiffness change and the maximum value of the load are the same.

For Cases 2, 3, and 4, the overlay concrete had more bond with the reinforcing steel. The loading continued to increase after the initial crack (first change in stiffness) and, with a further increase in load, total separation was observed at the greater load. As the concrete removal depth increased, the maximum failure load increased slightly.

The maximum load values showed an increase with the increase in the concrete removal depth level. The variation in the load at the stiffness change also showed a slight increase with an increased concrete removal depth level.

Similar behavior was observed for the shear stress values at the stiffness change and at maximum load. The stiffness values had slight changes in values irrespective of the concrete removal depth level.

Overall, Case 1 specimens (with concrete removal down to the surface of the top reinforcing bars) showed significantly lower bond strength. The load at the stiffness change and the shear stress at the stiffness change showed insignificant variation from Case 2 to Case 4. The maximum load and the shear stress at failure had a 33% increase from Case 2 to Case 4. The stiffness values showed relatively insignificant changes, yet the increase in the value from Case 1 to Case 4 was observed to be 14%.

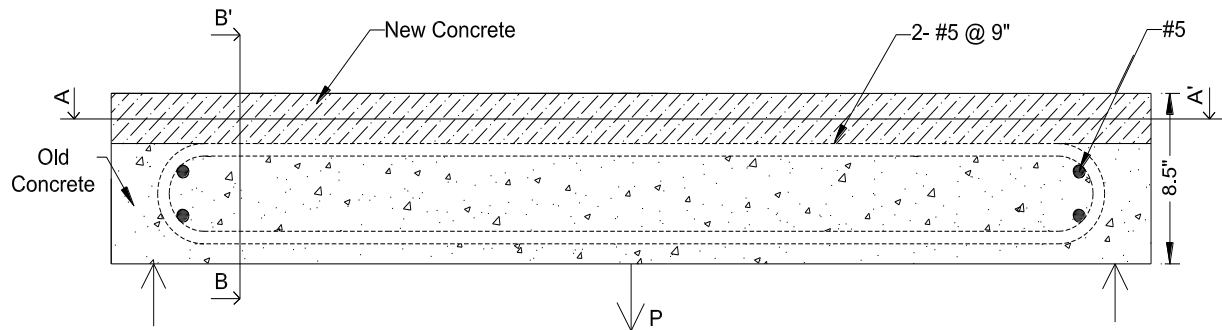
Even though a significant increase in the maximum load was observed, pure shear conditions never occur on an actual bridge deck, so the maximum load applied in this test may not be an appropriate measure of performance.

3.4.4 Positive bending flexural test

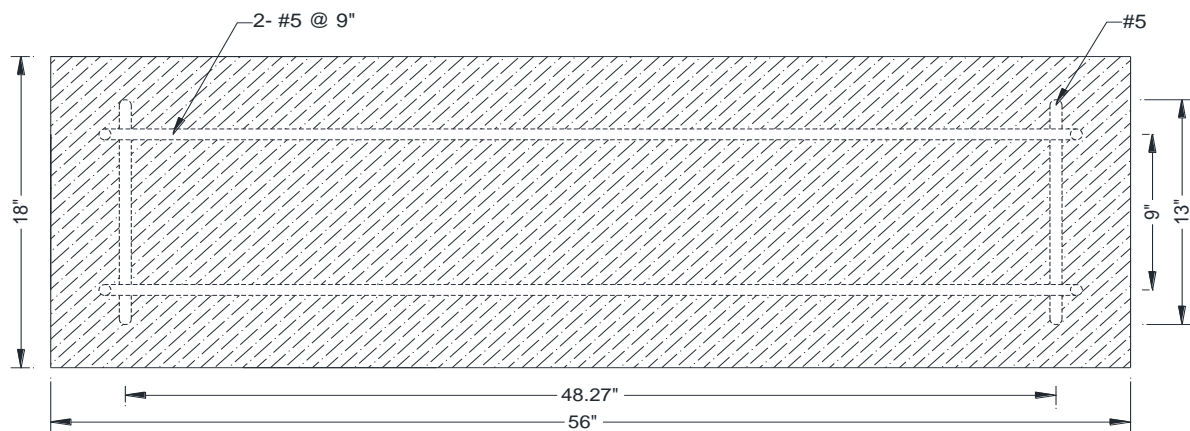
A bridge deck under traffic loading undergoes positive bending between the girders. This bending of the deck can cause compression in the top fibers of the concrete deck where the overlay is placed. The compression in the top fibers leads to horizontal shear stress, which can affect the bond between the overlay and the substrate concrete.

3.4.4.1 Specimen details

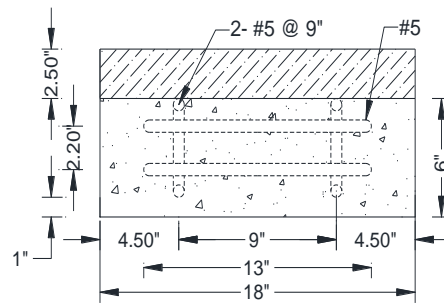
In this flexural test, beam specimens that resembled a bridge deck were constructed. The four concrete removal depth levels were evaluated using three specimens for each case. The details of the specimens including the reinforcing steel arrangement are shown in Figure 80.



a) Front view



b) Section A-A'



c) Section B-B'

Figure 80. Positive bending flexural test specimen schematic (Case 1)

To apply the force on the bottom of the specimen (P as shown at the bottom of Figure 80(a)), the shear studs on a metal plate were embedded in each specimen. Note that a pull down force was used to avoid providing a clamping force between the new overlay concrete and the substrate concrete. The size of the plate was 10 x 18 x 0.5 in. and each plate had 12 shear studs on it as shown in Figure 81.

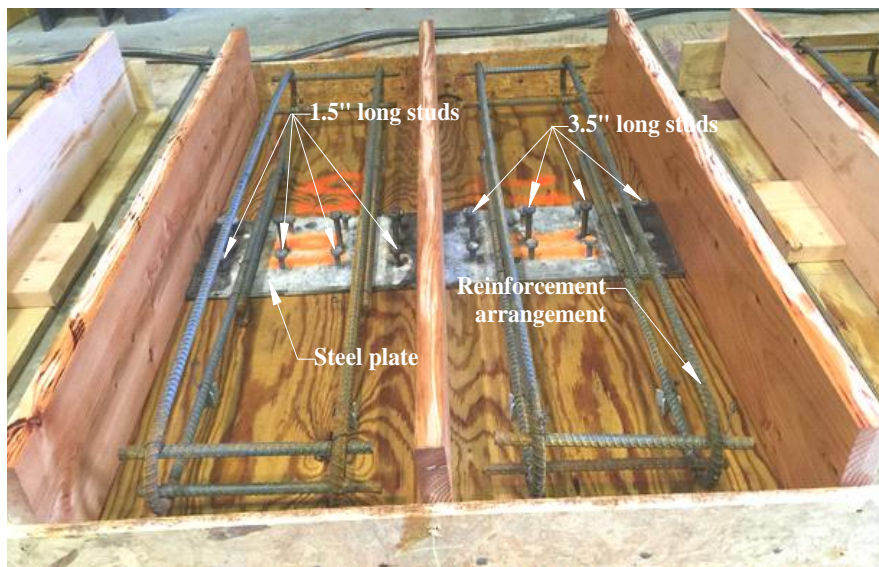


Figure 81. Positive bending flexural test formwork for substrate concrete placement

On each steel plate, the four studs in the middle were 3.5 in. long with 1 in. diameter head and the two sets of four shear studs on the sides were 1.5 in. long with 1 in. diameter heads. The plate also had four holes with threads, which were used to attach a 1 in. thick steel plate to which the force P was applied. This plate with the shear studs was placed below the reinforcement arrangement at the mid-span of the specimen before placement of the concrete as shown in Figure 81.

The substrate concrete was placed 0.5 in. above the required concrete removal depth level of each specimen so that a 0.5 in. of concrete could be chipped using a jackhammer to give it a proper roughened finish. Figure 82 shows a Case 4 specimen with the substrate concrete placed up to the bottom of the top reinforcing steel bars (i.e., 0.5 in. extra on top of the concrete removal depth level for Case 4).



Figure 82. Positive bending flexural test specimen after substrate concrete placement (Case 4)

This concrete was then cured with regular water application and covered with plastic. After two days of curing, the plastic cover was removed and the chipping process was started. Figure 83 shows the typical roughness of a substrate surface.



Figure 83. Positive bending flexural test specimen after roughening of substrate concrete (Case 1)

After curing the substrate concrete for 28 days, the specimens were prepared for the overlay concrete layer. The grout material as described in the previous tests was applied on the roughened surface with a brush as shown in Figure 84.



Figure 84. Application of grout to positive bending flexural test specimen (Case 1)

Immediately after applying the grout, the HPC-O mix overlay concrete was placed on top to create a 8.5 in. total specimen depth. After overlay placement, the specimens were covered with plastic to maintain the moisture level. These specimens were cured for three days.

3.4.4.2 Testing arrangement

Each flexural test for positive bending started 1.5 hours prior to 72 hours after overlay placement. Figure 85 shows the load frame with a specimen mounted in it.

The specimens were supported with pin and roller supports. A deflection transducer was attached on each side of the specimen to measure the deflection. The deflection transducers were mounted 2 to 3 in. right of center. The load was gradually applied to pull the steel plate down, thereby inducing positive bending in each specimen.

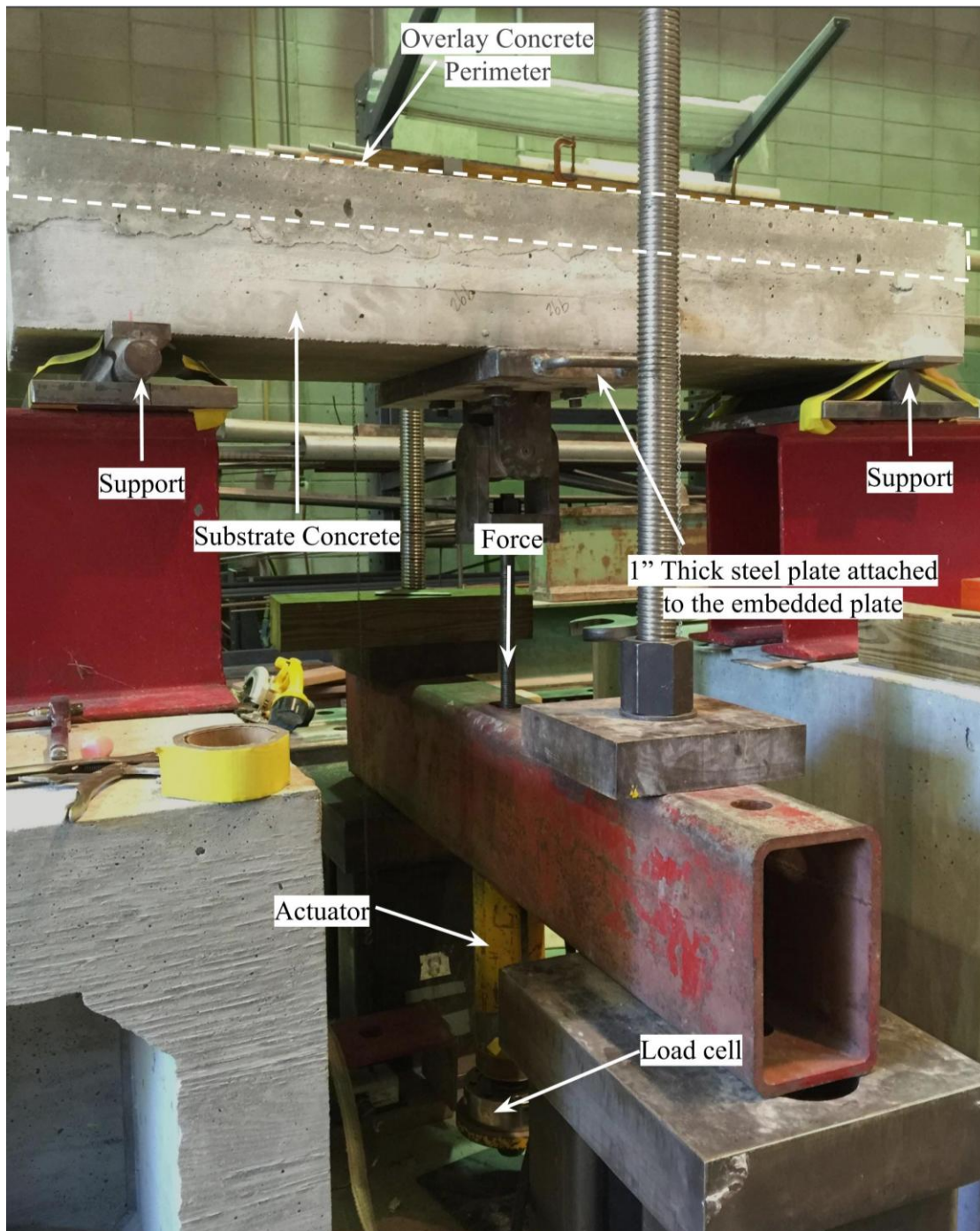


Figure 85. Testing arrangement for positive bending flexural test

3.4.4.3 Results

The factors that were considered for comparison using this test were the maximum load attained, the elastic shear stress at the bond interface at the maximum load, and the stiffness.

During testing, two types of cracks were observed. Flexure cracks were formed at the bottom of the specimen near mid-span and shear cracks were formed at the interface of the concrete bond. These cracks were found in specimens for all four cases (concrete removal depth levels). When the loads were increased, failures of the bond between the substrate concrete and the new overlay concrete were in the form of a visible separation at the interface.

Figure 86 through Figure 89 show one specimen for each case after failure. All three failed specimens for each case were similar.



Figure 86. Case 1 positive bending flexural test specimen failure at concrete bond interface

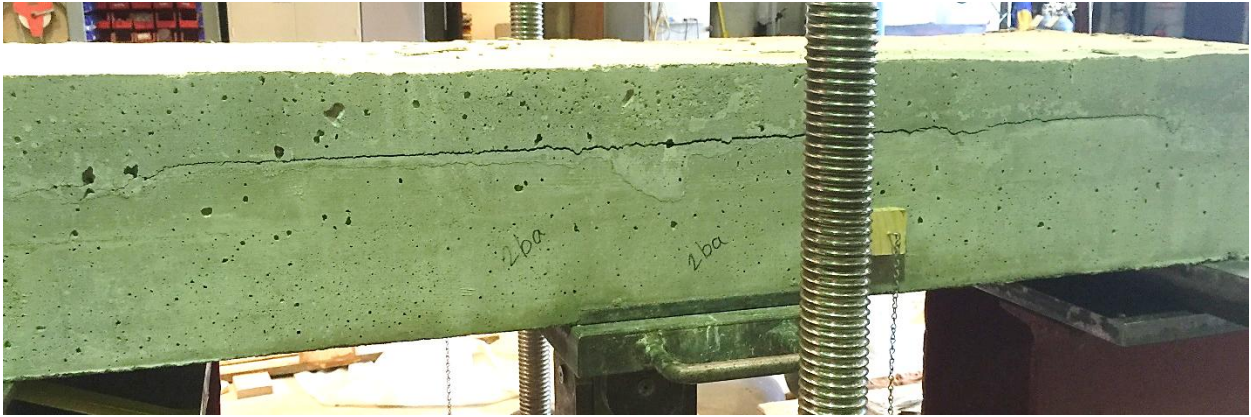


Figure 87. Case 2 positive bending flexural test specimen failure at concrete bond interface



Figure 88. Case 3 positive bending flexural test specimen failure at concrete bond interface



Figure 89. Case 4 positive bending flexural test specimen failure at concrete bond interface

Table 14 shows the test values for maximum load, elastic shear stress at the bond interface at maximum load, and stiffness as well as the average values for each concrete removal depth (Case 1 through 4).

The elastic shear stress at maximum load was calculated on the basis of section properties of an un-cracked section. Note that the distance of the bond interface from the neutral axis was different for each case of the concrete removal depth level, which led to a different value of shear stress at the bond interface for each case, even though the value for the maximum load could be the same.

Figure 90 shows the variation of the maximum load with the change in the removal depth level (Case 1 through 4).

Table 14. Positive bending flexural test results

Concrete		Elastic* Shear		
Removal		Maximum	Stress at	
Depth/ Case No.	Specimen No.	Load (kips)	Max. Load (psi)	Stiffness (kips/in.)
1	1	16.8	66	423
1	2	18.4	72	440
1	3	17.9	70	394
1	Average	17.7	70	419
2	1	16.6	70	376
2	2	16.6	70	497
2	3	18.9	79	417
2	Average	17.3	73	430
3	1	17.7	78	351
3	2	16.6	73	377
3	3	19.6	86	512
3	Average	18.0	79	413
4	1	16.6	78	437
4	2	16.2	77	399
4	3	16.8	79	412
4	Average	16.6	78	416

* All assumed section properties are for an un-cracked section

Removal Depth/Case No.:

- 1 – To top of the reinforcing steel
- 2 - Half the diameter of the reinforcing steel
- 3 - Full diameter of the reinforcing steel
- 4 - Full diameter of the bar and 0.5 to 1 in. additional

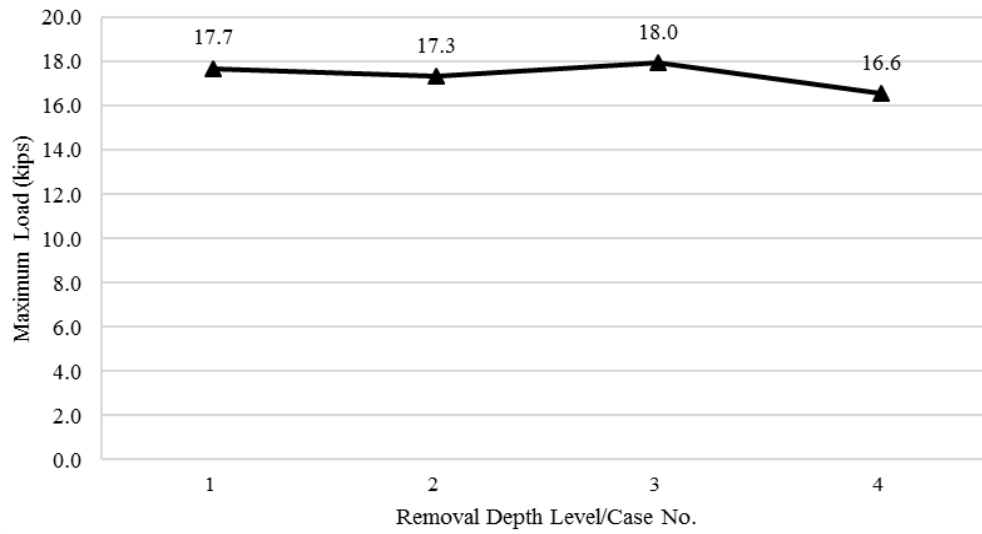


Figure 90. Average maximum load versus concrete removal depth (positive bending flexural test)

Figure 91 shows the variation of elastic shear stress at the interface at the maximum load relative to the concrete removal depth level.

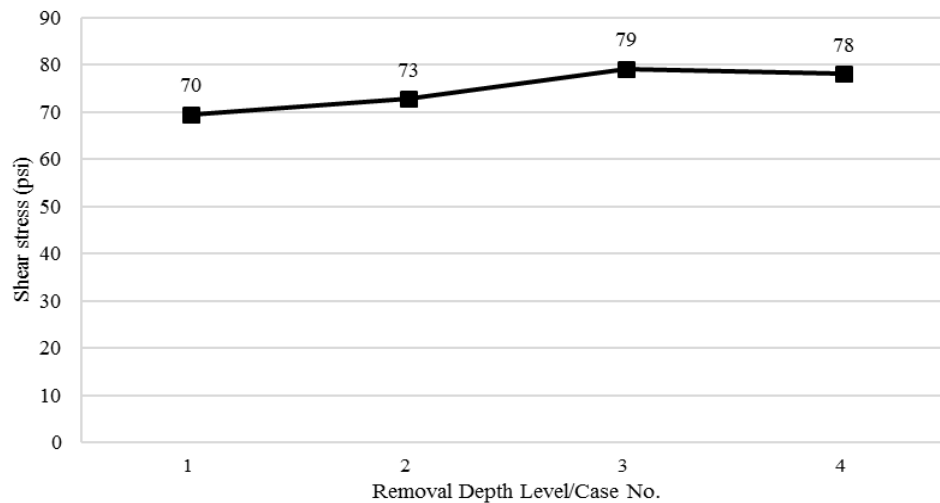


Figure 91. Average elastic shear stress at maximum load at interface versus concrete removal depth (positive bending flexural test)

Figure 92 shows the variation of average stiffness of the specimen depending on the change in concrete removal depth level.

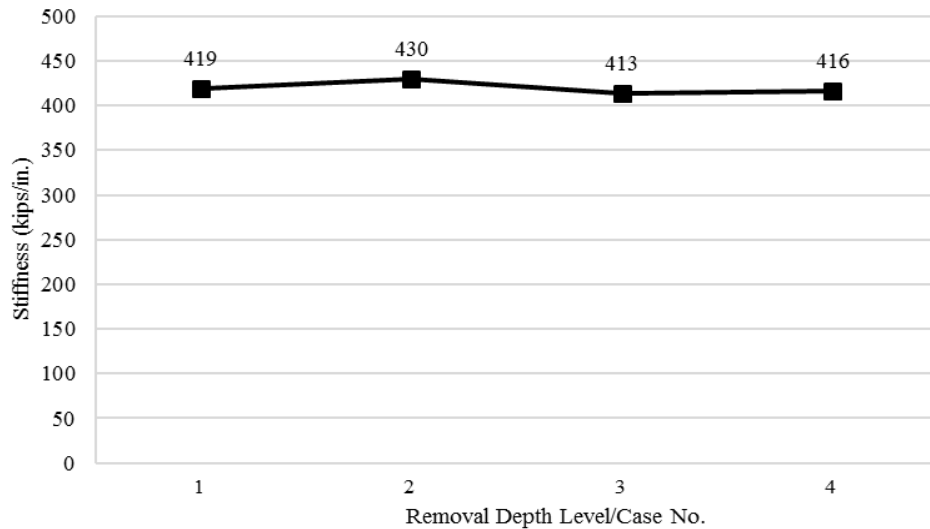


Figure 92. Average stiffness versus concrete removal depth (positive bending flexural test)

The stiffness was calculated as the slope of the load versus deflection data up to the point where the specimen started showing non-linear behavior or a large stiffness change.

3.4.4.4 Statistical analysis of the test data

A multiple comparison with Tuckey's procedure (the T Method) was performed using the maximum load values against the exposure depth. The recorded data values are independent of each other, the number of data points is too small and hence assumed to be normally distributed and there is equal within-group variance across the groups associated with each mean, which satisfies the assumptions for the Tuckey's procedure.

The analysis results showed that the mean values for the maximum load for all the different exposure depths were statistically indifferent. The P-value was 0.4558 which is greater than α ($\alpha = 0.05$), which means there is not enough evidence to say that the maximum load is dependent on the exposure depth.

3.4.4.5 Summary

For the flexural tests with positive bending, the gradual increase in the loading led to sudden failures where a large drop in the load and a shear crack at the bond interface was observed. Some flexure cracks were also observed near mid-span.

The variation in all of the parameters depending on the concrete removal depth level was small. The greatest values for maximum load and elastic shear stress were for Case 3 specimens, while the greatest value for stiffness was for Case 2 specimens.

The maximum load values showed a 6% decrease from Case 1 to Case 4; whereas, the elastic shear stress showed a 10% increase from Case 1 to Case 4. The stiffness of the specimens showed very slight changes in the values with less than a 1% decrease from Case 1 to Case 4.

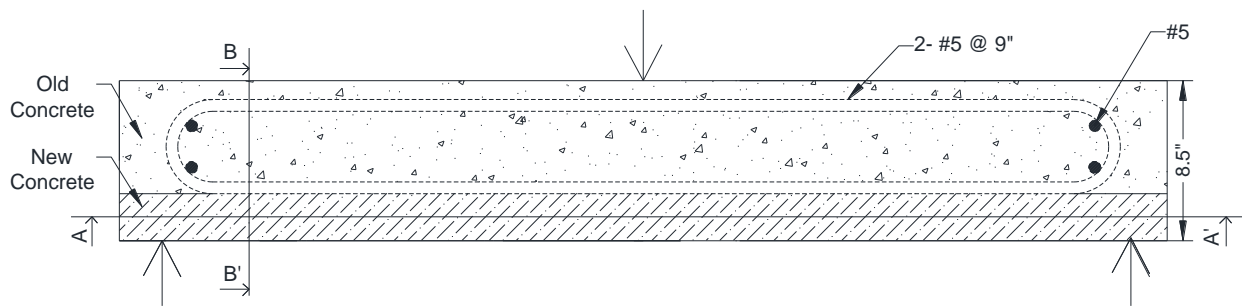
3.4.5 Negative bending flexural test

While the bridge deck experiences positive bending between the girders, negative bending is observed in the regions over the beams. This negative bending can cause tension in the top fibers of the bridge deck. The tension can induce horizontal shear stress in the top fibers, leading to damage to the bond between the overlay concrete and the substrate concrete.

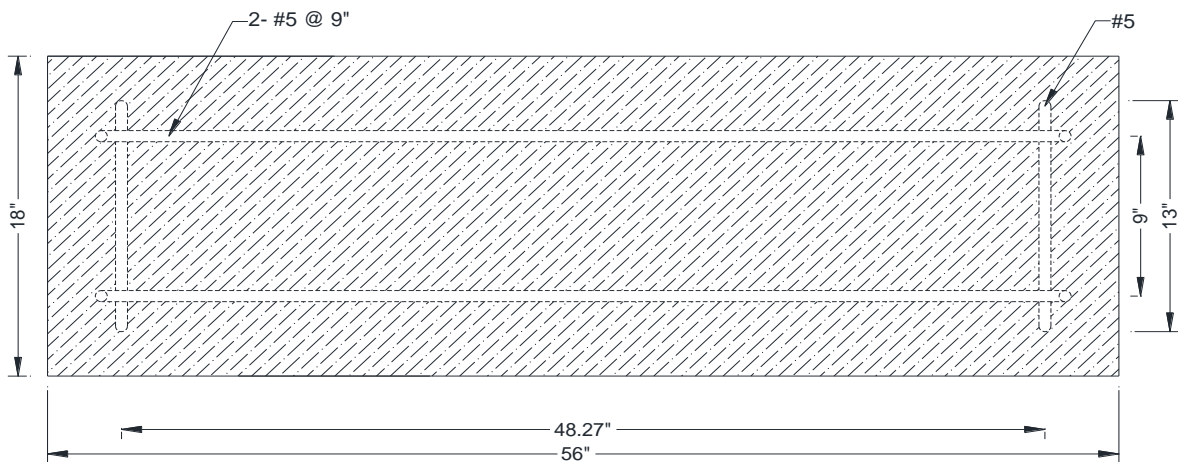
With this test, specimens were tested for negative bending to further evaluate the effects of concrete removal depth.

3.4.5.1 Specimen details

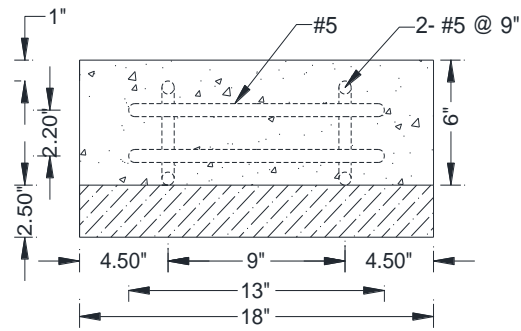
Specimens similar to those for the positive bending flexural tests were fabricated for the negative bending flexural tests; however, during the tests, the specimens were placed upside down while applying the load to simulate negative bending. Figure 93 shows the specimen dimensions and reinforcing steel details.



a) Front view



b) Section A-A'



c) Section B-B'

Figure 93. Negative bending flexural test specimen schematic

Figure 94 shows the formwork for the specimens.



Figure 94. Negative bending flexural test formwork for substrate concrete placement

The substrate concrete was placed into the formwork first. As with the other tests, C4 concrete was used. After curing the concrete for about two days, the concrete was removed by chipping it to its required depth with an electric demolition jackhammer, as shown in Figure 95, also giving the surfaces the proper roughness.



Figure 95. Chipping of substrate concrete for negative bending flexural tests

The typical roughness of the surface after chipping and roughening is shown in Figure 96.



Figure 96. Negative bending flexural test specimen after concrete removal to required depth (Case 3)

As described for the other tests, the same grout material was applied with a brush to the surface of the substrate concrete, as shown in Figure 97, before placement of the overlay concrete.



Figure 97. Application of grout to negative bending flexural test specimen

The overlay concrete was placed on the substrate concrete up to the total depth of the specimen.

3.4.5.2 Testing arrangement

Each flexural test for negative bending started 3 hours prior to the typical 72 hour curing.

Figure 98 shows the testing arrangement with the overlay concrete on the bottom.

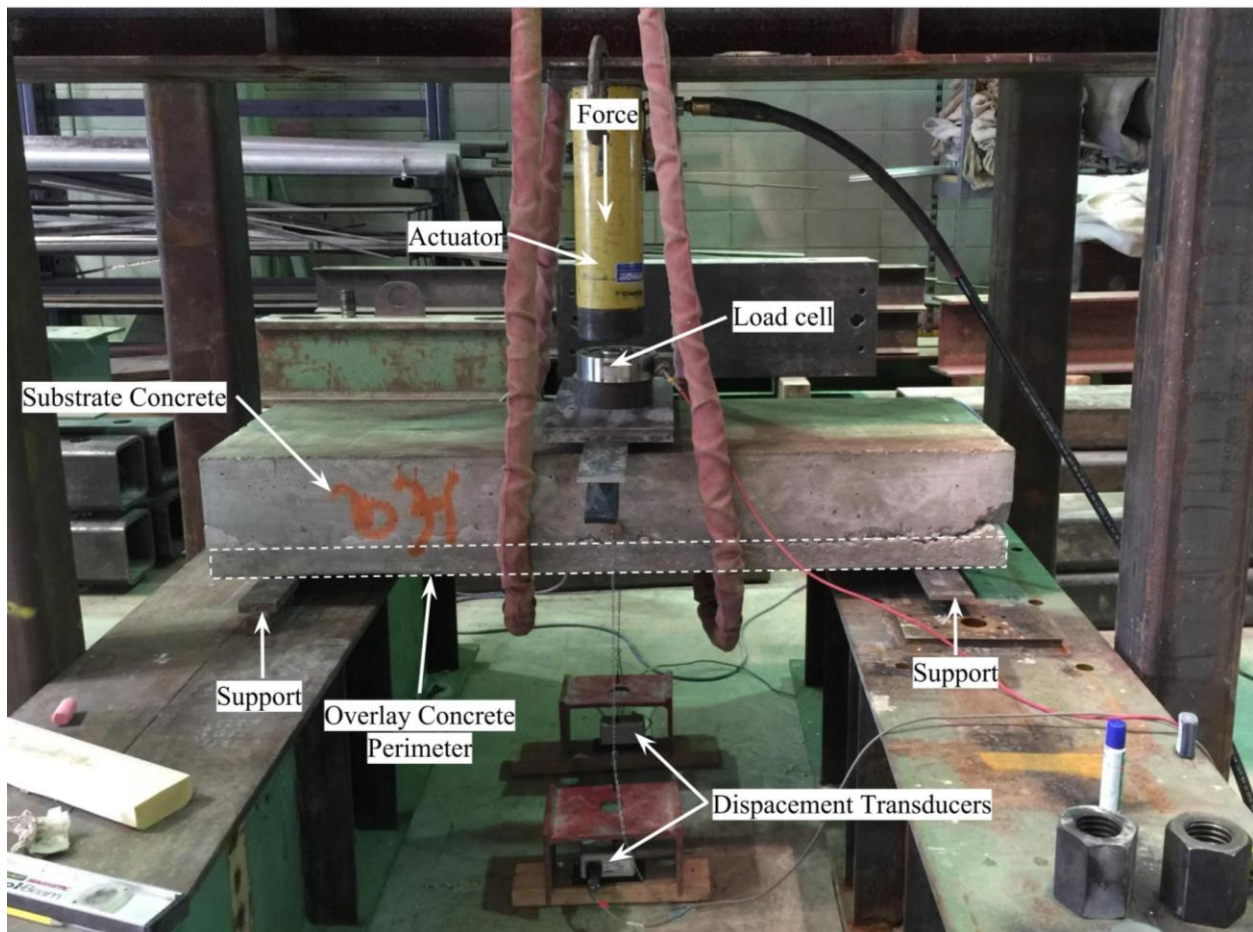


Figure 98. Testing arrangement for negative bending flexural test

The new overlay side of each specimen was supported on each end with a roller and a pin. A neoprene strip was placed at the center of the specimen and the load was applied with a hydraulic loading system. Displacement transducers were mounted on both sides of the specimen at the center to measure the vertical deflection of the specimen on both sides.

3.4.5.3 Results

In this flexural test, the specimens were subjected to loading that simulated negative bending. When the gradually increasing loads were applied to the specimens, shear cracks at the bond interface and some flexure cracks were observed on the specimens. Figure 99 through Figure 102 show specimens after testing.



Figure 99. Case 1 negative bending flexural test specimen failure at concrete bond interface

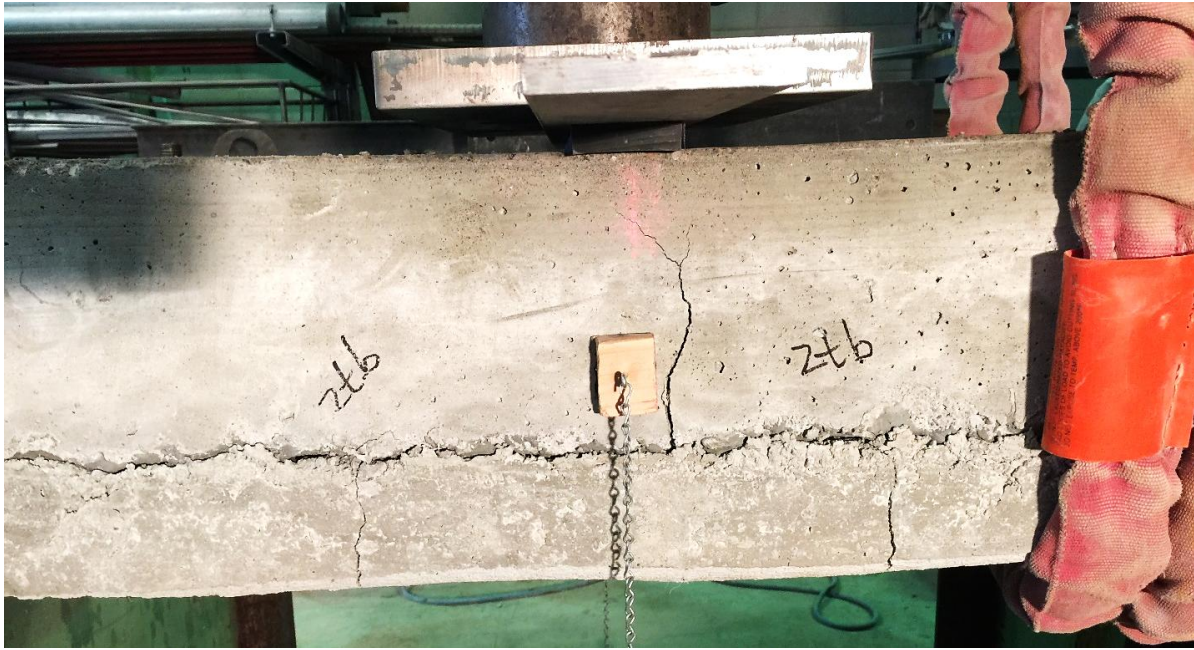


Figure 100. Case 2 negative bending flexural test specimen failure at concrete bond interface



Figure 101. Case 3 negative bending flexural test specimen failure at concrete bond interface

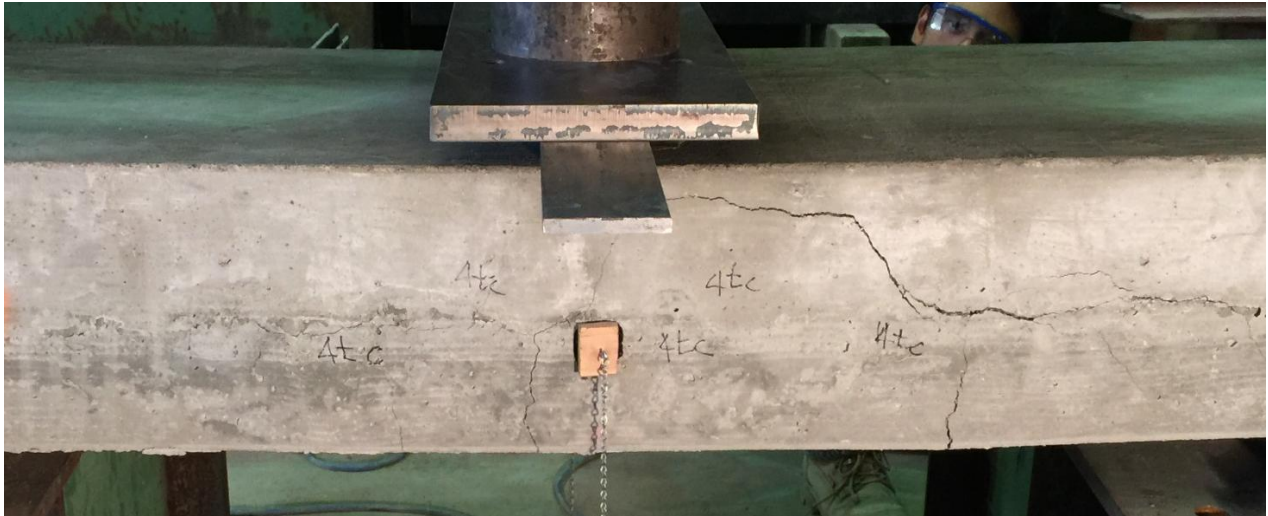


Figure 102. Case 4 negative bending flexural test specimen failure at concrete bond interface

The shear cracks and the flexure cracks are clearly visible in these images. Even though shear cracks were formed in the specimens at the bond interfaces, the cracks did not propagate all the way to the ends (i.e., the two layers of concrete on each specimen were not completely separated from each other). All three specimens for each concrete removal depth level (Case 1 through 4) showed similar failure patterns.

For the first three concrete removal depth level specimens (Cases 1 through 3), the stiffness change was observed only one time; but, for the Case 4 specimens, the change in the stiffness was observed twice. The first stiffness change for the Case 4 specimens was small and occurred at a lower load value of 6 kips, compared to 10 kips, which was the average stiffness change value for the for the other cases. However, the second change in stiffness for the Case 4 specimens was approximately 10 kips. Therefore, only the second stiffness change for Case 4 specimens were compared with the stiffness change from the other cases.

Table 15 shows the values for maximum load, elastic shear stress, and stiffness for all specimens along with the average values for each concrete removal depth (Case 1 through 4).

Table 15. Negative bending flexural test results

Concrete Removal Depth/ Case No.	Specimen No.	Elastic* Shear		Elastic*		
		Load at Stiffness Change (kips)	Stress at Stiffness Change (psi)	Max. Load (kips)	Max. Shear Stress (psi)	Stiffness (kips/in.)
1	1	7	28	26	102	211
1	2	8	31	25	98	183
1	3	8	31	20	79	215
1	Average	8	30	24	93	203
2	1	10	42	25	105	210
2	2	9	38	25	105	181
2	3	11	46	24	101	243
2	Average	10	42	25	103	211
3	1	11	48	24	106	245
3	2	10	44	26	115	198
3	3	11	48	23	101	162
3	Average	11	47	24	107	202
4	1	10	47	21	99	204
4	2	9	42	21	99	169
4	3	10	47	22	104	219
4	Average	10	46	21	101	197

* All assumed section properties are for an un-cracked section

Removal Depth/Case No.:

1 – To top of the reinforcing steel

2 - Half the diameter of the reinforcing steel

3 - Full diameter of the reinforcing steel

4 - Full diameter of the bar and 0.5 to 1 in. additional

Due to the change in the section properties (depth of substrate concrete and overlay concrete) for each removal depth level case, the average elastic shear stress at the bond interface at the maximum load and the stiffness change showed a dissimilar pattern compared to the average load values.

Figure 103 shows the variation of the average load at the stiffness change and the maximum load with the change in the concrete removal depth level.

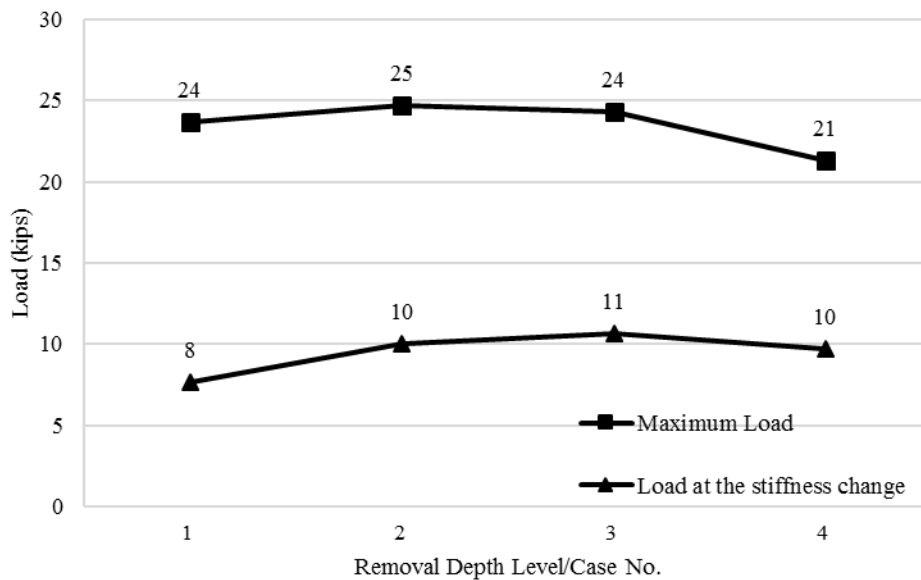


Figure 103. Average load versus concrete removal depth (negative bending flexural test)

Figure 104 shows the variation of the average elastic shear stress (at the bond interface) at the maximum load and at the stiffness change depending on the concrete removal depth level.

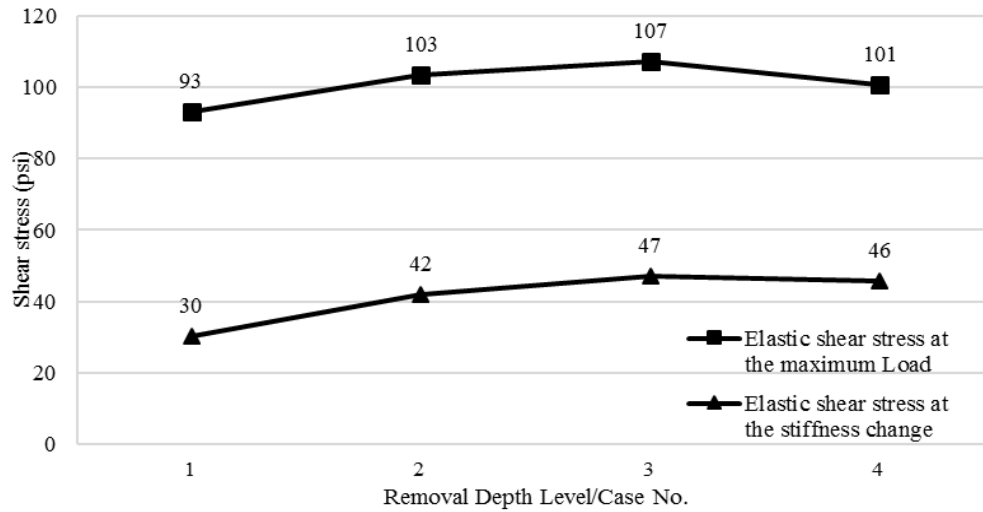


Figure 104. Average elastic shear stress versus concrete removal depth (negative bending flexural test)

Figure 105 shows the variation of the linear stiffness with the change in the concrete removal depth level.

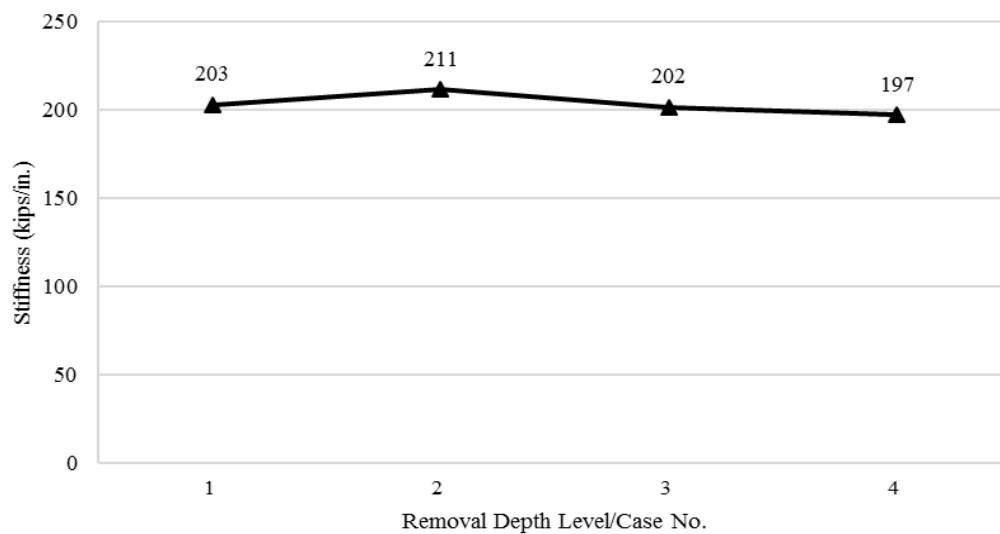


Figure 105. Average stiffness versus concrete removal depth (negative bending flexural test)

The stiffness was calculated as the slope of the linear portion of the load-deflection curve. For Case 4 specimens, the slope of the curve was taken from the starting point to the second change in the stiffness, given that the first stiffness change was small.

3.4.5.4 Statistical analysis of the test data

A multiple comparison with Tuckey's procedure (the T Method) was performed using the load at second stiffness change values against the exposure depth. The recorded data values are independent of each other, the number of data points is too small and hence assumed to be normally distributed and there is equal within-group variance across the groups associated with each mean, which satisfies the assumptions for the Tuckey's procedure.

The analysis results showed that the mean value for the load at second stiffness change for exposure depth 1 was different from rest of the depths while 1, 2 and 3 were statistically indifferent from each other. The P-value was 0.0044 which is less than α ($\alpha = 0.05$), which means there is enough evidence to say that the load at second stiffness change is dependent on the exposure depth.

The analysis on the maximum load values showed that the average maximum load value for all the exposure depths is significantly indifferent. The P-value is 0.1878 which is greater than 0.05, meaning that there is no significant evidence to say that the maximum load values are dependent on exposure depth.

3.4.5.5 Summary

For the flexural tests with negative bending, the gradually increasing loads caused shear and flexural cracks in the specimens. Loading was stopped after it was clear that the steel in the specimens had started to yield.

The values for both the load at the stiffness change and the maximum load for each concrete removal depth level were not much different. Overall, the maximum load decreased 13% from Case 1 to Case 4, while the load at the stiffness change increased by 25%. The elastic shear stress at the maximum load and at the stiffness change increased by 9% and 53%, respectively, from Case 1 to Case 4. Stiffness of the specimens showed very little variation with concrete removal depth.

From Case 2 to Case 4, the difference in the values of all parameters was observed to be insignificant.

CHAPTER 5. CONCLUSION

Time constraints on bridge construction is increasing day by day with the increase in the traffic demands. New bridge construction or rehabilitation can take a significant amount of time causing inconvenience to travelers and increase in construction cost. The “Get in, get out, stay out” strategy is a solution to this avoid these obstacles, by increasing the life span of the new bridge that are being built and to decrease the maintenance for the bridge. This was achieved in the first project of this thesis by incorporating three different innovative ideas like Geo-synthetic Reinforced Soil (GRS) abutments, using prefabricated beams for superstructure and using internal curing concrete in the construction of a bridge in Iowa.

From the innovative concepts that were used and the load test results that were obtained, following conclusions can be made

- The use of internal curing aggregates for the concrete leads to higher strength of concrete and lower weight of the beams which made it easier to move those and the additional concrete strength leads to longer service life
- Prefabrication of the beams and then lifting the beams from both ends using two backhoes and moving them over the creek was a successful time saving approach and did not cause any damage to the beams.
- The load tests performed on the bridge over three years indicated that, the bridge beams and the beam joints are structurally performing well.

Another way to prolong a bridge service life is by bridge deck overlay construction, and accelerating the overlay construction is important in re-opening bridges to traffic as quickly as

possible. This was investigated in the second project with three major tasks of literature review, field investigation, and laboratory testing.

The literature review on fast-curing concrete mixes led to a conclusion that CTS Rapid Set Low-P cement mixes, 4×4 concrete mix, polyester polymer concrete, and very-early-strength LMC may be possible substitutes for Class HPC-O and O concrete, and therefore could be used for overlay construction to reduce curing time without having any loss in the necessary strength requirements. Out of all the overlays mentioned above, very-early-strength LMC would be a best option for the state of Iowa because of its verified use by other states for about 25 years and the various properties it provides for prolonging to service life of deck.

Investigation of the ongoing overlay construction project concluded that some minor improvements such as use of additional machinery like sandblasting setup, jackhammers (and the workers using them), and dump trucks could lead to time savings.

Based on the laboratory testing to determine the required removal depth level, the following results were found.

- For the pull-off test, the load at failure and the tensile bond stress at failure showed slight variation with respect to the concrete removal depth. This suggests that the removal of the additional sound substrate concrete beyond half the diameter of the reinforcing steel bar would not have a significant effect on the bond strength.
- Push-out test results showed that the concrete removal depth Case 1 showed significantly lower bond strength than the other removal depths. The load and the shear stress values at the

stiffness change for the concrete removal depths Case 2 through 4 showed insignificant variation. The stiffness values for all cases showed very small variation. The load and the shear stress at a stiffness change (i.e., crack development) are important parameters when it comes to ensuring long-lasting structural performance of a bridge deck. The push-out test indicates that the removal of the additional sound concrete below half the diameter of the reinforcing steel bar would not result in a significant difference in the bond strength.

- Results from flexural tests with positive bending showed that the maximum load, stiffness, and elastic shear stress at the bond interface were slightly different for different concrete removal depths. The results show that Case 2 provides sufficient bond strength and no additional bond strength is achieved with additional sound concrete removal.
- For the flexural tests with negative bending, the load at stiffness change, maximum load, and elastic shear stresses showed relatively small change in values with changes in concrete removal depths. This shows that the removal of sound concrete below half the diameter of the reinforcing steel bar would not lead to a significant increase in bond strength.

Overall, from all of the laboratory tests and statistical analysis of the data, it can be concluded that the removal of the substrate concrete to half the diameter of the reinforcing steel bar provides as much bond strength as removing additional sound concrete. If unsound substrate concrete exists below half the diameter of the reinforcing steel bar, removing only the unsound concrete would likely be sufficient (contrary to the current standards where it needs to be removed half to one inch below the reinforcing steel bar).

With the concepts and techniques investigated in this thesis, the bridge construction time can be reduced significantly while increasing the life span and decreasing the cost.

5.2 Limitations of the research

- The victor avenue bridge was limited to single and small span of 50'.
- The method of lifting the beams using tow backhoes has the limitation of the weight/length of the beams that are safe to lift using backhoes.
- The different types of overlay mixes that were suggested in the project were based on literature review only and not tested in the laboratory to verify their properties.

5.1 Future study

- The method of cast-on-site beams should be attempted and tested for a longer span, multiple span with change in construction material.
- The lifting of the cast-on-site beams using backhoes may have a limit of span length, which should be further investigated.
- A bridge constructed using the philosophy of “get in, get out, stay out” should be inspected for structural soundness for a longer time period.
- CTS Rapid Set Low-P cement mixes, 4×4 concrete mix, polyester polymer concrete, and very-early-strength LMC should be further evaluated for use as overlay materials. The performance of overlays should be evaluated over a period of years following installation.

- During the removal of the unsound substrate concrete on an actual bridge, a trial attempt should be made with the following removal conditions:
 - If unsound concrete exists to or above half the diameter of the reinforcing steel bar, all concrete should be removed to half the diameter of the reinforcing steel bar.
 - If unsound concrete exists below half the diameter of the reinforcing steel bar, all the unsound concrete should be removed until the depth to which it exists, but no additional sound concrete should be removed.

REFERENCES

- AASHTO. 2011, *The Manual for Bridge Evaluation*, 2nd edition. AASHTO, Washington, DC.
- AASHTO. 2012, *AASHTO LRFD Bridge Design Specifications*. AASHTO, Washington, DC.
- AASHTO. 2014, *Standard Method of Test for Surface Resistivity Indication of Concrete's Ability to Resist Chloride Ion Penetration*. AASHTO TP 95. January 2014.
- ACI. 2016, *Guide to External Curing of Concrete*. ACI 308R-16. ACI, Farmington Hills, MI. May 2016.
- Anderson, Keith W., Jeff S. Uhlmeier, Mark Russell, Chad Simonson, Kevin Littleton, Dan McKernan, and Jim Weston. 2013, *Polyester Polymer Concrete Overlay*. Washington State Department of Transportation (WSDOT) Materials Laboratory. Olympia, WA.
- ASTM. 2005, *Standard Test Method for Compressive Strength of Cylindrical Concrete Specimens*. ASTM C39/C39M – 05, West Conshohocken, PA
- Babcock Anthony and Taylor Peter. 2015, *Impacts of Internal Curing on Concrete Properties*. National Concrete Pavement Technology Center, Ames, IA. January 2015
- BASF. 2011. *4×4™ Concrete System Product Information*. BASF Corporation Admixture Systems Master Builders. Cleveland, OH.
- . 2016 BASF 4×4 Concrete for Strength-on-Demand. BASF Corporation. Cleveland, OH.
www.master-builders-solutions.basf.us/en-us/functions-and-applications/producing-concrete/4x4-concrete-for-strength-on-demand.

Bentz Evan and Collins Michael. 2001, *Response-2000*. University of Toronto, Toronto, Canada.

September 2001

CTS Cement. 2014. *Rapid Set[®] Low-P[™] Cement Datasheet*. CTS Cement Manufacturing Corp.

Cypress, CA. www.ctscement.com/wp-content/uploads/2014/02/LOW-

[P_CEMENT_Datasheet_DS_016_EN_3.pdf](http://www.ctscement.com/wp-content/uploads/2014/02/LOW-P_CEMENT_Datasheet_DS_016_EN_3.pdf).

———. 2016. *Rapid Set[®] Low-P Cement[™]*. www.ctscement.com/low-p-cement/.

Iowa DOT. 2012. *Standard Specifications for Highway and Bridge Construction*. Series 2012.

Iowa Department of Transportation. Ames, IA.

www.iowadot.gov/specifications/Specificationsseries2012.pdf.

Kosmatka, Steven H., Beatrix Kerkhoff, and William C. Panarese. 2003. *Design and Control of*

Concrete Mixtures: The Guide to Applications, Methods, and Materials. 14th Edition.

Portland Cement Association, Skokie, IL.

Maggenti, Ric. 2001. *Polyester Concrete in Bridge Deck Overlays Report*. California

Department of Transportation (Caltrans) District 4 Bay Toll Bridge Program.

Meyers, Rod. n.d. *High Early Strength Portland Cement Concrete for Rapid Concrete Repair*.

4x4[™] Concrete Master Builders. www.virginiadot.org/business/resources/bu-mat-05vcc-rmeyer.pdf.

Mistry Vasant and Mangus Al. 2006, *Get In, Stay In, Get Out, Stay Out*. Public Roads, Federal

Highway Administration (FHWA), Washington, DC. November/December, 2006

- Nmai, Charles. 2016. Personal communication. BASF Corporation Admixture Systems. Cleveland, OH. May 2, 2016.
- Oberoi, Rajesh. 2012. *Polyester Polymer Concrete*. DDR Global Infrastructure Pvt. Ltd. Gurgaon, Haryana, India.
- Ohio DOT. 2007. *High Early Strength Concrete Overlays*. Ohio Department of Transportation Office of Materials Management Cement & Concrete Section.
- Ramey, G. Ed and Russell S. Oliver. 1998. *Rapid Rehabilitation/Replacement of Bridge Decks*. Highway Research Center, Harbert Engineering Center, Auburn University for the Alabama Department of Transportation.
- Smith, Karl, Raul Alarcon, and Doran Glauz. 2001. *Portland Cement Based Fast-Setting Concrete Demonstration*. California Department of Transportation (Caltrans) Materials Engineering and Testing Services Office of Rigid Pavements and Structural Concrete. Sacramento, CA.
- Sprinkel, Michael. 1988. High early strength latex modified concrete. The Aberdeen Group. UK.
- Sprinkel, Michael M. 1998. *Very-Early-Strength Latex-Modified Concrete Overlay*. Virginia Transportation Research Council. Charlottesville, VA.
- . 2011. *LMC Overlays for Bridge Deck Preservation*. 2011 Southeast Bridge Preservation Partnership Meeting, Raleigh, NC, April 13-15, 2011.
- Taylor Peter. 2013, *Curing concrete*. CRC Press, London. September 2013